Cooperative Science and Monitoring Initiative (CSMI)

Lake Michigan 2015 Report

Edited by Carolyn Foley and Paris Collingsworth, Illinois-Indiana Sea Grant

---

Contact:

Carolyn Foley
Research Coordinator
Illinois-Indiana Sea Grant
Purdue University
195 Marsteller Street
West Lafayette, IN 47907-2033
765-494-3601 | cfoley@purdue.edu

Paris Collingsworth
Great Lakes Ecosystem Specialist
Illinois-Indiana Sea Grant
Purdue University
195 Marsteller Street
West Lafayette, IN 47907-2033
312-886-7449 | pcolling@purdue.edu

IISG18-HCE-RLA-013

Table of Contents

Executive Summary iii

List of Tables xiv

List of Figures xv

Describing the Distribution and Productivity of Biota Along a Nearshore to Offshore Gradient 1

Temporal and Spatial Coupling of Nutrients and Food Web—Microbes to Fish 16

Major Findings from the CSMI Benthic Macroinvertebrate Survey in Lake Michigan in 2015 With an Emphasis on Temporal Trends 44

A Summary of Mid-Continent Ecology Division Efforts Associated With the 2015 Lake Michigan Cooperative Science Monitoring Initiative (CSMI) 81

Water Quality and Lower Trophic Level Summary from the 2015 Lake Michigan CSMI 82

Application of a Nutrient Model to Address Nearshore Phosphorus Levels in Lake Michigan 96

"Data in Motion" - Continuous Water Sensor Data Collection for the 2015 Lake Michigan CSMI 102

Atrazine Concentrations in Lake Michigan: Investigating Causes of the Recent Decline 117

Examining Legacy and Emerging Contaminants in Lake Michigan Tributaries 121

Key Findings

Dreissenids and *Diporeia*. Lakewide quagga mussel density declined between 2010 and 2015, but biomass increased slightly over the same period. Discrepancies between the trends in density and biomass are due to population dynamics in the mid-depth (31–90 m) regions of the lake, where most quagga mussels reside. In these regions quagga mussel densities are decreasing but the remaining population consists of larger individuals. Meanwhile, in deeper regions of the lake (> 90 m), quagga mussel populations continue to expand, both in terms of density and biomass, but there are still fewer mussels overall in this region. *Diporeia* populations continue to decline in Lake Michigan. In the 2015 benthic survey, *Diporeia* were only found in 10 sites, most of which were deeper than 90 m.

Pelagic food web. In 2015, CSMI sampling was undertaken to address the hypothesis that primary and secondary production are higher in regions of the lake adjacent to high loading tributaries, particularly in nearshore areas. Results show very little support for this hypothesis. Nearshore total phosphorus was significantly higher at only one shallow (18 m) station off the Muskegon River, whereas chlorophyll *a* concentrations were higher along transects adjacent to high loading tributaries at shallow stations during May and July and at offshore stations (> 90 m) during July. Zooplankton density was higher at nearshore stations only during the month of July, and no differences were found in larval and adult fish density at different sampling depths. Finally, larval fish growth rates did not differ across transect or sampling depths, but larval fish are growing about half as fast as they did prior to the establishment of quagga mussels in the early 2000s. Collectively, these results suggest that resource limitation is prevalent across the pelagic food web in Lake Michigan. Further, the 2015 study design may not have been adequate to fully address this

this hypothesis. Future studies should consider sampling areas that are shallower than 18 m.

Contaminants. Atrazine in open lake water and PCB concentrations throughout the Lake Michigan ecosystem are declining at a rate that exceeds the predictions of the Lake Michigan Mass Balance Study from the 1990s. In addition, tributary loadings of PCBs and mercury were approximately 50–70% lower in 2015 relative to loads calculated for 1994–1995. Collectively, the results from CSMI contaminant monitoring efforts suggest that remediation efforts in Lake Michigan are meeting or exceeding their goals.

Lake Michigan CSMI 2015 Executive Summary

The role of the Cooperative Science and Monitoring Initiative (CSMI) is to provide enhanced monitoring and research activities that provide relevant information to address the science priorities of the Lake Partnerships (established under the Lakewide Management Annex of the 2012 Great Lakes Water Quality Agreement) across the Laurentian Great Lakes. The Lake Michigan Partnership, a collaborative team of natural resource managers led by the U.S. Environmental Protection Agency with participation from federal, state, tribal, and local governments or agencies, uses the information collected through CSMI to help develop long term ecosystem-based management strategies for protecting and restoring Lake Michigan's water quality. On a practical level, CSMI is an intensive effort to collect information on the health of each lake, rotating to one Great Lake each year. In 2015, it was Lake Michigan’s turn. The following is an executive summary of the 2015 research results and the associated white paper containing more specific information.

One of the primary ecosystem stressors in Lake Michigan is the proliferation of invasive species. Many invasive species have entered the Great Lakes since the 1800s, but none have been as

prolific as dreissenid mussels, the collective term for zebra mussels (*Dreissena polymorpha)* and quagga mussels (*Dreissena rostriformis bugensis*). Quagga mussels were first detected in Lake Michigan in 1997 and became well established by 2004. Since their introduction, quagga mussel populations have widely and rapidly expanded, blanketing a huge portion of the lake bottom such that they are now one of the most abundant organisms in the lake. As quagga mussels filter water, they remove nutrients, bacteria, and phytoplankton from the lake, which means that much of the nutrients that would have been available at the base of the food web under pre-invasion conditions is now bound up in quagga mussel tissue and shells. In this way, the proliferation of quagga mussels has disrupted the flow of energy up the food chain—from small zooplankton to top predator fish—and therefore, quantifying the effects of quagga mussels on energy flow throughout the lake is an important concern for the management community of Lake Michigan.

The most prevalent mechanistic hypothesis invoked to describe the negative effects of quagga mussels on the Lake Michigan food web emphasizes their influence on the distribution of nutrients in the water column. According to this hypothesis, commonly referred to as the nearshore shunt hypothesis, nutrients entering Lake Michigan, coming primarily from agricultural watersheds and large urban population centers around the southern basin, remain shunted in nearshore areas due to the filtering activity of quagga mussels, which, in turn, leads to high primary production in nearshore areas. While adequate levels of primary production are necessary to support a vibrant Lake Michigan food web, nuisance levels of algal production, including harmful algal blooms in productive embayments and *Cladophora* stands in coastal areas, represent a problem for the Lake Michigan management community. Despite the long-term changes in food web structure that have been documented since the establishment of quagga mussels in the early 2000s, the hypothesized

effects of quagga mussel grazing, and subsequent localized increases in primary production, on the food web had not been fully tested. In response to this pressing management concern, many of the enhanced monitoring and research activities undertaken during the 2015 CSMI field year in Lake Michigan sought to explicitly test this hypothesis on a lake wide scale.

The current status of the lake drove the following research priorities developed by the Lake Michigan Partnership:

1) What is the status of the lower food web and can the lower food web be an indicator for detecting ecological change?
2) What is the distribution, abundance, and movement of nutrients and biota across a nearshore-offshore gradient?
3) What are the nearshore water-quality effects from tributary nutrient loading?
4) What is the current status of contaminant loads and cycling in the ecosystem?

The scientific approaches to addressing these priorities were not mutually exclusive, and in this report the enhanced monitoring and research activities undertaken during the 2015 Lake Michigan CSMI will be presented in three categories:

1) The status of the lower food web today versus the historic structure.
2) The status of the pelagic food web with respect to the timing of delivery and spatial distribution of nutrients in Lake Michigan.
3) The status of loading and in-lake concentrations of contaminants in Lake Michigan.

The main results from this effort are summarized in the following sections. In addition, full reports from each research group that participated in 2015 field year sampling are included after this executive summary.

Lower Food Web and Ecological Change

Scientists working with the National Oceanic and Atmospheric Administration (NOAA) and the U.S. Environmental Protection Agency (EPA) have been monitoring components of the lower Lake Michigan food web, including zooplankton and benthic macroinvertebrates, since the mid-1980s. Sampling schemes for 2015 used historical methods with a few key additions. In 2015, CSMI partners from EPA, NOAA, Cornell University, the University at Buffalo, and University of Michigan, monitored the whole benthic community rather than only zebra mussels, quagga mussels, and *Diporeia spp.* (as had been done previously), and used additional sampling techniques such as a benthic sled and optical plankton counters to complement historic sampling methods. The technological advances in the 2015 CSMI sampling year greatly improved the scientists' abilities to assess trends in Lake Michigan. However, standard techniques, such as PONAR grabs for benthic invertebrates and zooplankton net tows, are important to maintain, not only for their ability to assess trends over time, but to complement and validate the newer methods (e.g., using empty shell estimates from PONAR samples to calibrate video captured by the benthic sled, and using traditional net tows to calibrate zooplankton density estimates from towed laser optical particle counters).

Benthic trends included in this report are summarized from the 1990s through 2015. Sampling sites varied slightly by sampling year. Benthic samples were collected at 140 stations in July of 2015 (135 in the main basin of the lake, and five in the outer portion of Green Bay). Dreissenid density declined significantly between 2010 and 2015 (and dreissenids are now comprised of quaggas mussels only). Dreissenid densities declined 79%, 56%, and 40% at < 30 m, 31–50 m, 51–90 m intervals, respectively, but increased 37% at depths > 90 m. Despite general declines in density, overall biomass of dreissenids increased in 2015 over 2010. The discrepancy

between the trends in density and biomass of dreissenids can generally be attributed to a shift toward fewer but larger-bodied individuals. In 2015, much of the dreissenid biomass was found at depths of 30–90 m. *Diporeia* and Sphaeriidae continue to decline in 2015 from previous time periods sampled. Currently, *Diporeia* are only found in very few areas (n = 10 sites), and are generally found deeper than 90 m. Oligochaeta have progressively increased in shallower and mid-depth regions between 1992 and 2015, especially in southeastern Lake Michigan.

Scientists from EPA, the US Geological Survey (USGS), NOAA, and Cornell University assessed zooplankton community dynamics. Measurements of zooplankton biomass along transects off Frankfort (Michigan), and Sturgeon Bay (Wisconsin), suggest that total zooplankton biomass did not differ between 2010 and 2015 (although biomass of Cladocera such as *Daphnia galeata mendotae* and *Bythotrephes longimanus* declined, and *Mysis relicta* biomass increased over this time period). In June, dreissenid veligers were the dominant zooplankton in numbers and biomass all along the Muskegon transect. Zooplankton were also found deeper in the water column in 2015 as compared to previous years. Quagga mussel filtration activities have led to increased levels of water clarity throughout the photic zone (i.e., surface layer of the lake that receives sunlight) over time, and zooplankton may be seeking refuge in murkier waters near the metalimnion. Both larval fish and another relatively recent invader, *Bythotrephes longimanus*, visually prey on zooplankton. Vertical distribution of fish larvae have indeed shifted from the top meter of the water column in 1983 down to the metalimnion in 2015. This supports the notion that the fish are visually tracking the downward movement of zooplankton prey.

Stable isotope analyses of lower food web members suggest that quagga mussels and zooplankton may be competing for resources at a different time of year than previously assumed. Quagga mussels and zooplankton exhibited well-differentiated $\delta^{13}C$ and $\delta^{15}N$ isotopic composition

in May, indicating that they were not feeding on similar algae or other particles during winter or spring. The reason for isotopic differentiation of mussels and zooplankton during unstratified conditions is not known, however, the two organismal groups became increasingly isotopically similar through summer and fall, such that they were not different from each other by September. These results suggest that quagga mussels are competing with zooplankton for food resources during stratified lake conditions. Direct competition between quagga mussels and zooplankton throughout the summer growing season could ultimately reduce zooplankton production in the offshore food web, thereby reducing the amount of food available for prey fish and sportfish alike.

Pelagic food web and nutrients

Uncertainty in exactly how hypothesized nearshore increases in nutrient concentrations affect in-lake processes such as water quality, primary productivity, and fish production led to the development of two 2015 CSMI research priorities. To address these uncertainties, EPA, USGS and NOAA designed a large-scale collaborative field effort to examine trends in nutrients and biota (from micro-plankton to fish) along nearshore to offshore gradients in Lake Michigan and formulated two specific hypotheses:

1) Nearshore-offshore transects located near high phosphorus (P) loading tributaries have higher productivity levels than those located near low P-loading tributaries.

2) Nearshore areas have higher productivity than offshore areas.

Scientists from USGS and the EPA established eight fixed location sampling transects based on their proximity to tributaries. Based on previous modeling efforts, the tributaries were

designated: “no” loading—Waukegan (Illinois), Frankfort (Michigan), and Sturgeon Bay (Wisconsin); “low” loading—Root River/Racine (Wisconsin) and Pere Marquette River/Ludington (Michigan); or “high” loading—St. Joseph River (Michigan), Kalamazoo River (Michigan), and Manitowoc River (Wisconsin). The distance from the tributary varied slightly between transects, and three fixed sampling locations along each transect were designated nearshore (18 m), mid-depth (45 m), or offshore (> 90 m). Most transects were sampled once each season (spring, summer, and fall). One transect, off Muskegon, Michigan, relatively close to both Muskegon Lake and the mouth of the Grand River, was sampled by NOAA scientists almost monthly to capture localized fine-scale temporal food-web dynamics.

Results of the fixed sampling transect work showed little evidence for a positive relationship between proximity to high loading tributaries and the shoreline and the spatial distribution of total phosphorus (TP) and chlorophyll *a* concentrations in Lake Michigan. Broadly speaking, TP and chlorophyll *a* were more variable along the western shore of the lake (versus the eastern), and in the northern basin (versus the southern). However, at the individual transect level, nearshore TP was significantly higher at only one shallow (18 m) station off the Muskegon River. When averaging across months, mean chlorophyll *a* concentrations were consistently higher for stations that were near high-loading tributaries, but these differences were not statistically significant from lower-loading tributaries. Looking at specific sampling months, chlorophyll *a* concentrations were higher along transects adjacent to high loading tributaries at shallow stations during May, and at both shallow and offshore stations (> 90 m) during July.

The spatial and temporal relationships between TP, chlorophyll *a,* and productivity at higher trophic levels is even less clear. For example, along the Muskegon transect, nearshore and offshore zooplankton had distinct differences, with smaller, epilimnetic species found nearshore.

Lake-wide, stable isotope results for benthic macroinvertebrates and zooplankton demonstrate a shift from relatively low $\delta^{15}N$ and high $\delta^{13}C$ values nearshore to higher $\delta^{15}N$ and lower $\delta^{13}C$ offshore. The $\delta^{13}C$ patterns may suggest a greater contribution of nearshore carbon sources (i.e., benthic algae) to the food web, higher production in nearshore versus offshore waters, or both. The $\delta^{15}N$ patterns are consistent with previous observations regarding nitrogen cycling in Lake Michigan. Relatively low $\delta^{15}N$ values of animals collected in the nearshore areas (i.e., 18 m depth) suggest that animals in these areas are not strongly reliant on anthropogenic inputs of nitrogen.

Fish data suggest that nearshore areas, and potentially the entire Lake Michigan ecosystem, may be resource-limited. High mortality rates during the larval period have long been believed to be a bottleneck to fish production. Along the Muskegon transect, decreasing cyclopoid copepod biomass is coincident with increased abundance of *Dreissena* veligers, and changing prey types and availability may have a negative effect on larval fish growth. In offshore areas, densities and growth rates of larval bloater remained low compared to previous years. Conversely, in nearshore areas, larval densities of alewife and yellow perch increased in 2015 over previous years. Along the Muskegon transect, larval alewife growth rates and condition were extremely low as compared to the early 2000s. Catches of adult pelagic prey fish declined by more than 91% between 2010 and 2015 along the Frankfort and Sturgeon Bay transects (declines by species: alewife 90%, rainbow smelt 99%, bloater 86%). Adult alewife energetic condition was similar in 2015 to values measured in the early 2000s when quagga mussel proliferation was underway; however, alewife production continues to be "squeezed" from both limited prey resources and the well-documented predation pressure from piscivorous salmon and trout.

Loading and in-lake concentrations of contaminants

Human activities have led to contamination of Lake Michigan water, sediment, and biota. Pollutants found include certain chemicals used as pesticides on agricultural fields and polychlorinated biphenyls (PCBs) used in industrial practices. Much of our current knowledge about the dynamics of pollutants in Lake Michigan comes from the Lake Michigan Mass Balance (LMMB) study conducted by EPA in the 1990s. The LMMB research team measured common pollutants and developed models to predict the fate of these pollutants under different management scenarios. To this day, the study results are the baseline for measuring progress. Scientists from EPA, USGS, and Indiana University specifically addressed the loading of PCBs and mercury and estimated in-lake concentrations of atrazine during the 2015 CSMI field year. They also estimated the loadings of organophosphate esters (OPEs), brominated flame retardants (BFRs), and dechlorane-related compounds, many of which are chemicals of emerging concern.

Atrazine concentrations measured in Lake Michigan in 2015 were lower than what had been forecasted by the LMMB study. Water samples collected from EPA Great Lakes National Program Office (GLNPO) Lake Michigan open water stations in August of 2015, at both the mid-epilimnion and mid-hypolimnion depths, reflected a mean atrazine concentration of 36 ng/L. This concentration fell between the LMMB model predictions for 100% reduction of tributary loading and 100% reduction of total loading scenarios. Literature reviews, plus examination of atrazine use in the Lake Michigan basin, suggest that a combination of decreased atrazine use on land and higher than originally estimated degradation rates resulted in lower atrazine concentrations than those forecasted.

PCB, mercury, and flame retardants were analyzed from water samples collected every three weeks from April through December in 2015. Five tributaries, namely the Grand,

Kalamazoo, St. Joseph, and Lower Fox rivers, plus the Indiana Harbor and Ship Canal (IHSC), were selected for sampling because they showed the highest loads of PCBs in the LMMB study. The geometric mean concentrations of ΣPCB (sum of 85 congeners) ranged from 1.52 to 22.4 ng/L. The highest concentrations of PCBs were generally found in the Lower Fox River and the IHSC. The highest BFR concentrations were measured in either the IHSC or the St. Joseph River. OPEs were the most abundant among the targeted compounds with geometric mean concentrations ranging from 20 to 54 ng/L, and concentrations were similar across tributaries. BFR concentrations were about 1 ng/L while dechlorane-related compounds were less than 0.001 ng/L. Mercury loads from all five tributaries were on the order of 50% to 75% lower in 2015 relative to loads calculated for 1994–1995. The Lower Fox River remains the highest loading tributary of mercury into Lake Michigan (43 kg/yr in 2015), with other tributary loadings ranging from 1.7 kg/yr to 12.6 kg/yr.

PCB data from this study were combined with open-lake water, air, and sediment PCB concentration data from other studies to calculate an updated mass budget for Lake Michigan. The estimated net transfer of PCBs out of the lake is 1240 ± 531 kg yr-1, which is 46% lower than that estimated in the 1994–1995 LMMB study. In most lake matrices, PCB concentrations are decreasing, which drives the decline of all the individual input and output flows. Tributary loads at the Lower Fox River and the Indiana Harbor and Ship Canal both decreased substantially relative to 1994–1995 loads. Atmospheric deposition to Lake Michigan has become negligible, while volatilization from the water surface is still a major route of loss, releasing PCBs from the lake into the air. Large PCB masses remain in the water column and surface sediments and are likely to contribute to future efflux of PCBs from the lake to the air.

List of Tables

GLERL sampling activities during the 2015 Lake Michigan CSMI field season 43

Location, depth, and described substrate of sites sampling in Lake Michigan in 2015 (benthos) ... 61

Sites where additional *Dreissena* was collected for determination of length-weight relationships in 2010 and 2015 65

Relationship between shell length (SL in mm) and tissue ash-free dry weight (AFDW in mg) for *D. polymorpha* and *D. r. bugensis* at various depth intervals in Lake Michigan in 2004, 2008, 2010, and 2015 66

Mean (± SE) density (no./m^2) of *Diporeia, Dreissena polymorpha*, and *Dreissena r. bugensis* at four depth intervals (< 30 m, 31–50 m, 51–90 m, and > 90 m) in each survey year 67

Percentage of measured *D. r. bugensis* within various size categories at four depth intervals (< 30 m, 31–50 m, 51–90 m, and > 90 m) in 2010 and 2015 68

Mean (± SE) density (no./m^2) of major macroinvertebrate taxa at four depth intervals (< 30 m, 31–50 m, 51–90 m, and > 90 m) at 40 sites in the southern basin of Lake Michigan 69

Mean (± SE) biomass (gAFDW/m^2) of *Dreissena* at < 30 m, 31–50 m, 51–90 m, and > 90 m depth intervals based on the latest lake-wide surveys in Lake Michigan, Lake Ontario, and Lake Huron 70

Data collection dates for 2015 Lake Michigan CSMI (transect and glider) 108

Sensors on various sampling platforms used for CSMI 108

List of Figures

Expected loading level for different CSMI sites based on historical models 9

Mean chlorophyll a concentrations estimated at nearshore sampling sites categorized as “no” (i.e., Waukegan, Frankfort, Sturgeon Bay), “low” (i.e., Root, Pere Marquette), and “high” (i.e., St. Joseph, Kalamazoo, Manitowoc) total phosphorus loading sites. 10

Mean chlorophyll a concentrations estimated by depth zone for three different seasons in 2015 ... 11

Mean zooplankton biomass (natural-log transformed) estimated by depth zone for three different seasons in 2015 12

Mean *Mysis* biomass estimated by depth zone for three different seasons in 2015 13

Mean energetic condition for commonly sized large alewife (135-165 mm) and commonly sized small round goby (45–95 mm) at two different depth zones during the fall of 2015 near Waukegan 14

Location of sampling sites for 2015 CSMI (transects) 15

Sampling sites along the Muskegon transect in Lake Michigan 22

Daytime PSS long transect results from M10-M110 on May 20, 2015 23

Seasonal zooplankton composition at M15. 24

Seasonal zooplankton composition at M110 25

Density of predatory cladocerans at Muskegon transect 15, 45, and 110 m sites during 2015 26

Fine scale spatial distribution of zooplankton from diel sampling at night on June 25, 2015 at M110 27

Daytime PSS long transect results from M10–M110 on June 23, 2015 along with corresponding net tows 28

Larval densities pre (2001–2002) and post (2010–2014) quagga mussel invasion for alewife, yellow perch and bloater. 29

Larval alewife and bloater growth rates along Muskegon transect pre- and post-quagga mussel invasion 30

Nearshore/offshore diet contents of alewife, bloater and yellow perch 31

Regression analysis of factors influencing larval alewife daily growth rates from 2001–2002, 2010–2011, 2013–2015 32

PSS plots of temperature (A) and chlorophyll (B) show an upwelling event on July 13, 2015 that displaced nearshore larval alewife offshore 33

Attenuation coefficients of nearshore, mid-depth and offshore sites in Lake Michigan 34

Comparing 1983 to 2010, a decline in offshore bloater larvae density, and change in vertical distribution 35

Density of Mysis at Muskegon transect 45 and 110 m sites during 2015 36

Total seasonal phosphorous concentration along the Muskegon transect in 2015 37

Acoustics transects show the seasonal succession of planktivore overlap with their zooplankton prey.. 38

UV Irradiance at M110 on July 25, 2015. UV-B (305 nm) radiation could have a potentially negative effect on some zooplankton and larval fish in the upper 5 m of the water column 39

Dominant nano and micro-plankton grazers in Lake Michigan 40

Flow cytometric analysis of the bacterial community across the Muskegon transect 41

Abundance-weighted bacterial community composition dynamics 42

Location of sampling sites in the southern region of Lake Michigan in 2015 (benthos) 71

Location of sampling sites in the central region of Lake Michigan in 2015 (benthos) 72

Location of sampling sites in the northern region of Lake Michigan in 2015 (benthos) 73

Density (no. per m^2) of *Dreissena polymorpha* in Lake Michigan based on lake-wide surveys in 1994/1995, 2000, 2005, 2010, and 2015 74

Density (no. per m^2) of *Dreissena r. bugensis* in Lake Michigan based on lake-wide surveys in 1994/1995, 2000, 2005, 2010, and 2015 75

Long-term trends of total *Dreissena* in Lake Michigan in 1994/1995, 2000, 2005, 2010, and 2015 76

Ash free dry weight (AFDW, mg) of a standard 15 mm *D. r. bugensis* at four depth intervals intervals in Lake Michigan between 2004 and 2015 77

Relationship between ash free dry weight (AFDW) and total wet weight (TWW, whole mussel, tissue and shell) of *D. r. bugenisis* at each sampling site in the main basin of Lake Michigan in 2015 78

Density (no. per m^2) of *Diporeia* spp.in Lake Michigan based on lake-wide surveys in 1994/1995, 2000, 2005, 2010, and 2015. 79

Density (no. per m^2) of total *Dreissena* at < 30 m, 31-90 m, and > 90 m in Lake Ontario, Lake Michigan, and Lake Huron 80

Transects sampled by CSMI in 2015 and associated rivers and loading categories, overlain on a map of TP loading differences among shoreline locations 88

Relationship between surface-water TP measured on the May or July 2015 CSMI cruises vs. 2002–2008 avg annual TP loading from the adjacent tributary (the three no-tributary transects were assigned to zero load) 89

Relationship between surface-water planktonic CHLA measured on the May or July 2015 CSMI cruises vs. 2002–2008 avg annual TP loading from the adjacent tributary (the three no-tributary transects were assigned to zero load) 90

1982–2015 time-series of upper-water column total phosphorous concentrations (mean ± 1 standard deviation) from a set of long-term monitoring stations (i.e., GLNPO monitoring data) measured in either spring (April or May) or summer (August or September) 91

1982 to 2015 time-series of upper-water column chlorophyll a (CHLA) concentration (mean ± 1 standard deviation) from a set of long-term monitoring stations (i.e., GLNPO monitoring data) measured in either spring (April or May) or summer (August or September) 92

Box plots comparing levels of TP (left panels) and CHLA (right panels) across depths in 1983 (GLNPO monitoring data) relative to 2015 CSMI stations 93

Carbon and nitrogen stable isotope ratios of quagga mussel, zooplankton (Zoop.), and oligochaetes (Oligo.) at the 18 m, 46 m, and 110 m stations 94

The difference between zooplankton and quagga mussel carbon and nitrogen stable isotope ratios by month (May, July, September).. 95

Computational grid (1km x 1km) of the study area (nutrient model) 99

Model phosphorus results versus observational data (in µg/L): Base TP load 100

Model phosphorus results versus observational data (in µg/L): 30% reduction of the base TP load 100

Nearshore spatial patterns of TP in the Lake Michigan for two dates in summer (2015) 101

Lake Michigan 2015 CSMI transects with dots indicating vertical CTD casts 109

Clockwise from top left: Photos of Slocum Glider, tow body, CTD Rosette glider, Research vessel the Lake Explorer II and tow body ready to be deployed 109

Screen shot of Cesium software animation of glider mission track displaying chlorophyll sensor data 110

Screen shot of ESRI Story Map developed for Lake Superior glider data. 110

Dates of glider deployment segments 111

Cross section of Lake Michigan temperature and chlorophyll-a from 2015 Deployment 2, segment 7 112

Comparison of wind data measured by different platforms 113

Lake Michigan surface temperature on Sept. 26, 2015 and Oct. 10, 2015 114

Lake Michigan Upwelling index summed from 1994 through 2013 using methods developed by Plattner et al 2006 114

Vertical CTD Cast for the Ludington, MI transect at depths of 110, 46 and 18 meters collected on Sept. 21, 2015 (before the upwelling event) 115

Tow temperature data from all four transects during September 2015 116

Lake Michigan atrazine concentration prediction modeling (Kreiss, Rygwelski) 118

Sampling locations related to the 2015 CSMI Lake Michigan contaminant study.. 125

Tributary loading of organophosphate esters (OPEs), non-BDE novel flame retardants (nFRs), and polybrominated diphenylethers (PBDEs) to Lake Michigan. 126

Box and whisker plots of concentrations of individual congeners and ΣPCBs in 2015 tributary water samples 127

Tributary ΣPCB flows to Lake Michigan for 1994–1995, 2005–2006, and 2015 128

Estimated total PCB mass budget flows (kg/yr) and inventories (kg) for 2010–2015 and comparison to the 1994–1995 mass balance results based on the MICHTOX model16 in Lake Michigan. 129

Box and whisker plots of concentrations of organophosphate esters (OPEs) in tributary water samples 130

Box and whisker plots of concentrations of polybrominated diphenyl ethers (PBDEs), non-BDE novel flame retardants (nFRs), and dechlorane related compounds (Decs) in tributary water samples. 131

Report: Describing the Distribution and Productivity of Biota Along a Nearshore to Offshore Gradient

Authors:

David Bunnell, USGS Great Lakes Science Center
Patricia Armenio, USGS Great Lakes Science Center
David Warner, USGS Great Lakes Science Center
Lauren Eaton, University of Toledo
Drew Eppehimer, University of Arizona

Contact:

David Bunnell

Email: dbunnell@usgs.gov

Phone: 734-214-9324

Address:

Great Lakes Science Center

1451 Green Rd

Ann Arbor, MI 48105

Background

The Lake Michigan Lakewide Action and Management Plan (LAMP) proposed adding nutrients (phosphorus) to its "pollutant of concern" list in 2002, given that excessive nutrients were causing impairments in nearshore waters. Since that time, scientists have highlighted the "shunting" of nutrients to the nearshore (Hecky et al. 2004), owing to the ability of invasive dreissenid mussels to capture some portion of allochthonous phosphorus that enters the lake through tributaries. These changes are believed to increase productivity in the nearshore, reflected in increased benthic and pelagic primary production and nuisance *Cladophora* (Auer et al. 2010). Whether increases in primary productivity lead to concomitant increases for secondary (by zooplankton) and tertiary (by fish) production remains largely untested. Hence, understanding the distribution and abundance of nutrients and biota (e.g., zooplankton, fish) across a nearshore to offshore gradient was identified as a Cooperative Science and Monitoring Initiative (CSMI) priority in 2015. Increased understanding of the Lake Michigan nearshore will also facilitate the development of a Nearshore Strategy by the LAMP, which is called for in the 2012 Great Lakes Water Quality Agreement.

Working collaboratively with Environmental Protection Agency (EPA) and National Oceanic and Atmospheric Administration (NOAA), United States Geological Survey (USGS) described the distribution of nutrients and biota across nearshore to offshore transects in 2015 (see Appendix 1). At each transect, we sampled the food web at three sites with differing bottom depths: 18 m, 46 m, and 91-110 m. We purposefully chose transects near tributaries of varying total phosphorus (TP) input (see Figure 1, Dolan and Chapra 2012): three transects that were not associated with any large tributary where total phosphorus would be loaded (Waukegan IL, Frankfort MI, Sturgeon Bay WI), three transects adjacent to tributaries presumed to be relatively low loaders of TP (Pere Marquette MI, Root WI, Muskegon MI), and three transects adjacent to tributaries presumed to be relatively high loaders of TP (St. Joseph MI, Kalamazoo MI, Manitowoc WI). USGS estimated chlorophyll concentrations, zooplankton, *Mysis*, larval fish, and juvenile and adult fish seasonally (April/May, July, October/November) at eight of these transects (all but Muskegon).

From this design, we tested two hypotheses that organize our results below. 1) Among nearshore sites, productivity should be greater at sites near tributaries with higher TP loading. Because we do not have 2015 estimates of TP loading, we substituted chlorophyll a, the most relevant index of productivity from the next lower trophic level, when seeking to explain variation in productivity across nearshore sites. 2) The nearshore should be more productive than the offshore. We used several different response variables for productivity in these hypotheses, including chlorophyll *a*, zooplankton biomass and production, larval fish density and growth (for alewife only), and prey fish biomass and energetic condition. We hypothesized that enhanced productivity for lower trophic levels would lead to greater prey resources to support fish production or fish condition. We also provide results for *Mysis diluviana*, a large native zooplankton that is omnivorous but is well known to reach higher densities in deeper waters. We acknowledge that benthic invertebrates (e.g., quagga mussels) would be another important response variable to evaluate for these hypotheses, but these data were collected by Buffalo State University and NOAA and should be integrated in future analyses. We used Pearson correlation coefficient to determine whether variation in nearshore productivity corresponded with lower

trophic level indicators of productivity. We also used Analysis of Variance to determine whether productivity response variables differed between nearshore and offshore depths. Where differences were found, we used Tukey's multiple comparison test to determine which means are different from one another.

Hypothesis 1. Among nearshore sites, productivity should be greater at sites near tributaries with higher TP loading.

Chlorophyll a: For each sampling event in each season, we averaged the estimated chlorophyll concentration for the entire water column or euphotic zone, which ever was deeper. The maximum depth of the euphotic zone was 65 m, so we only averaged chlorophyll over this depth range for the offshore sites. Water column chlorophyll was predicted based on fluorescence data calibrated with at least three *in situ* estimates of chlorophyll throughout the water column. We categorized the sites into one of three groups (no loading, low TP loading, high TP loading) based on historical TP loadings from the adjacent tributaries. Chlorophyll concentrations did not differ among groupings for any of the seasons (spring: $F = 0.86$, $P = 0.48$; summer: $F = 0.24$, $P = 0.80$; fall: $F = 2.20$, $P = 0.21$). The high TP loading category always had the highest mean chlorophyll, but the variation surrounding the mean of each group was relatively high (Figure 2). Hence there was no support for the hypothesis that chlorophyll concentrations increased with expected increases in TP loading.

Zooplankton biomass and production: Zooplankton biomass and production were lower in spring, compared to summer and fall. Zooplankton production was estimated through temperature and size-based regressions (Shuter and Ing 1997; Stockwell and Johannsson 1997). For each season, we correlated zooplankton with coincident chlorophyll *a* estimates. During spring, neither zooplankton biomass ($r = -0.46$, $P = 0.26$) nor zooplankton production ($r = -0.49$, $P = 0.21$) was positively correlated with chlorophyll concentrations. Similarly, during summer, neither zooplankton variable (biomass: $r = 0.18$, $P = 0.68$; production: $r = 0.41$, $P = 0.31$) was positively correlated with chlorophyll. Finally, chlorophyll was not positively correlated with zooplankton biomass ($r = 0.38$, $P = 0.36$) or production ($r = 0.46$, $P = 0.25$) in the fall either. Hence there was no support for the hypothesis that zooplankton biomass or production increased with nearshore productivity.

Larval fish densities: The majority of nearshore larvae sampled in late April and early May were deepwater sculpin (42%), followed by lake whitefish (41%), and round goby (16%). The highest densities of larvae (all species) were sampled at Frankfort (4.2/100m^3) and Sturgeon Bay (2.5/100m^3). Lower densities (<1/100m^3) were samples at Root, Pere Marquette, and Manitowoc. No larvae were sampled at the Kalamazoo, St. Joseph, and Waukegan sites. During spring, total larval density (natural log transformed) was not positively correlated with any lower trophic level measurements from the same sampling day: chlorophyll ($r = 0.54$, $P = 0.35$), zooplankton biomass ($r = 0.19$, $P = 0.76$), or zooplankton production ($r = 0.09$, $P = 0.88$).

For the July samples, the majority of nearshore larvae sampled were alewife (89%), followed by yellow perch (6%), slimy sculpin (3%), and burbot (1%). The highest densities of larvae (all species) were sampled at St. Joseph (54/100m^3) and Kalamazoo (32/100m^3). Intermediate densities were sampled at Root (4.2/100m^3), Manitowoc (1.3/100m^3) and Pere Marquette

(1.3/100m^3). The lowest densities (<1/100m^3) were sampled at Waukegan and Sturgeon Bay. No larvae were collected at Frankfort. During summer, total larval density (natural log transformed) was not positively correlated with any lower trophic level measurements from the same sampling day: chlorophyll (r = 0.58, P = 0.17), zooplankton biomass (r = 0.41, P = 0.37), or zooplankton production (r = 0.55, P = 0.20). No larval fish were collected during the fall sampling effort. Hence there was no support for the hypothesis that production of larvae increased with nearshore productivity.

Larval alewife growth rates: Alewife are a key prey fish species in Lake Michigan and are a large proportion of Chinook salmon and lake trout diets. Annual production of new alewife is highly variable across years, and we estimated growth rates of alewife larvae sampled in July to determine whether spatial variability in growth could be explained by variation in nearshore productivity. We assume that faster larval growth rates increase the probability of survival to sizes large enough to feed key salmonines. Alewife larvae of comparable ages (≤ 20 days old) were only collected from four of the nearshore sites from July 12-22, 2015. Growth rates differed among sites, with larvae from Waukegan growing the fastest (0.58 mm/day) and those from the Kalamazoo site growing the slowest (0.39 mm/day). Sites with intermediate growth rates included St. Joseph (0.47 mm/day) and Root (0.48 mm/day). Although we had limited power (N = 4) to detect correlations, there was no positive correlation between larval growth rate and any lower trophic level: chlorophyll (r = 0.27, P = 0.73), zooplankton biomass (r = -0.70, P = 0.30), zooplankton production (r = -0.43, P = 0.57). Hence there was no support for the hypothesis that larval growth rate increased with nearshore productivity.

Fish biomass: Fish biomass was estimated through the summation of estimates derived from the bottom trawl, midwater trawl and acoustics. Nearshore fish biomass varied seasonally, likely owing to fish migrations associated with occupying optimal temperature or accessing spawning habitat. For spring, nearshore fish biomass was diverse, with round goby, alewife, lake whitefish, bloater, and lake trout being the most common. Total fish biomass (all species pooled) was not positively correlated with either chlorophyll (r = 0.43, P = 0.34) or either measure of zooplankton (biomass: r = -0.27, P = 0.56; production: r = -0.15, P = 0.75). During summer, fish biomass was mostly alewife and bloater, and total fish biomass was weakly positively correlated with chlorophyll (r = 0.70, P = 0.05), but not with either measure of zooplankton (biomass: r = 0.18, P = 0.68; production: r = 0.42, P = 0.30). During fall, fish biomass was mostly round goby and alewife and was unrelated to chlorophyll (r = -0.25, P = 0.55), and strongly negatively related to zooplankton biomass (r = -0.87, P = <0.01) and production (r = -0.79, P = 0.02). In total, there was very limited support for the hypothesis that fish biomass increased with nearshore productivity.

Fish energetic condition: We estimated whole fish energy density (Joules/gram of fish) to index energetic condition of alewife and round gobies collected at our sites. When comparing similar sized fish, those with higher energetic condition have more lipids, and likely have exploited prey resources better than those with lower energetic condition. Only small alewife (i.e., (< 13 g, wet weight) in the fall had sufficient sample sizes across nearshore sites to make a comparison. Mean energetic condition of small alewife was unrelated to chlorophyll (r = 0.04, P = 0.94) or either measure of zooplankton (biomass: r = 0.48, P = 0.34; production: r = 0.35, P = 0.49).

Hence there was no support for the hypothesis that fish energetic condition increased with nearshore productivity.

Hypothesis 2. The nearshore should be more productive than the offshore.

Chlorophyll a: Chlorophyll concentrations did not differ among nearshore, intermediate depth, and offshore sites in spring ($F = 2.75$, $P = 0.09$), summer ($F = 1.34$, $P = 0.28$) or fall ($F = 1.16$, $P = 0.34$). The variation among the sites within a depth zone was relatively high, and the mean chlorophyll was only highest in the nearshore zone in the fall (Figure 3). Hence there was no support for the hypothesis that chlorophyll concentrations were higher in the nearshore zone than in the other zones.

Zooplankton biomass and production: Zooplankton biomass ($\mu g/m^3$) was lower in spring than in summer and fall (Figure 4). Zooplankton biomass did not differ among nearshore, intermediate depth, and offshore sites in spring ($F = 1.69$, $P = 0.21$). During summer, however, zooplankton biomass was significantly higher at 18 m than at 110 m ($F = 5.62$, $P = 0.01$); biomass at 46 m was similar to the other two depth zones. During fall, only two of the offshore sites were sampled. Hence we limited the statistical comparison to 18 m and 46 m, and found no difference in zooplankton biomass between these two depth zones ($F = 0.55$, $P = 0.47$). Zooplankton production results revealed the exact same pattern as zooplankton biomass: during summer zooplankton production average 706.2 $\mu g/m^3/d$ in the nearshore, which was significantly higher than the average of 209.2 $\mu g/m^3/d$ in the offshore. Hence there was seasonal support (i.e., summer only) for the hypothesis that zooplankton biomass or production was higher in the nearshore than in other zones. It is noteworthy that the summer season can be a critical period for many larval fishes that hatch in the nearshore zone (e.g., alewife, yellow perch).

Larval fish densities: Density ($\#/m^3$) of all larval fish did not differ among nearshore, intermediate depth, and offshore sites in spring ($F = 0.74$, $P = 0.49$) or summer ($F = 0.99$, $P = 0.39$); larvae were not sampled in fall. Because more than 88% of all larval fish sampled in summer were alewife, and alewife hatch in the nearshore, it was surprising that larval fish densities were not highest in this zone. Larval alewife were likely advected offshore through currents and may even navigate into deeper waters when they reach sizes large enough to be active swimmers. The distance between the nearshore and offshore sites ranged from 7 km (Frankfort) to 36 km (Kalamazoo), with the average distance across all transects being 19 km. Hence there was no support for the hypothesis that larval fish density was higher in the nearshore than in other zones.

Larval alewife growth rates: Larval alewife growth rates in the summer were slower for those sampled in the nearshore (mean = 0.47 mm/d) compared to those sampled in the offshore (0.52 mm/d; $F = 5.12$, $P = 0.006$); those sampled in the intermediate depths were not different from any other depth (mean = 0.50 mm/d). Hence there was no support for the hypothesis that larval fish grow faster in the nearshore than in other zones, despite zooplankton biomass (and production) being higher in the nearshore than the offshore during summer.

Mysis biomass: Mysis biomass is commonly known to increase with depth in the Great Lakes. Hence, we did not hypothesize that *Mysis* biomass would be higher in the nearshore than in the

offshore in 2015. During spring, summer, and fall, we observed the expected result that *Mysis* biomass (mg/m^2) was higher in the offshore than in the nearshore (Figure 5, spring: $F = 11.18$, $P < 0.001$); summer: $F = 10.54$, $P < 0.001$; fall: $F = 7.07$, $P = 0.007$). Fall offshore collections were limited to two sites with high variability between sites.

Fish biomass: Biomass of fish was never highest in the nearshore. During spring, nearshore fish biomass was lower than the biomass in the intermediate or offshore depth zones ($F = 6.92$, $P = 0.005$). During summer, there was no difference in fish biomass across the three zones ($F = 1.28$, $P = 0.30$). During fall, there was no difference between fish biomass at 18 and 46 m depth zones ($F = 0.16$, $P = 0.70$; only 2 offshore sites were sampled). Hence there was no support for the hypothesis that fish biomass was higher in the nearshore than in other zones.

Fish energetic condition: To compare alewife energetic condition across depth zones, we only had one sampling occasion with similar-sized fish caught at both 18 m and 46 m depths. In the fall at Waukegan, alewife energetic condition was 26% greater at 46 m (i.e., 8066 J/g wet weight, see Figure 6) than at 18 m (i.e., 6403 J/g wet weight), a significant difference ($F = 76.8$, $P < 0.0001$). For a round goby comparison across depths, we also only had one comparative opportunity. At Waukegan in the fall, round goby energetic condition was not different ($F = 3.86$, $P = 0.052$) between those sampled at 46 m (i.e., 4227 J/g wet weight) and those at 18 m (i.e., 4352 J/g wet weight). Hence there was no support for the hypothesis that fish energetic condition was higher in the nearshore than in other zones. Round goby, a fish that relies on more benthic prey resources, was much closer to supporting the hypothesis than the more pelagic-oriented alewife.

Summary. Contrary to the hypotheses, our nearshore sampling sites were not sensitive to expected variable inputs of TP from tributaries, nor were they generally "hot spots" of productivity for chlorophyll, zooplankton, or larval, juvenile, and adult fish. From a whole lake perspective, the "nearshore" zone of the lake is widely considered to include depths 30 m and shallower, and this region only represents about 20% of the lake surface area (far less of a percentage by volume). Hence our 18 m nearshore sites were relatively centrally located within the nearshore habitat. Nonetheless, it remains possible that if we had sampled in even shallower waters or more immediately "downstream" of the tributary inputs, we might have detected higher productivity within an even shallower portion of the nearshore zone. The only support for nearshore "hot spot" in our study was for nearshore zooplankton biomass and production in the summer. Given that the eggs of many important fish species are hatching in the nearshore during summer, this could be advantageous for first-feeding fish larvae. Surprisingly, however, larval fish densities were just as high in the offshore zones as in the nearshore zones- even for nearshore spawning fish like alewife. This advection of young larvae to the offshore waters is likely driven by circulation and upwelling, which contribute to a nearshore habitat that is likely less stable in water temperatures than in the offshore. Furthermore, larval alewife growth rates were lower in nearshore waters than in offshore waters.

For the other instances where CSMI sampling revealed differences in biota along a nearshore to offshore gradient, the nearshore was typically the site where biomass (juvenile and adult fish in the spring fish, *Mysis* in all seasons) or energetic condition (large alewife) was lowest. Contrary

to our hypothesis, the offshore habitat was generally more productive than the nearshore habitat across trophic levels.

Temporal comparisons to other studies. Two of the nearshore to offshore transects sampled in 2015 were the same transects (Frankfort, Sturgeon Bay) that were sampled monthly in 2010. When we compared different trophic levels between the two years at these sites we found: total zooplankton biomass did not differ between years (although cladocerans such as *Daphnia galeata mendotae* and *Bythotrephes* declined in 2015), *Mysis* biomass was higher in 2015 than 2010, and pelagic prey fish biomass declined by more than 91% in 2015 relative to 2010 (90% decline for alewife, 99% decline for rainbow smelt, and 86% decline for bloater).

The 2015 intensive effort also afforded an opportunity to measure key variables for alewife, a prey fish species of high management concern given its importance to sustaining the recreationally important Chinook salmon fishery and the recent alewife collapse in adjoining Lake Huron. Larval alewife growth rates in 2015 were 43% and 38% slower than the rates estimated from comparable studies in 2001-2002 and 2004-2006, respectively (Höök et al. 2007; Weber et al. 2015). This slower growth rate, coupled with our finding that 67% of larval alewife stomachs in 2015 were devoid of prey suggests that the larval period could be a bottleneck to production of new alewife. At the same time, we determined that the energetic condition of juvenile and adult alewife in 2015 (that have survived a potential larval bottleneck) were in no worse condition than a study that measured alewife energetic condition in 2002-2004 (Madenjian et al. 2006). This result suggests that larger alewife appear to be doing just as well exploiting prey resources in 2015 as in the early 2000s when quagga mussel proliferation was underway. At the same time, alewife energetic condition in 2002-2004 and in 2015 was still about 25% lower than was measured in 1979-1981 when the lake was more productive (and when alewife densities were considerable higher). These data suggest that alewife production continues to be "squeezed" from both limiting prey resources, as well as the well documented predation pressure from piscivorous salmon and trout.

Implications for future 2020 CSMI: Should describing the productivity of the nearshore remain a goal in future CSMI efforts, 1) additional sampling efforts could be directed in this dynamic habitat, 2) hydrological models could be developed to place the data collected from discrete sampling events in greater context, and 3) remote sensing tools (e.g., profiling buoys/drifters, gliders, satellites) that were tangentially applied in 2015 could be more carefully considered for their role in 2020 to try and describe this dynamic environment between sampling events by research boats. Additional research into a potential "bottleneck" for larval fish survival may also continue to provide insights into how the changing lower trophic levels are influencing prey fish densities.

References:

Auer, M.T., L.M. Tomlinson, S.N. Higgins, S.Y. Malkin, E.T. Howell, and H.A. Bootsma. 2010. Great Lakes Cladophora in the 21st century: same algae- different ecosystem. Journal of Great Lakes Research 36: 248-255.

Dolan, D.M., and S.C. Chapra. 2012. Great Lakes total phosphorus revisited: 1. Loading analysis and update (1994-2008). Journal of Great Lakes Research 38: 730-740.

Hecky R.E., R.E.H. Smith, D.R. Barton, S.J. Guildford, W.D. Taylor, M.N. Charlton, and T. Howell. 2004. The nearshore phosphorus shunt: A consequence of ecosystem engineering by dreissenids in the Laurentian Great Lakes. Canadian Journal of Fisheries and Aquatic Sciences 61: 1285–1293.

Höök, T.O., E.S. Rutherford, D.M. Mason, and G.S. Carter. 2007. Hatch dates, growth, survival, and overwinter mortality of age-0 alewives in Lake Michigan: implications for habitat-specific recruitment success. Transactions of the American Fisheries Society 136: 1298-1312.

Madenjian, C. P., S.A. Pothoven, J.M. Dettmers, and J.D. Holuszko. 2006. Changes in seasonal energy dynamics of alewife (*Alosa pseudoharengus*) in Lake Michigan after invasion of dreissenid mussels. Canadian Journal of Fisheries and Aquatic Sciences 63: 891–902.

Shuter, B.J., and K.K. Ing. 1997. Factors affecting the production of zooplankton in lakes. Canadian Journal of Fisheries and Aquatic Sciences 54: 359-377.

Stockwell, J.D., and O.E. Johannsson. 1997. Temperature-dependent allometric models to estimate zooplankton production in temperature freshwater lakes. Canadian Journal of Fisheries and Aquatic Sciences 54: 2350-2360.

Weber, M.J., B. C. Ruebush, S. M. Creque, R. A. Redman, S. J. Czesny, D. H. Wahl, and J. M. Dettmers. 2015. Early life history of alewife *Alosa pseudoharengus* in southwestern Lake Michigan. Journal of Great Lakes Research 41: 436-447.

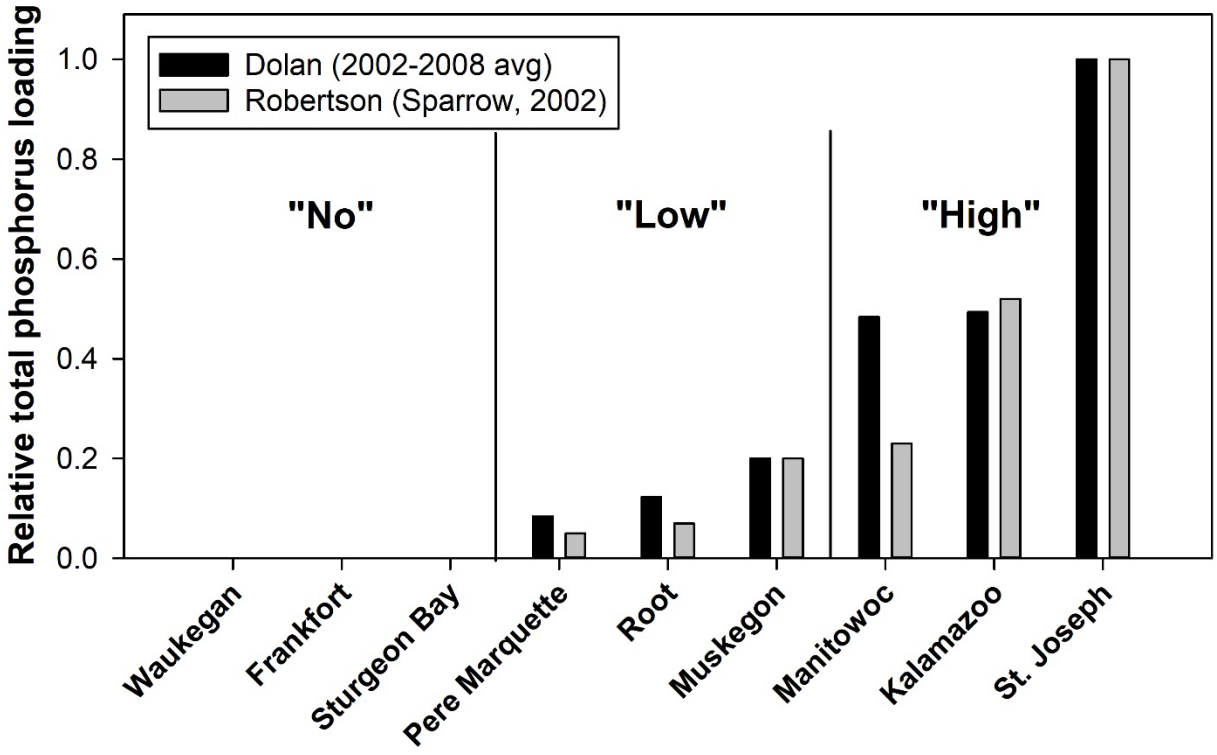

Figure 1. Expected loading level for different CSMI sites based on historical models.

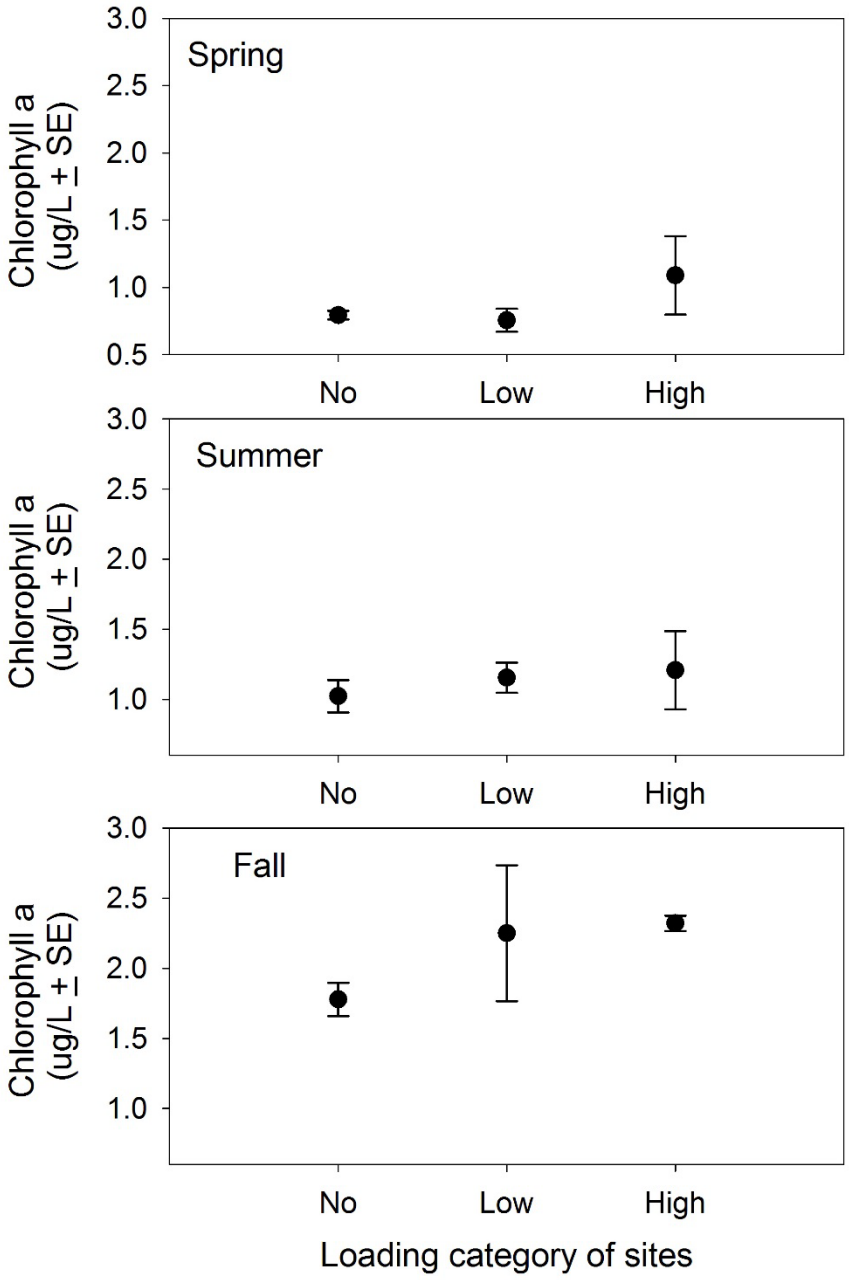

Figure 2. Mean chlorophyll a concentrations estimated at nearshore sampling sites categorized as “no” (i.e., Waukegan, Frankfort, Sturgeon Bay), “low” (i.e., Root, Pere Marquette), and “high” (i.e., St. Joseph, Kalamazoo, Manitowoc) total phosphorus loading sites. Mean chlorophyll did not differ across loading category for any season.

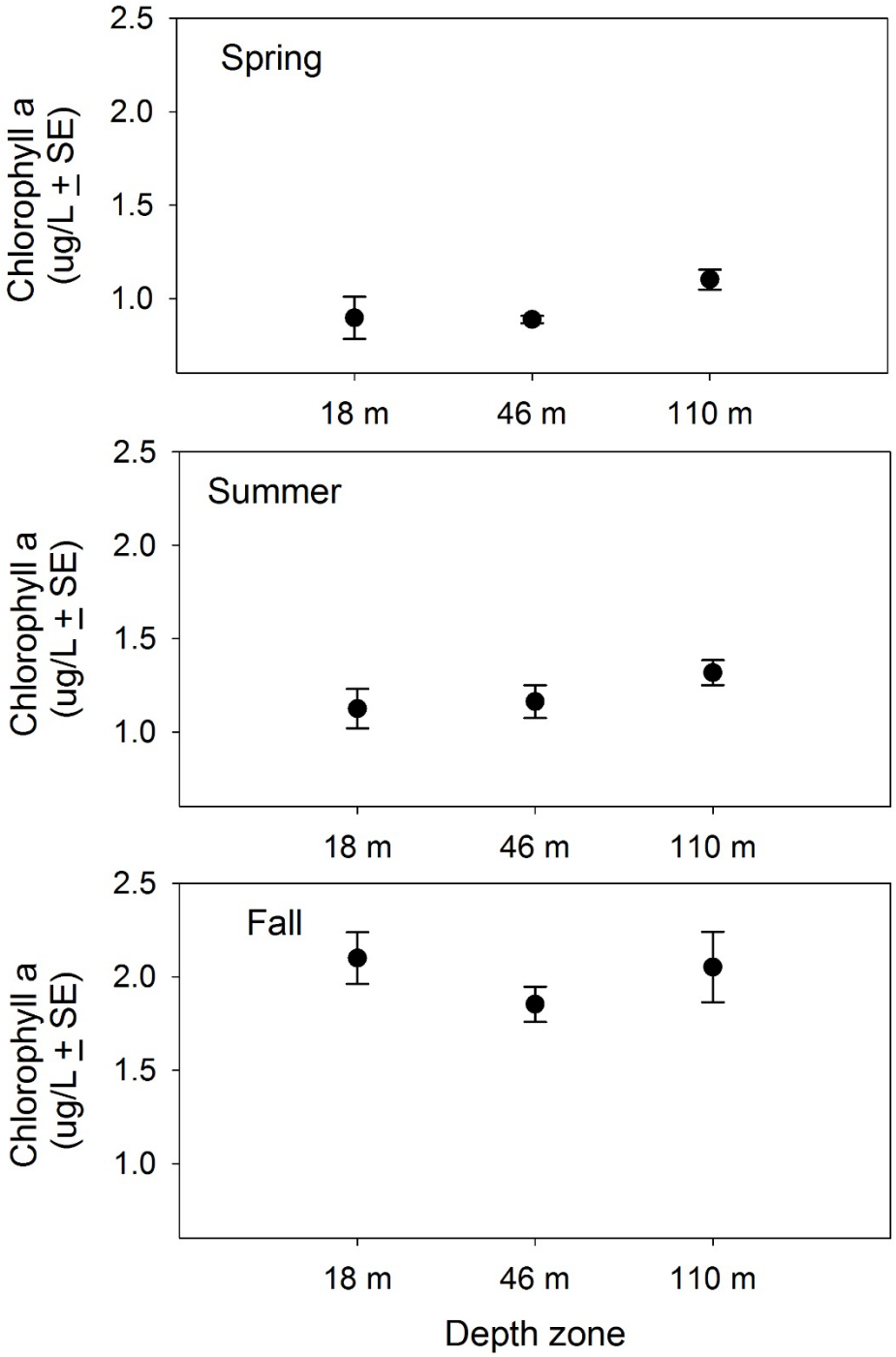

Figure 3. Mean chlorophyll a concentrations estimated by depth zone for three different seasons in 2015. Mean chlorophyll did not differ across depth zones for any season. Fall 110 m was only at the Frankfort and Sturgeon Bay sites (other offshore sites were unable to be sampled).

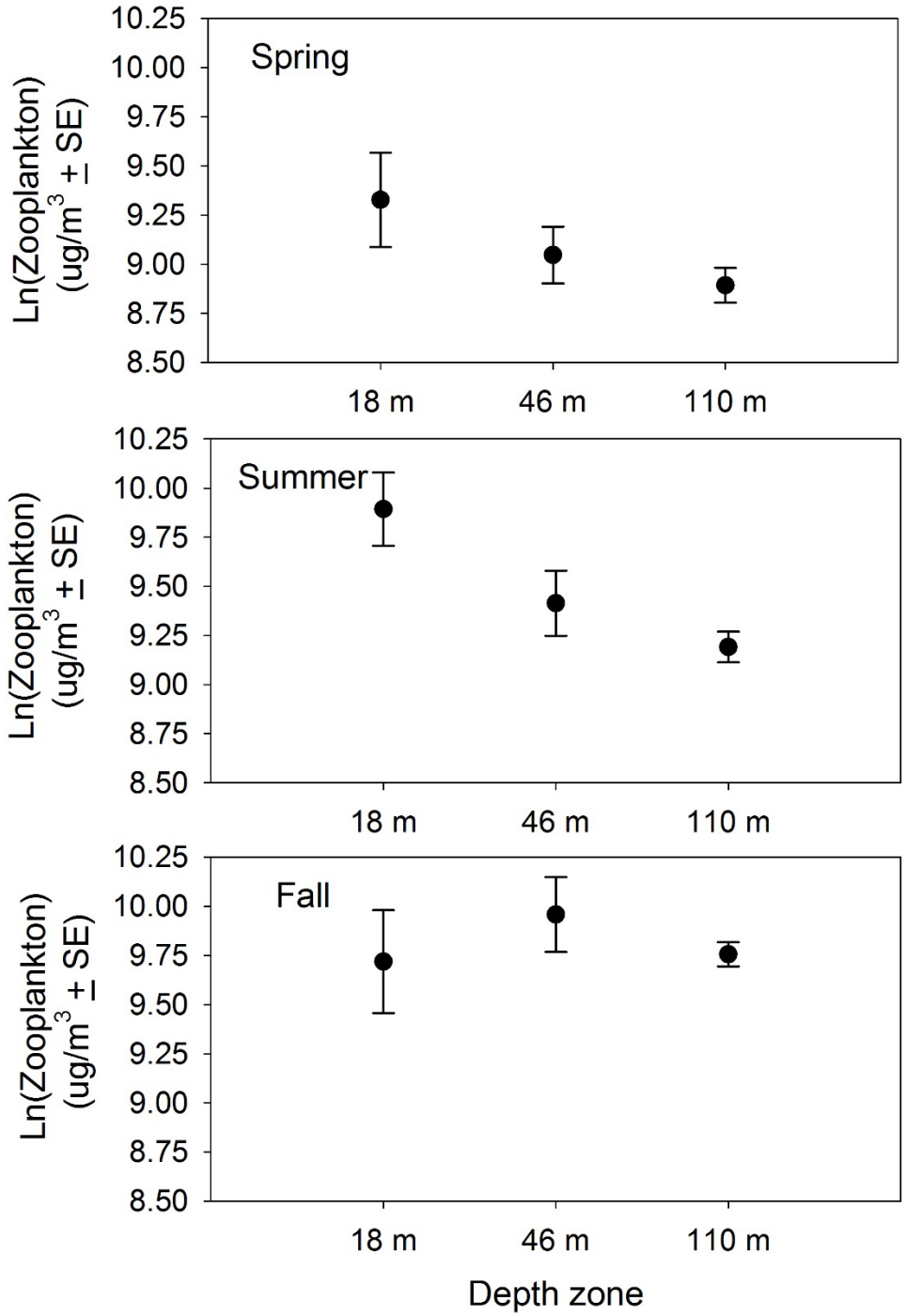

Figure 4. Mean zooplankton biomass (natural-log transformed) estimated by depth zone for three different seasons in 2015. Zooplankton biomass was higher at 18 than at 110 m only in summer. Fall 110 m was only at the Frankfort and Sturgeon Bay sites (other offshore sites were unable to be sampled).

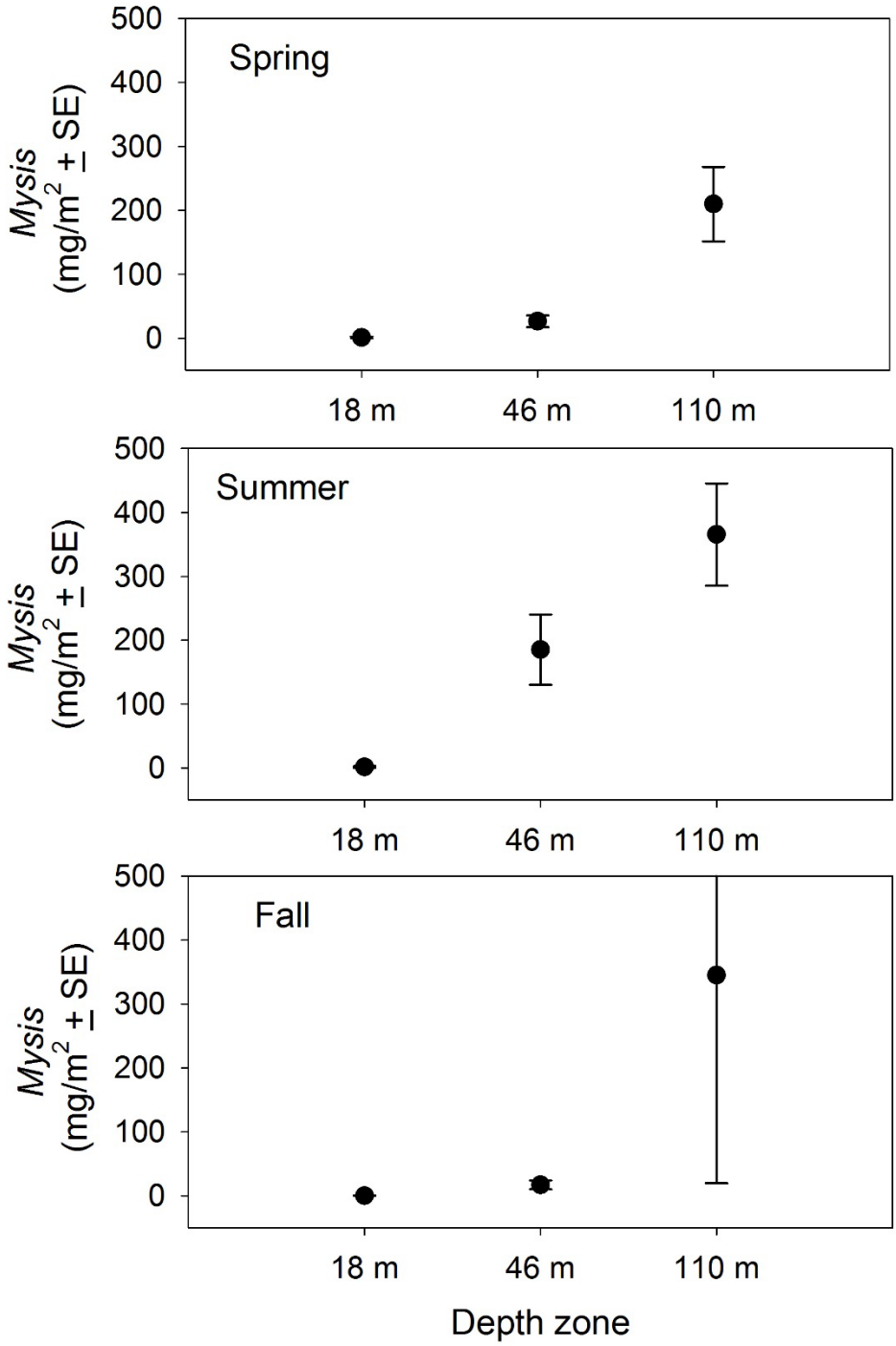

Figure 5. Mean *Mysis* biomass estimated by depth zone for three different seasons in 2015. *Mysis* biomass was higher at 110 m than at 18 m in all seasons. Fall 110 m was only at the Frankfort and Sturgeon Bay sites (other offshore sites were unable to be sampled).

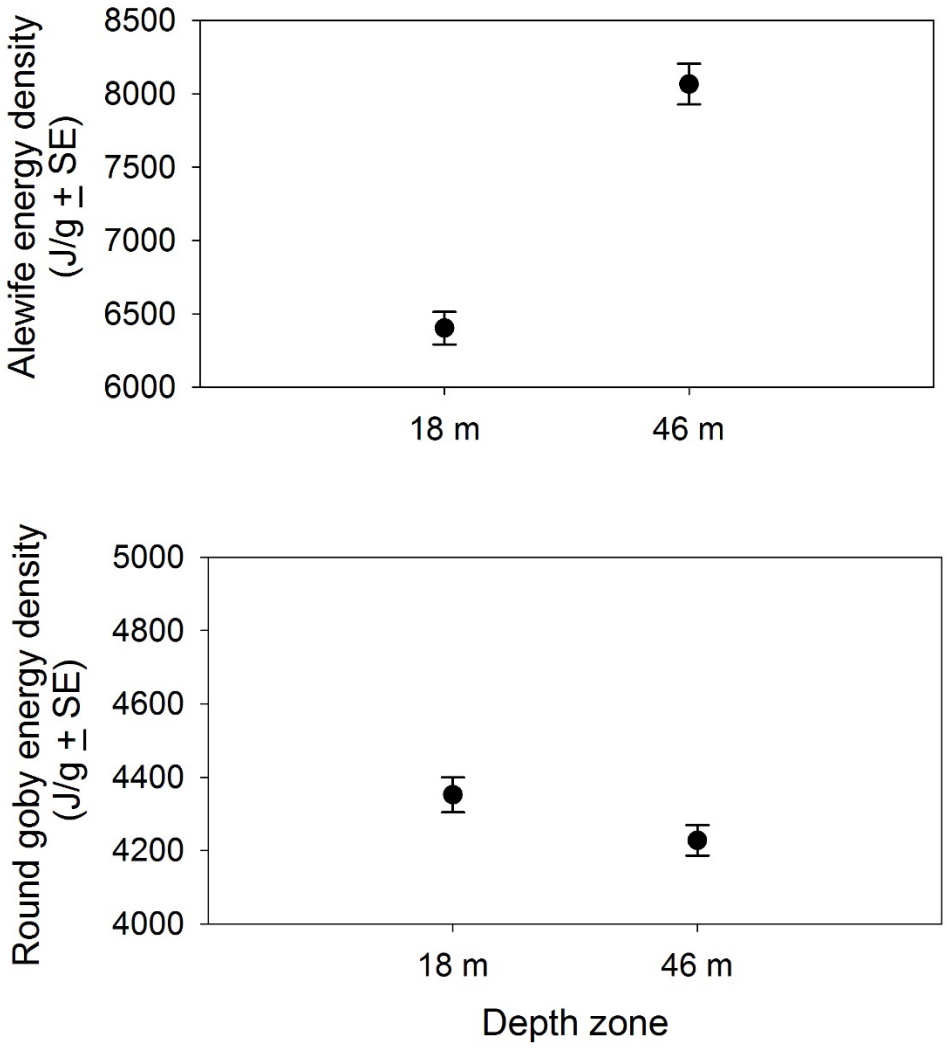

Figure 6. Mean energetic condition for commonly sized large alewife (135-165 mm, top panel) and commonly sized small round goby (45 – 95 mm, bottom panel) at two different depth zones during the fall of 2015 near Waukegan. Energetic condition was higher at 46 m than at 18 m for alewife, but there was no difference in energetic condition between depths for round goby.

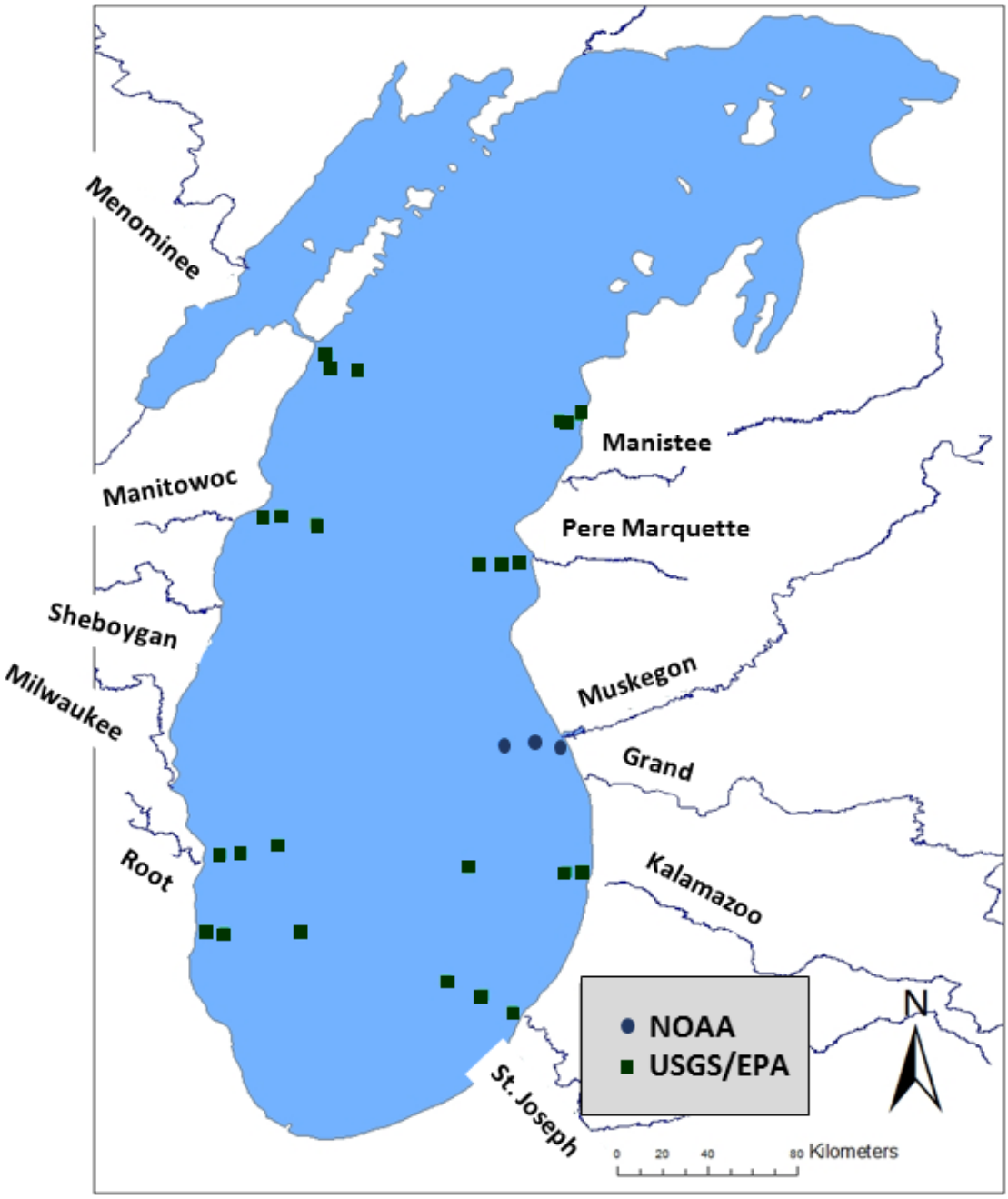

Appendix 1. Location of sampling sites for 2015 CSMI. At each nearshore to offshore transect, the food web was sampled at three depths: 18, 46, and 91-110 m.

Report: Temporal and Spatial Coupling of Nutrients and Food Web—Microbes to Fish

Authors:

Henry Vanderploeg, NOAA Great Lakes Environmental Research Laboratory
Edward Rutherford, NOAA Great Lakes Environmental Research Laboratory
Steven Pothoven, NOAA Great Lakes Environmental Research Laboratory
Joann Cavaletto, NOAA Great Lakes Environmental Research Laboratory
James Liebig, NOAA Great Lakes Environmental Research Laboratory
Doran Mason, NOAA Great Lakes Environmental Research Laboratory
Hunter Carrick, Central Michigan University
Vincent Denef, University of Michigan
Paul Glyshaw, Cooperative Institute for Great Lakes Research
David Wells, Cooperative Institute for Great Lakes Research

Contact:

Henry Vanderploeg

Email: henry.vanderploeg@noaa.gov

Phone: 734-741-2284 / 2292

Address:

NOAA GLERL

4840 S. State Rd.

Ann Arbor MI 48108

Brief Project Description

In support of EPA/USGS efforts to sample food web components at multiple transects around the periphery of Lake Michigan during two or three seasons, we conducted intensive temporal (including diel sampling) and fine-scale spatial sampling across seasons (April-October) in the Muskegon/Grand River Region. Moreover, we measured the microbial food web (MFW) as part of our study to describe the often ignored component of the food web. Our approach was similar to Year of Lake Michigan 2010 and Lake Huron 2012, where we examined, in detail, the seasonal changes in diel spatial coupling (April, July, and September) of the food web using a variety of advanced tools including plankton survey system (PSS) with Laser Optical Plankton Counter (LOPC) and fisheries acoustics. Further, a variety of collection methods to quantify larval fish and Mysis abundance, size structure, spatial distribution, and critical rates (growth, mortality), were utilized. Also, we measured depth profiles of UV radiation to examine the relationship between UV radiation penetration vs. plankton and larval fish vertical distribution.

There is little previous knowledge of spatial coupling during the time of early stratification, which is critical for deep chlorophyll layer formation as well as zooplankton and larval fish production. Therefore, we examined spatial coupling of the food web monthly April – October to understand nutrient flow and trophic dynamics from inshore to offshore. Our transect location was particularly important since it is near the Muskegon and Grand Rivers, the largest combined source of nutrient loading going directly into Lake Michigan (Figure 1).

Sampling (Day and Night)

Table 1 shows the sampling scheme for major variables collected in the Muskegon region. In summary, the following major sampling activities took place:

- Nearshore-offshore PSS/acoustics transects were completed and processed (April to October).
- Full column net zooplankton tows (64-µm and 153-µm mesh), at the end of all transects (15-m and 110-m depth stations), were completed and processed.
- Depth-stratified vertical opening-closing zooplankton net tows (to determine species-specific vertical depth distributions) were made at M45 or M110 or at both stations during both day and night in all months with the exception of August and October due to severe weather conditions. PSS transects that gave fine-scale vertical distribution of chlorophyll, photosynthetically active radiation (PAR), temperature and occasional measures of UV radiation complimented the net tow data.
- Abundance of pico- to microplankton were measured, and primary production and microbial grazing was estimated for most months (Table 1).
- Nutrients including total P, dissolved P, and particulate C, N, and P were measured in all months.

Findings

Mesozooplankton

- The PSS tows coupled with back-up information from net tows showed that chlorophyll levels and zooplankton were highest in the shallow epilimnion during both day and night during early stratification (Figure 2).
- We found distinct differences in nearshore and offshore zooplankton, with smaller epilimnetic species found nearshore. (Figure 3, Figure 4, Figure 5).
- We were able to specify both fine-scale horizontal and vertical distribution of some important species by combining net tow observations with LOPC size category data. (Figure 6). We are continuing to make progress in developing a method to define fine-scale spatial structure of zooplankton using the coarse vertical distribution from nets and fine-scale spatial data from the LOPC.
- Net tows (Figs. 3 and 4) and LOPC data revealed that during June *Dreissena* veligers were the dominant zooplankton (both number and biomass) from nearshore out to the 80-m depth contour, i.e., out to 14 km offshore. (Figure 7)
- Most of the summer-fall zooplankton biomass was found at night in the metalimnion and not, as expected, in the epilimnion. The exception was during October, when *Daphnia galeata* dominated the epilimnion in the offshore plankton.

Larval fish

- In the nearshore zone, density of alewife and yellow perch larvae in 2015 (Figure 8) was higher than in previous years (2010-11, 2013-14) but alewife growth and condition were extremely low, nearly half the rates as seen in 2001-2002 before quagga mussels irrupted (Figure 9). Diet analysis indicated alewife and yellow perch larvae consumed high proportions of mussel veligers which were extremely abundant in the epilimnion in June and July (Figure 10). Regression analysis of factors influencing larval alewife daily growth rates from 2001-2002, 2010-2011, 2013-2015 indicated cyclopoid copepod biomass, and not mean June-July temperature, positively affected alewife growth rate (Figure 11). These results suggest that the decline in cyclopoid copepod biomass, caused by reduced productivity in the nearshore zone and increased abundance of dreissena veligers, may have a negative effect on larvae growth. Given that larval consumption of veligers is increasingly common in studies of larval diets in the Great Lakes (Marrin Jarrin et al. 2014, Withers et al. 2015), and if larval growth rate is correlated with probability of their survival to the juvenile stage, then abundance of veligers in larvae diets may indicate how *Dreissena* mussels could disrupt the lower food web and effect fish recruitment. Currently, we are estimating alewife larvae survival for 2015 and comparing it to rates in 2010 and 2001-2002 (pre-quagga irruption) to see if there is a relationship between larval growth and survival, and size of juvenile alewives.

- In the offshore, bloater larvae density and growth rate in 2015 remained low compared to prior years (Figure 9). Bloater larvae consumed mainly small copepods and copepod eggs.
- We also are examining effects of an upwelling event in July 2015 on displacement of alewife larvae from nearshore to offshore (Figure 12). Preliminary results indicate the upwelling has had no effect on alewife survival or growth.
- Finally, we are comparing species composition and vertical distributions of fish larvae in 2015 with compositions and distributions of zooplankton and fish larvae measured during 1983 off Grand Haven by Richard Nash and Audrey Geffen. This comparison indicates a shift in vertical distribution of larvae from the top meter of the water column in 1983 to the metalimnion in 2015, a likely response to quagga mussel filtration increasing light levels (Figure 13), and foraging efficiency by the visually predaceous cladoceran *Bythotrephes*, that have resulted in deeper vertical distributions of zooplankton (Figure 14).

Mysis

- Mysis were collected at 45 and 110 m sites April-November; offshore abundance was higher than at the 45m transitional site (Figure 15). Abundance of Mysis in 2015 was relatively high compared to previous 3 years.

Nutrients

- C:N:P ratios of seston suggest only mild to moderate P limitation at most stations and depths along the transect. Some even show no P-limitation.
- Phosphorous was highest nearshore in the spring, reaching a maximum of 10.27 μgL^{-1} in late June, and then decreased to levels comparable to offshore beginning in July. Offshore phosphorous was lowest in late April, and increased to a maximum of 6.03 μgL^{-1} in late September. (Figure 16)

Fishery acoustics

- Preliminary examination of acoustic target strength (mostly small planktivorous fishes) showed not much overlap between fish and zooplankton until late summer and fall (Figure 17).

UV radiation and PAR

- UV depth profiles showed that UV-B (305 nm) radiation could have a potentially negative effect on some zooplankton and larval fish in the upper 5 m of the water column. There is no useful information as to effect of UV-B radiation on Great Lake zooplankton or fish larvae. Longer wavelengths of UV radiation and PAR can penetrate to greater depths than UV-B, and PAR levels remain relatively high to our near bottom sampling depths (Figure 18). PAR profiles indicate that *Bythotrephes* could visually detect prey down to depths of 40 m or greater (10 $\mu mol\ m^{-2}s^{-1}$) during midday. Most planktivorous fishes should be able to visually

detect prey throughout the water column during midday as PAR levels remain above threshold limits of 0.2 µmol $m^{-2}s^{-1}$ to depths greater than 85 m.

Microbial food web (Carrick)

- Lake Michigan has experienced recent changes in the phytoplankton assemblage coinciding with reductions in watershed nutrient loadings and the introduction of invasive species. As such, we evaluated the population dynamics of key plankton components in Lake Michigan along a series of near to offshore transects in southern Lake Michigan (2013-16). Chlorophyll analysis revealed that the picoplankton fraction (Ppico, < 2 µm) contributed an average of >50% to total phytoplankton biomass. Particulate P made up nearly all of the TP in the water column; this pool was composed of poly-P in the pico-sized particles (>80% of total) and bioassay experiments revealed that phytoplankton growth was limited primarily by P. The abundance of Ppico (5,200 to >70,000 cells/mL) was considerable and the assemblage was dominated by cyanobacteria taxa and pico-eukaryotes. The occurrence of diatoms (mainly *Cyclotella* and *Discotella* taxa) was limited to the nearshore region during the spring and early stratification periods. We estimated growth and grazing losses attributable to small grazers (microzooplankton, protists; Fig. 19) and large grazers (mesozooplankton, crustaceans) from enclosure experiments. Ppico had lower growth (0.19 +/- 0.27) relative to grazing losses by microzooplankton (-0.33 +/- 0.37), indicating tight coupling with small grazers. These results suggest that carbon (and phosphorus) flow from Ppico to metazoa may dominate the current, trophic dynamics in the lake.

Microbial food web (omics, Denef)

- **Bacterial abundance.** Though bacteria play a fundamental role in freshwater biogeochemical cycling and community dynamics, they are often left out of Great Lakes studies. We monitored total bacterial numbers and the fraction of cells in the so-called High-nucleic acid content fraction (HNA), as defined by flow cytometric analysis. The HNA fraction is thought to be representative of more active bacterial cells. Cell numbers declined from the estuary to offshore locations, increased during the year in the estuary, while being more variable over time in Lake Michigan itself, with a marked minimum in July (Figure 20A). The fraction of all cells that were deduced to be more active (HNA fraction) showed an opposite trend to total cell abundance in the estuary, while it more closely tracked cell abundance in Lake Michigan (Figure. 20B).

- **Bacterial community composition.** Typically, bacterial community composition is censused via high throughput sequencing of the 16S rRNA gene, providing insights into the diversity of all potentially active and dormant bacteria at the DNA level. However, the influence of bacteria on ecosystem function is most likely predominated by active organisms. One proxy for activity is the use of RNA to assess community composition rather than DNA. During the CSMI 2015 work, we high throughput sequenced the 16S rRNA gene using simultaneously

extracted DNA and RNA to evaluate the DNA versus the RNA community in samples collected monthly in 2015 from April until October along a eutrophic (Muskegon Lake) to oligotrophic (offshore regions) transect in Lake Michigan. In addition, we monitored DNA-level community composition of the sediment at each station. Richness and evenness of both the water and sediment bacterial communities consistently decreased from the estuary to the offshore station. Across seasons, diversity tended to increase from spring to fall. The sediment communities significantly differed from water column communities (Figure 21A), and strongly clustered by station with limited variability by month, except at the 45 m depth station (Figure 21B). Location along the transect explained the largest fraction of the observed variance is water column bacterial species presence/absence (22%), whereas season and whether DNA and RNA samples were used affected communities in similar ways (13 and 11% variance explained, respectively). When relative abundance of each species was taken into consideration, DNA vs RNA explained 30% of the variance, while station (14%) and season (9%) explained lower fractions of the observed variance in community composition (Figure 21A, C, D). Several microbial phyla differed between DNA and RNA samples and included five of the most abundant groups. *Verrucomicrobia*, *Alpha-*, and *Beta-proteobacteria* were overrepresented in the RNA pool while *Actinobacteria* and *Bacteriodetes* were overrepresented in in the DNA pool. These taxonomic differences between in the potentially active and total bacterial communities indicate that there may be multiple layers to the microbial communities that underpin lake community and ecosystem processes.

- **Dreissenid mussel feeding impacts on bacteria.** In a companion study [not GLRI funded] we showed that *Dreissena* grazed more heavily on the species that appear to be more metabolically active based on the RNA and DNA-based analyses during the CSMI work, which has potential implications for nutrient cycling {Denef et al., 2017; Props et al, 2018}.
- **References.**

Props, R., M.L. Schmidt, J. Heyse, H.A. Vanderploeg, N. Boon, and V.J. Denef. (2018) Flow cytometric monitoring of bacterioplankton phenotypic diversity predicts high population-specific feeding rates by invasive dreissenid mussels. Environ Microbiol 20 (2), 521-534.

Denef V.J., Carrick H.J., Cavaletto J., Chiang E., Johengen T.H., Vanderploeg H.A. 2017. Lake bacterial assemblage composition is sensitive to biological disturbance caused by an invasive filter feeder. mSphere 2 (3), e00189-17.

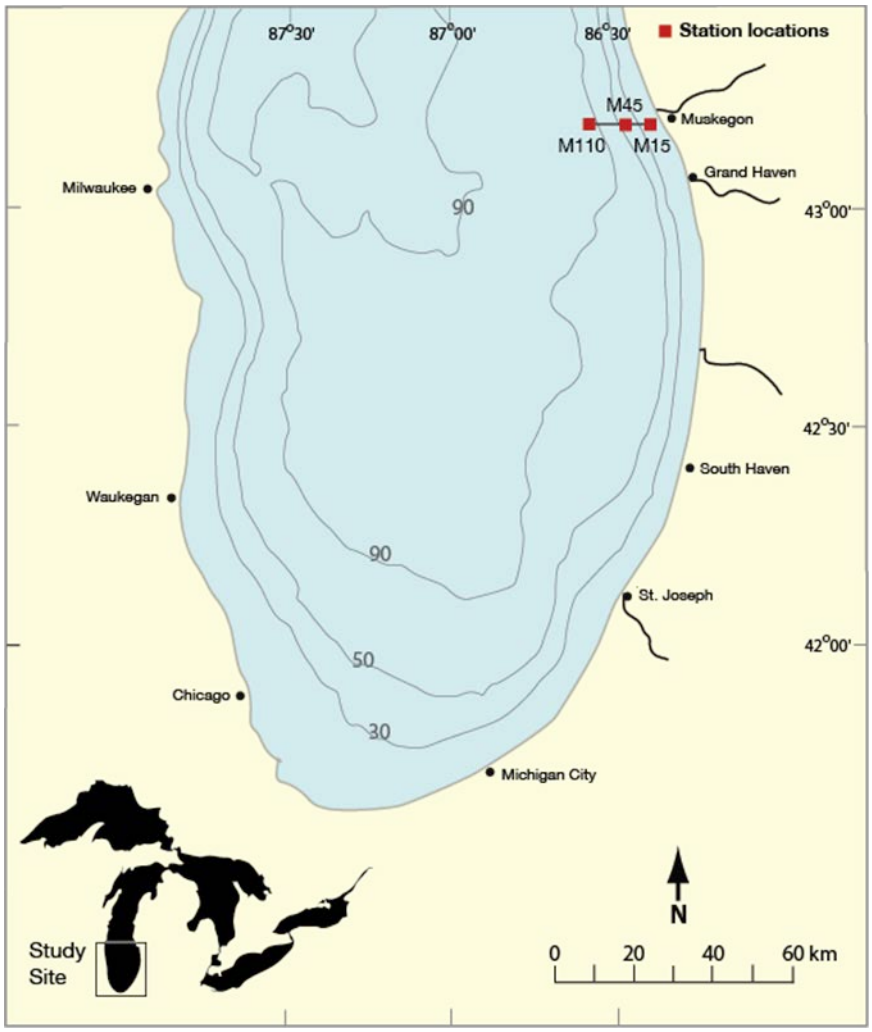

Figure 1: Sampling sites along the Muskegon transect in Lake Michigan.

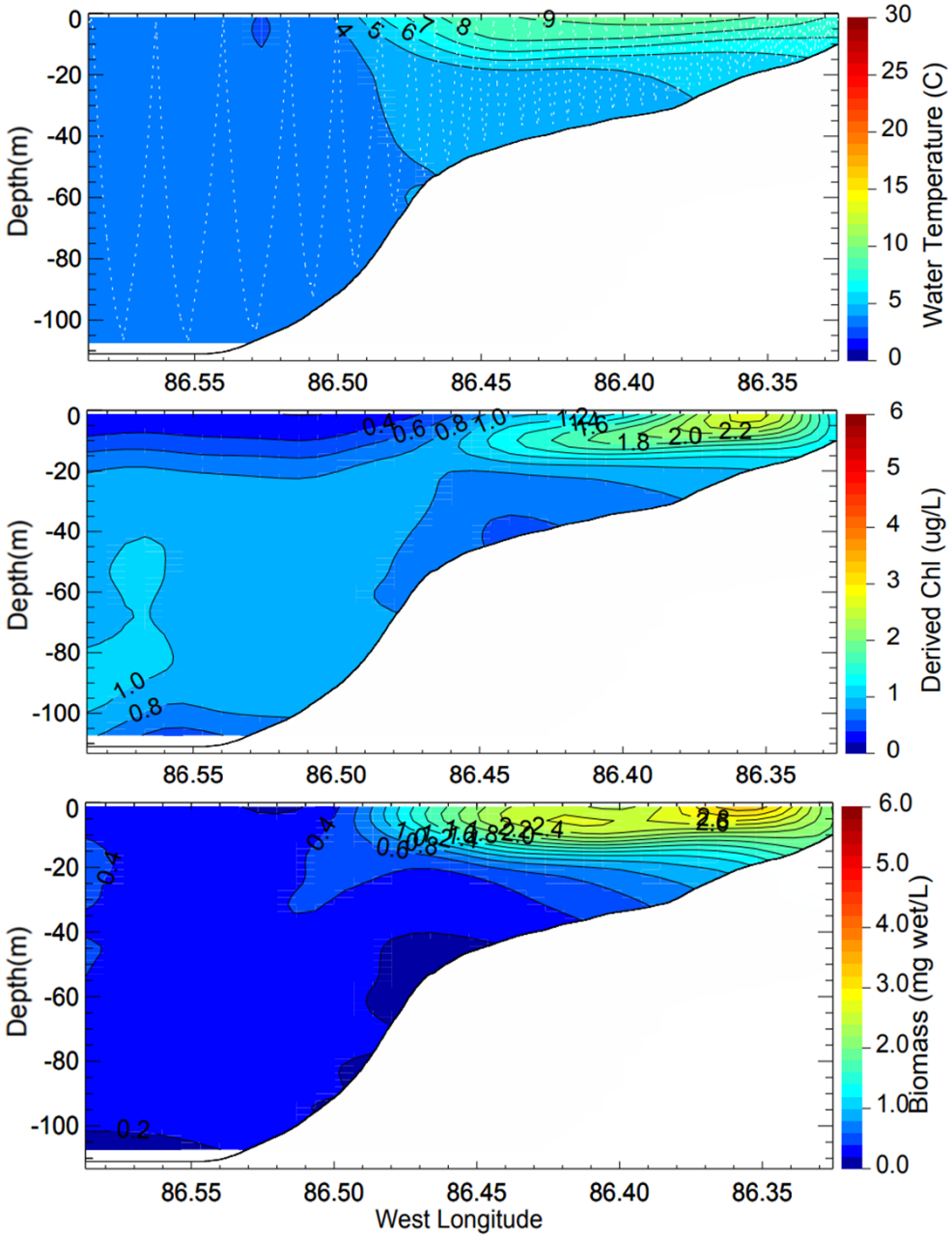

Figure 2: Daytime PSS long transect results from M10-M110 on May 20, 2015 show that chlorophyll and zooplankton were highest in the epilimnion and nearshore during early stratification.

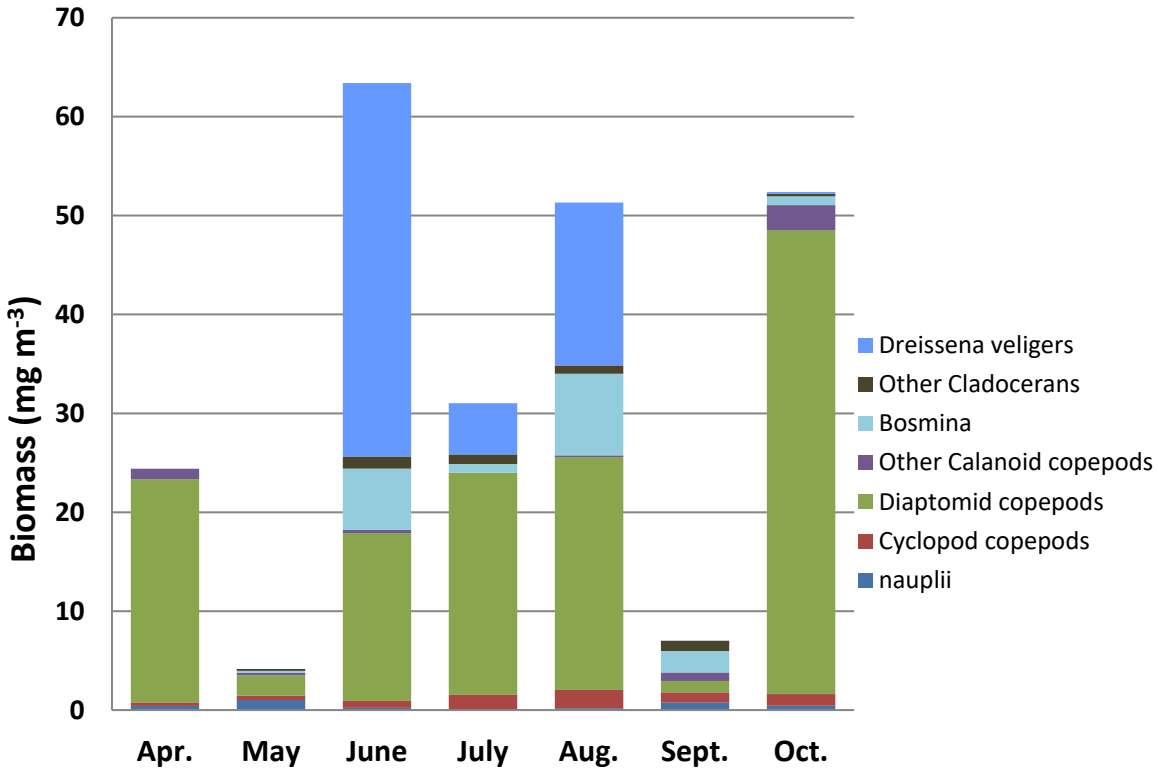

Figure 3: Seasonal zooplankton composition at M15.

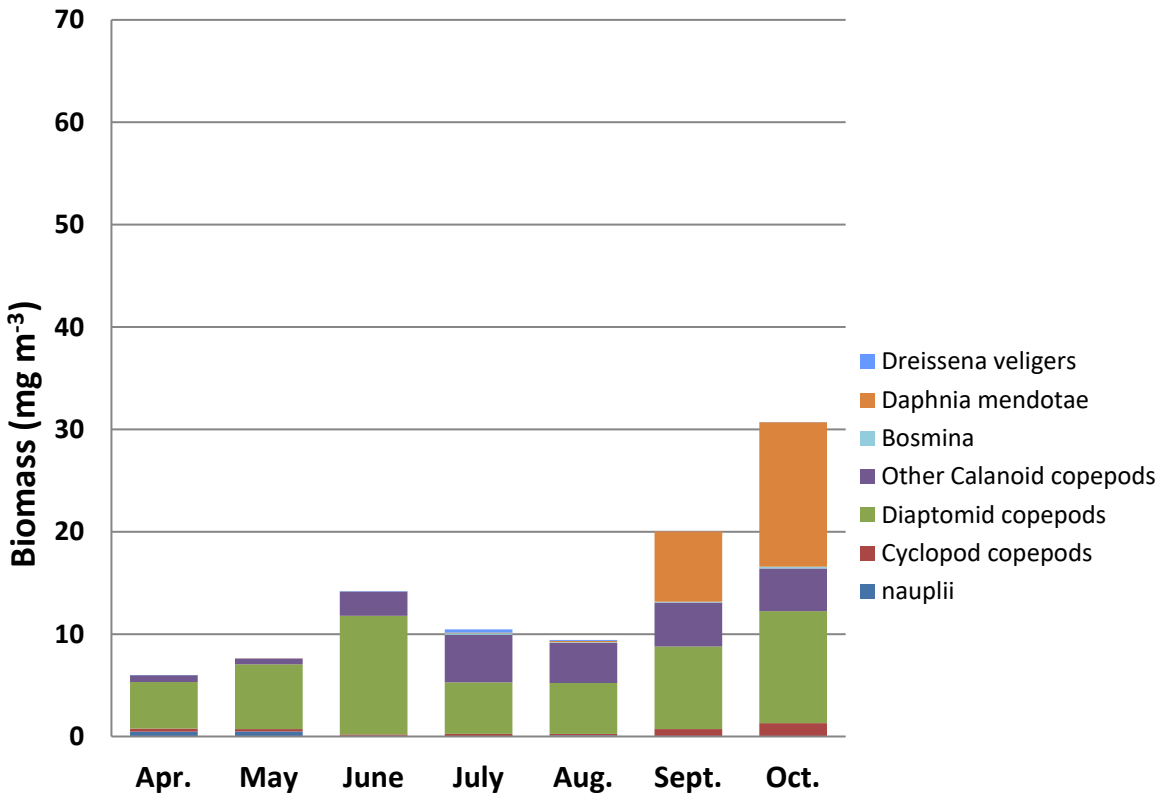

Figure 4: Seasonal zooplankton composition at M110.

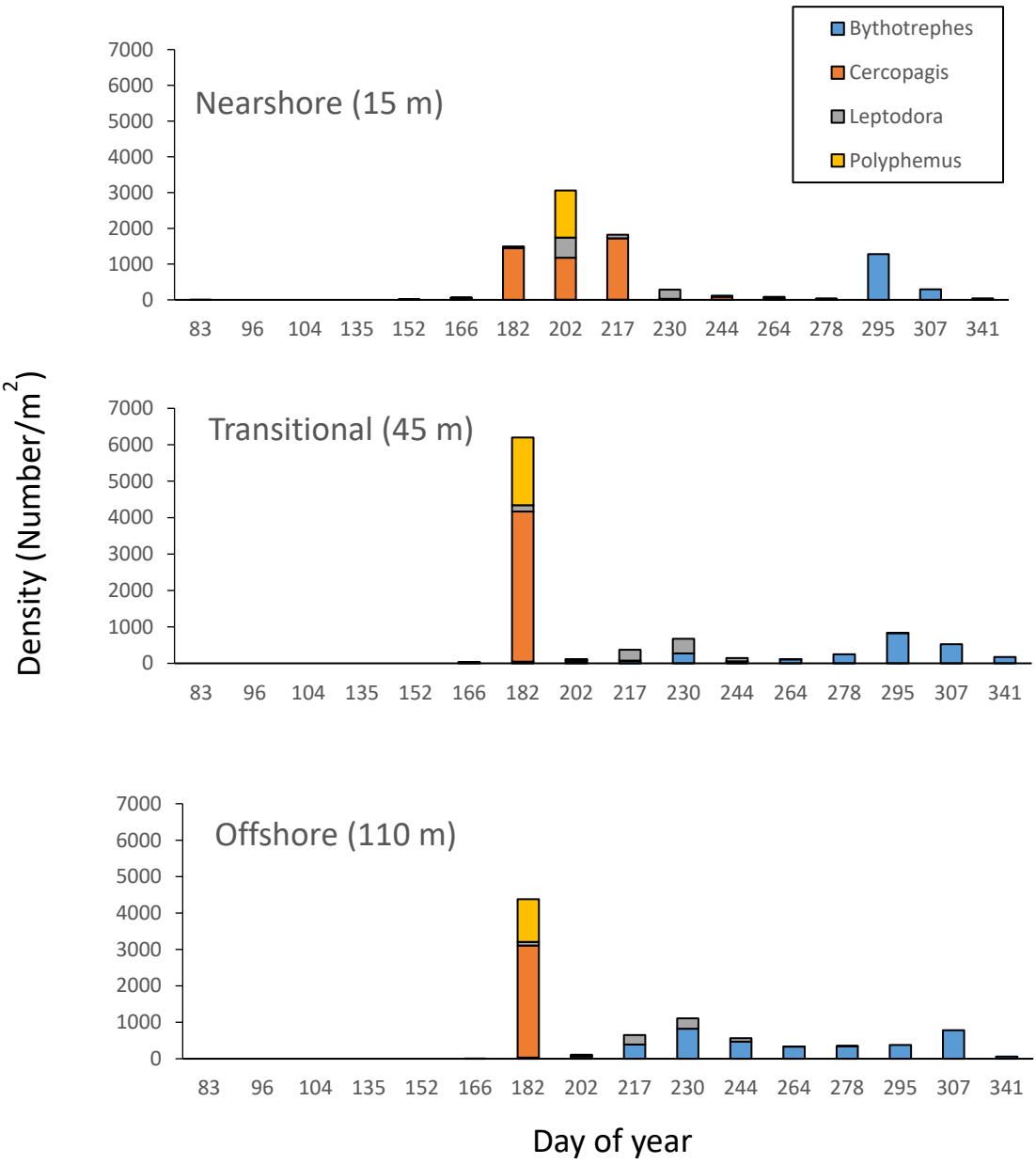

Figure 5: Density of predatory cladocerans at Muskegon transect 15, 45, and 110 m sites during 2015. High density of Polyphemus was very unusual.

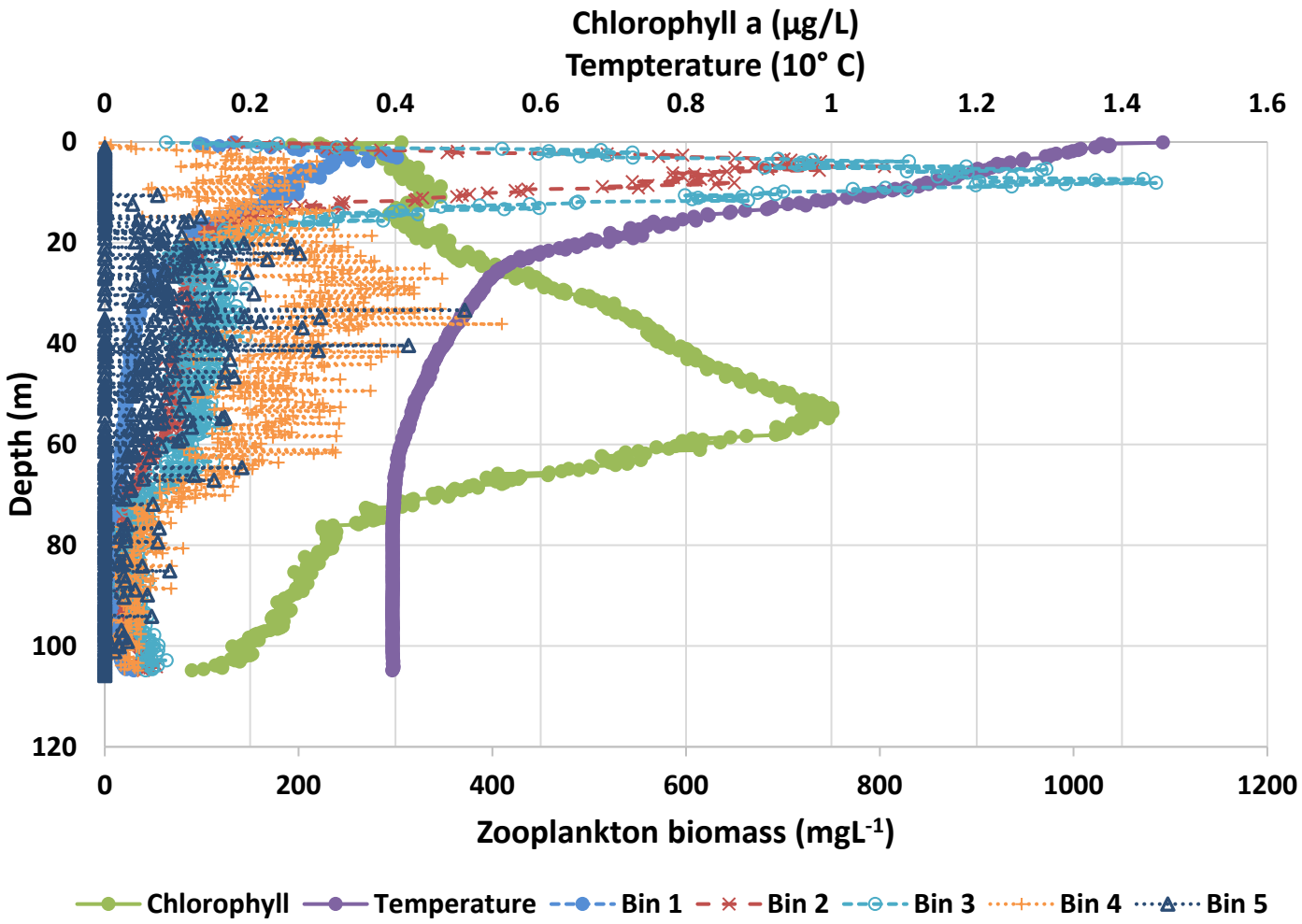

Figure 6: Fine scale spatial distribution of zooplankton from diel sampling at night on June 25, 2015 at M110. Bin 1=91-255 µm, Bin 2=256-495 µm, Bin 3=496-750 µm, Bin 4=751-1500 µm, Bin 5=1501-4005 µm. When the lake is stratified organisms found in each bin typically include: Bin 1= nauplii, *Bosmina*, *Dreissena* veligers; Bin2= copepodites, small copepods, *Bosmina*; Bin 3= *Daphnia*, large copepods; Bin 4= large *Daphnia*, *Cercopagis*, *Limnocalanus*; Bin 5= *Bythotrephes*, *Leptodora*, *Mysis*. We are currently working to assign species-specific biomass by combining this data with depth stratified zooplankton net tows.

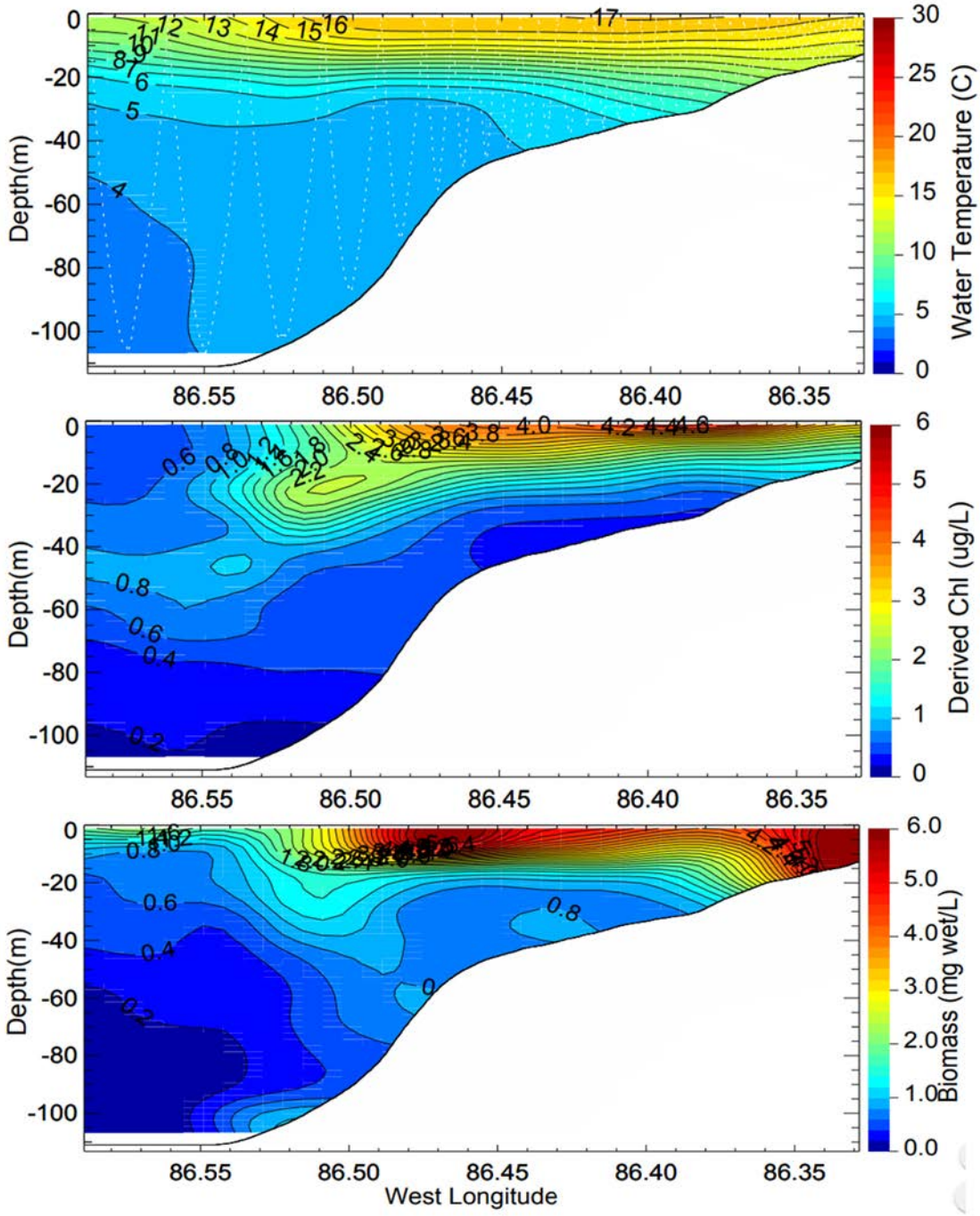

Figure 7: Daytime PSS long transect results from M10-M110 on June 23, 2015 along with corresponding net tows show that *Dreissena* veligers were the dominant zooplankton (both number and biomass) from nearshore out to the 80-m depth contour, i.e., out to 14 km offshore.

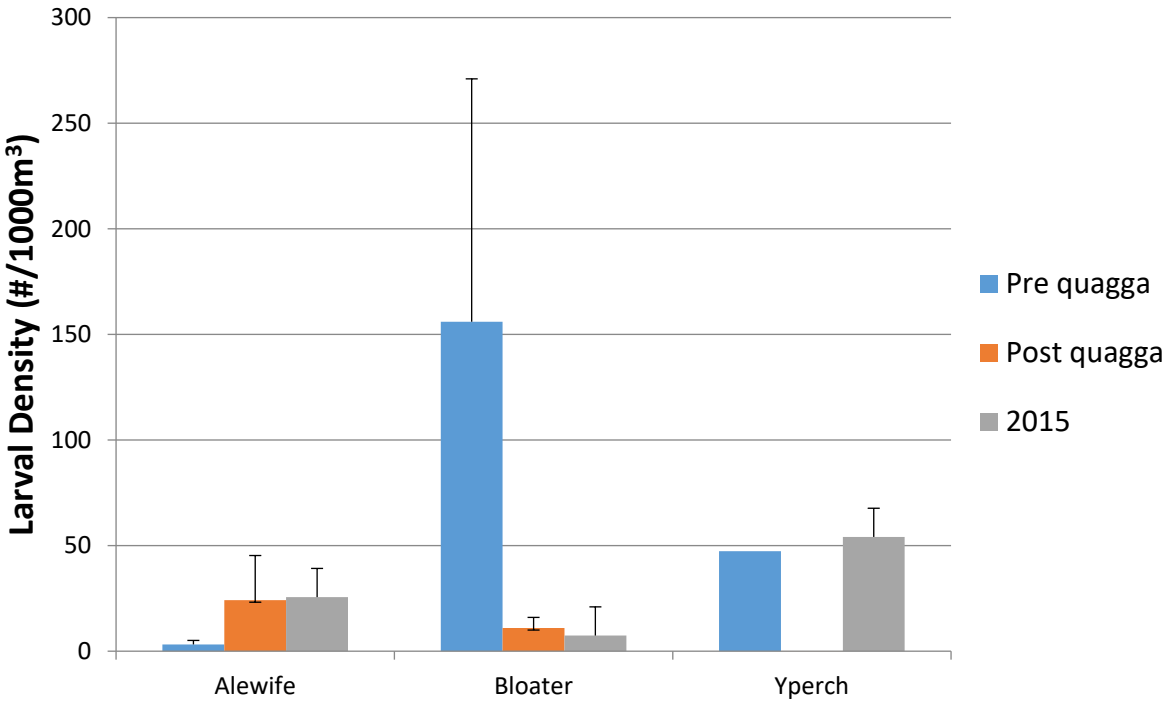

Figure 8: Larval densities pre (2001-2002) and post (2010-2014) quagga mussel invasion for alewife, yellow perch and bloater.

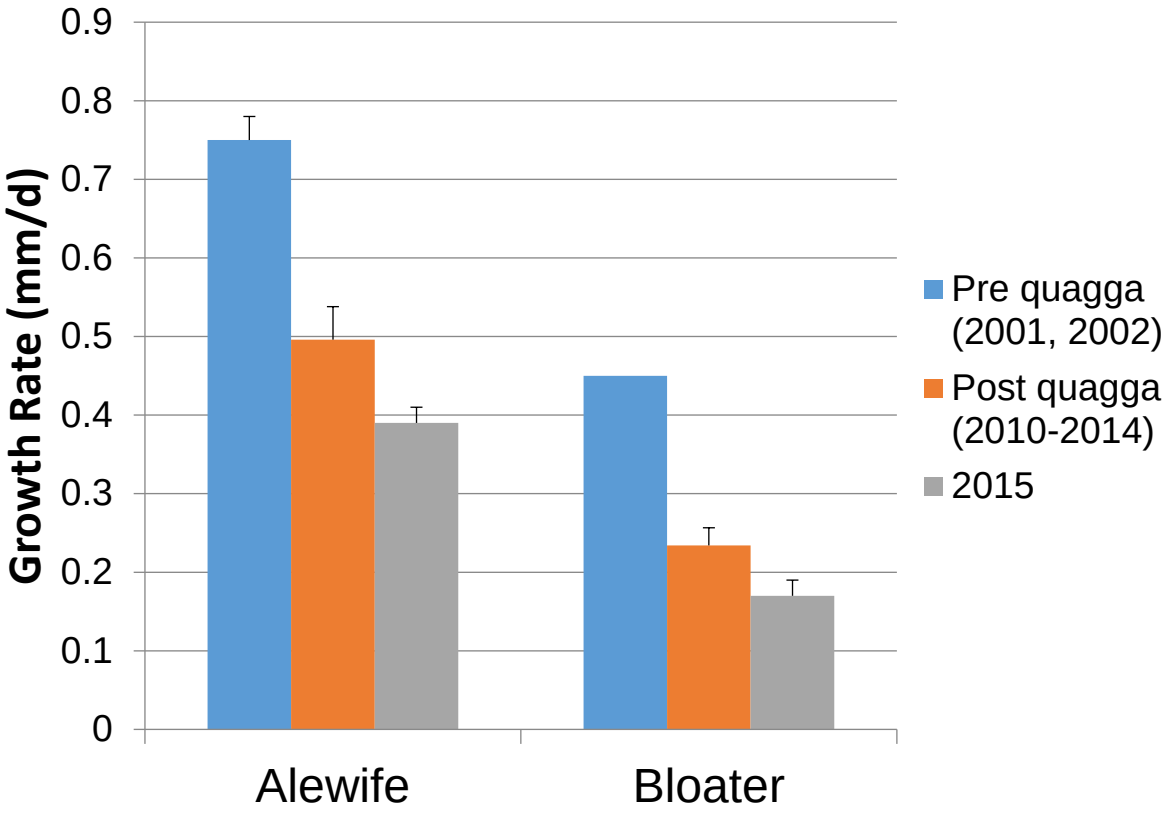

Figure 9: Larval alewife and bloater growth rates along Muskegon transect pre and post quagga mussel invasion. Yellow perch data not available.

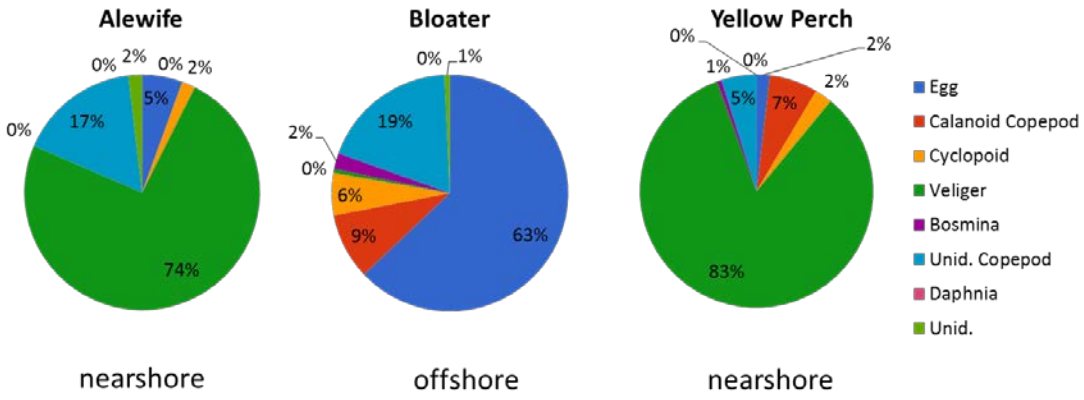

Figure 10: Nearshore/offshore diet contents of alewife, bloater and yellow perch.

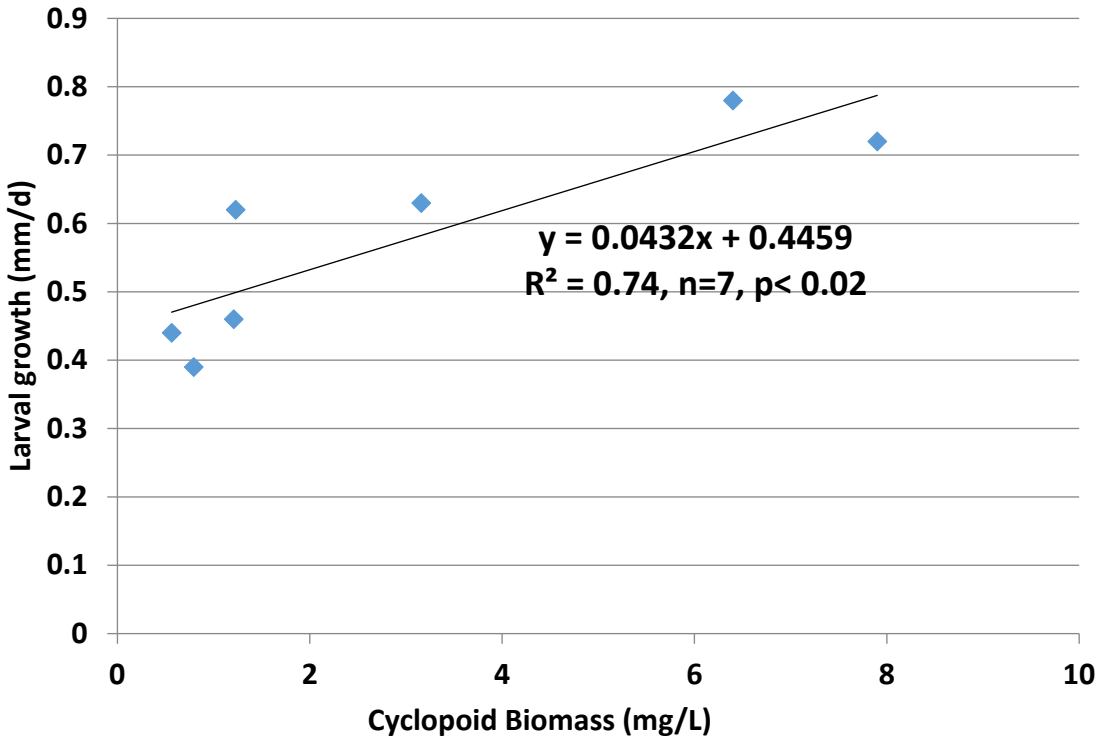

Figure 11: Regression analysis of factors influencing larval alewife daily growth rates from 2001-2002, 2010-2011, 2013-2015 indicated cyclopoid copepod biomass, and not mean June-July temperature, positively affected alewife growth rate.

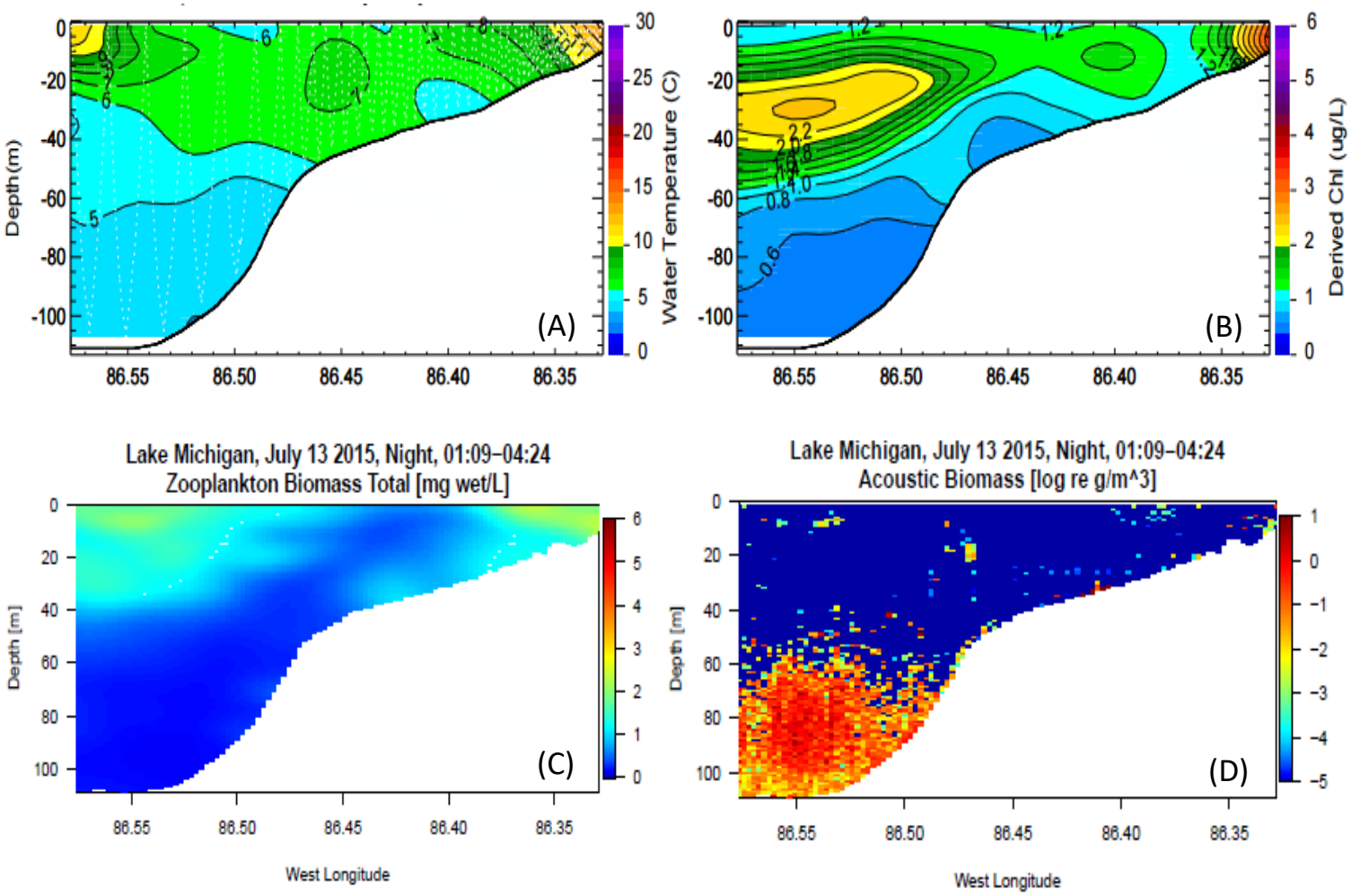

Figure 12: PSS plots of temperature (A) and chlorophyll (B) show an upwelling event on July 13, 2015 that displaced nearshore larval alewife offshore. Also shown are potential prey (C) and predator (D) fields for larval fish during the upwelling event.

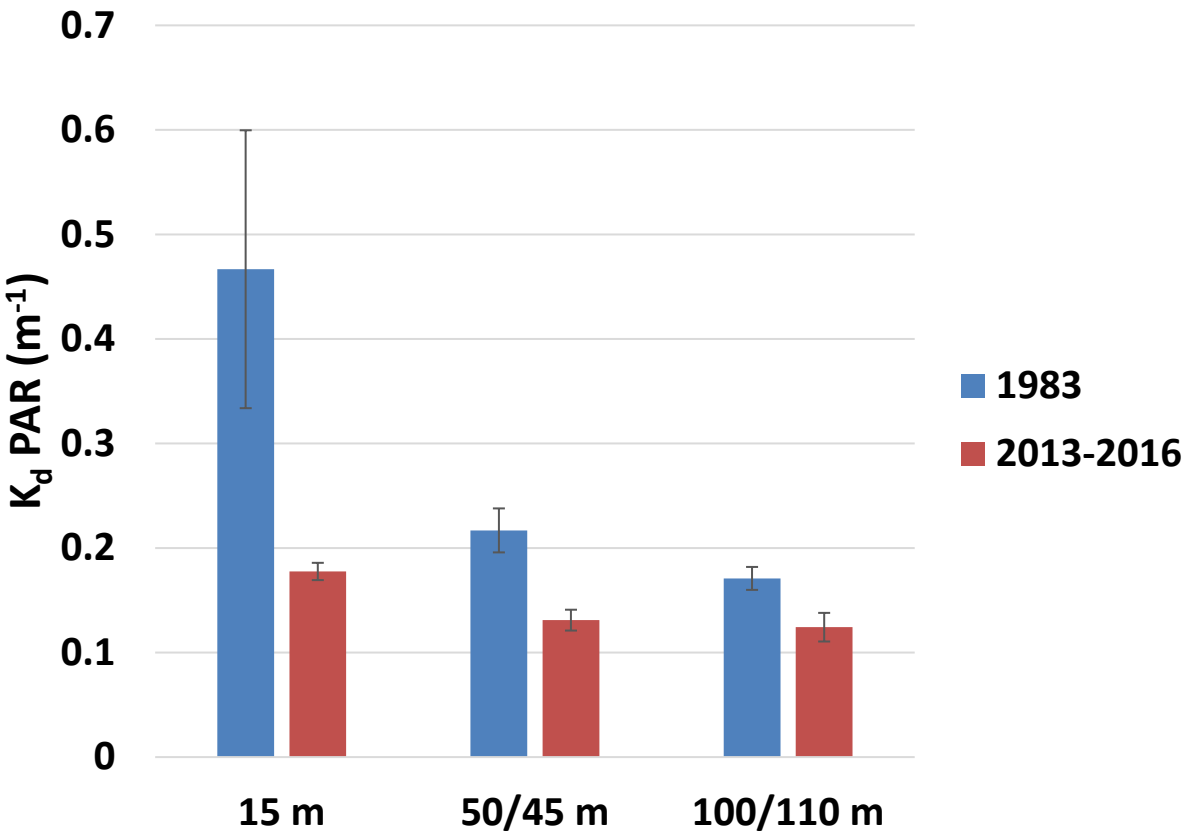

Figure 13: Attenuation coefficients of nearshore, mid-depth and offshore sites in Lake Michigan. 1983 data is from a transect off Grand Haven with depths of 15 m, 50 m, and 100 m; 2013-2016 data is from our 25 m, 45 m, and 90 m sites off Muskegon.

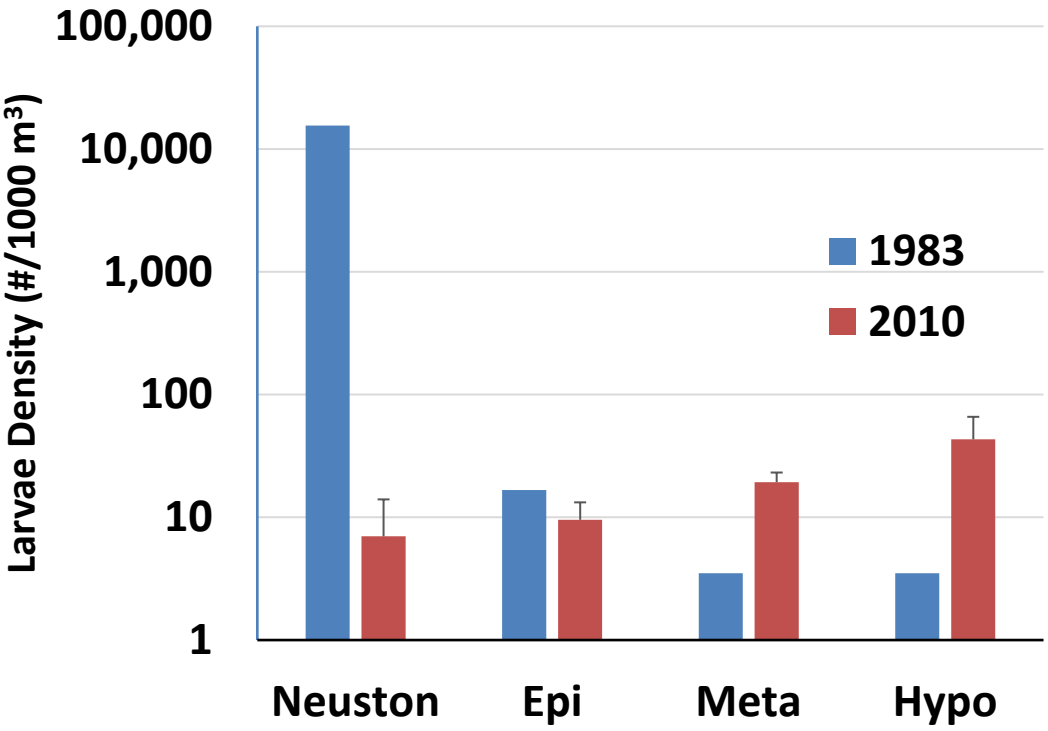

Figure 14: Comparing 1983 to 2010, a decline in offshore bloater larvae density, and change in vertical distribution.

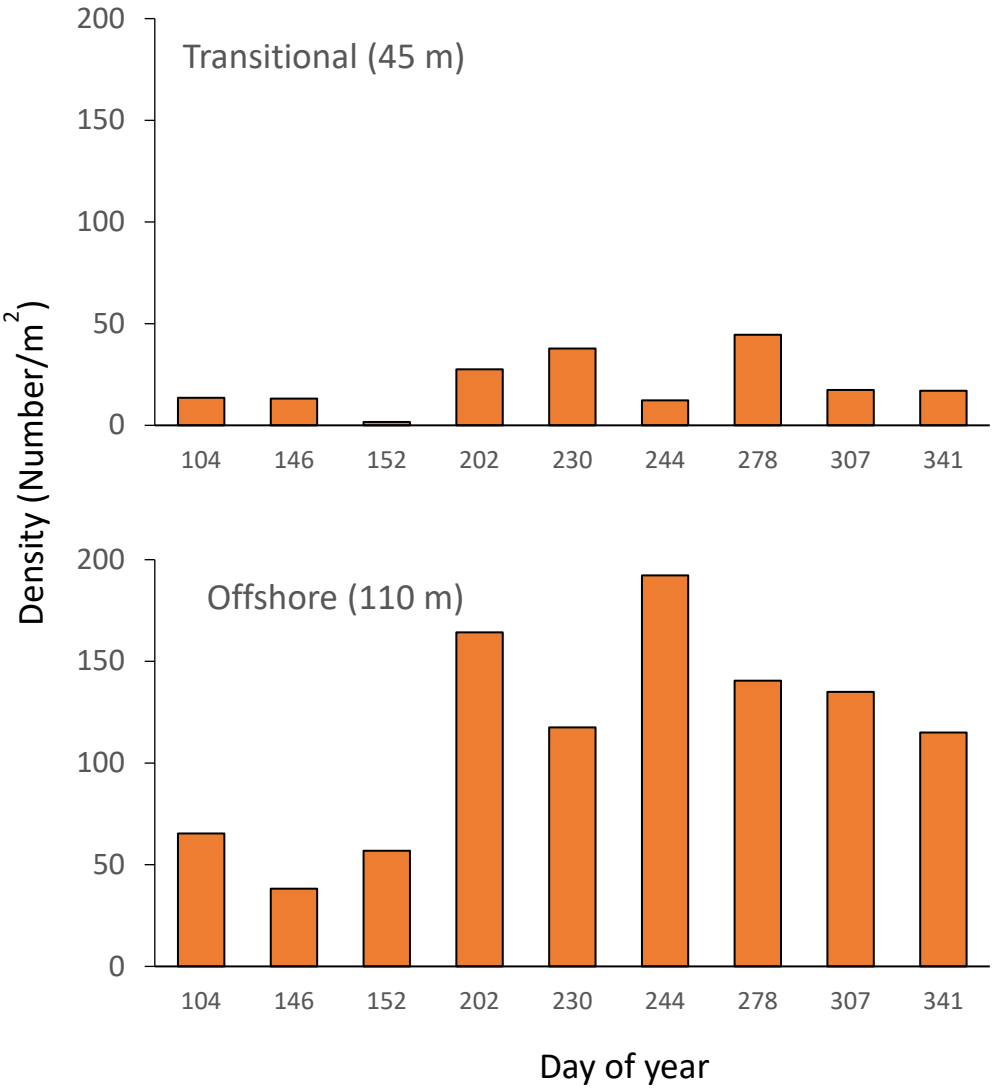

Figure 15: Density of *Mysis* at Muskegon transect 45 and 110 m sites during 2015.

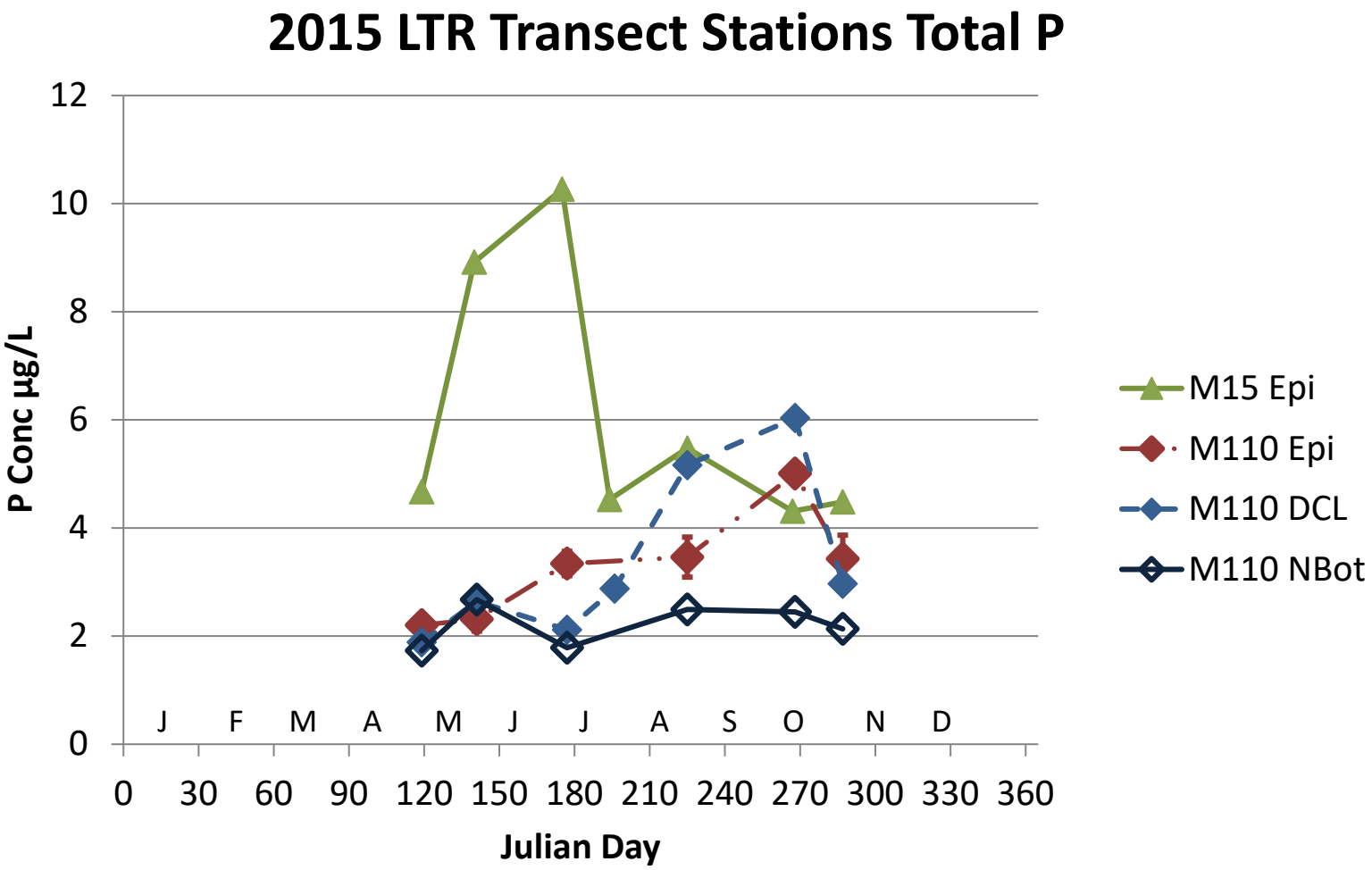

Figure 16: Total seasonal phosphorous concentration along the Muskegon transect in 2015.

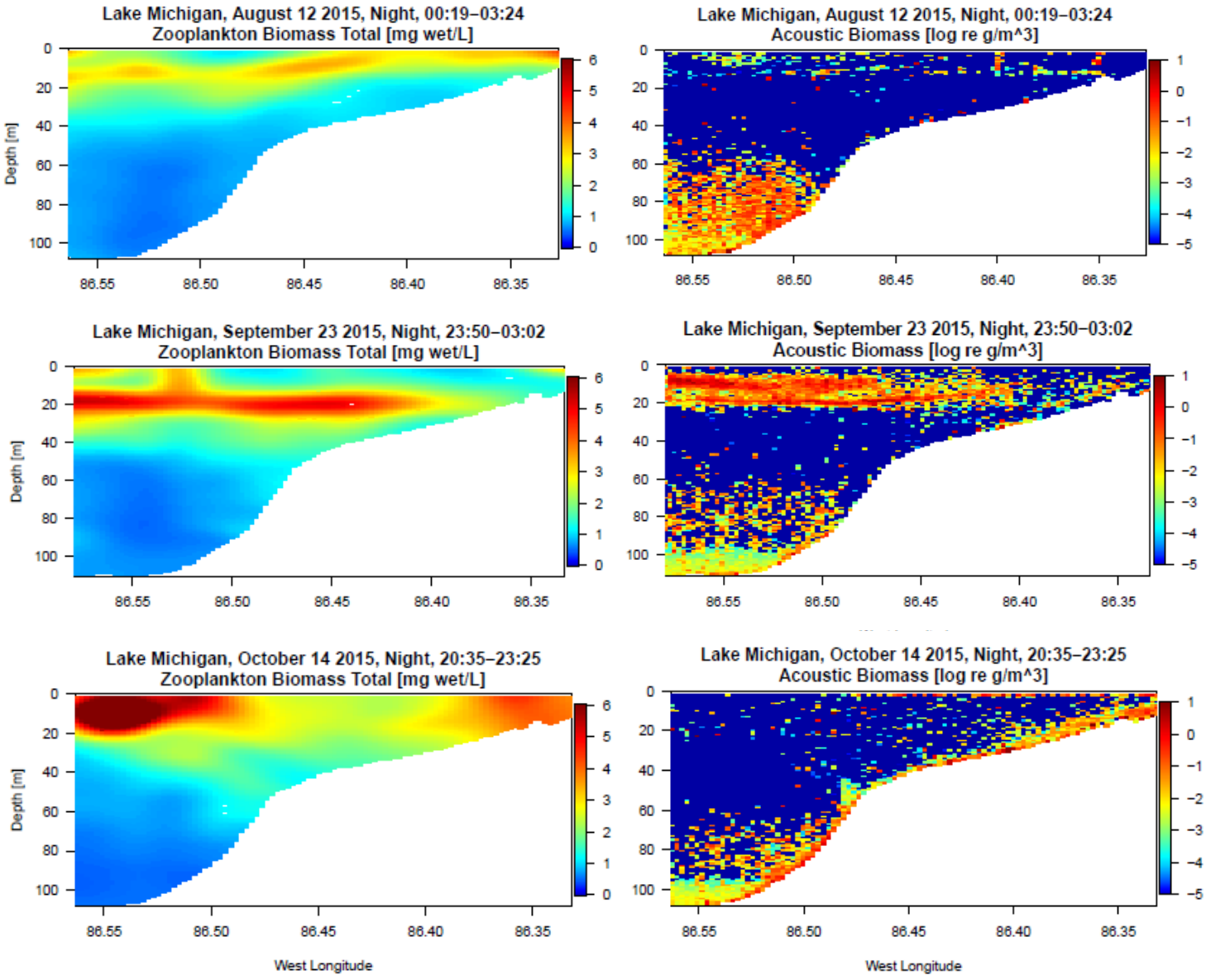

Figure 17: Acoustics transects show the seasonal succession of planktivore overlap with their zooplankton prey. Note, that the overlap with prey becomes greater as we progress through the seasons from mid-summer to late fall. The degree of predator and prey overlap appears to occur with the progression and strength of the thermocline where in July it's the weakest and in September it's the greatest. Note the lessening of the overlap in October as the thermocline begins to degrade.

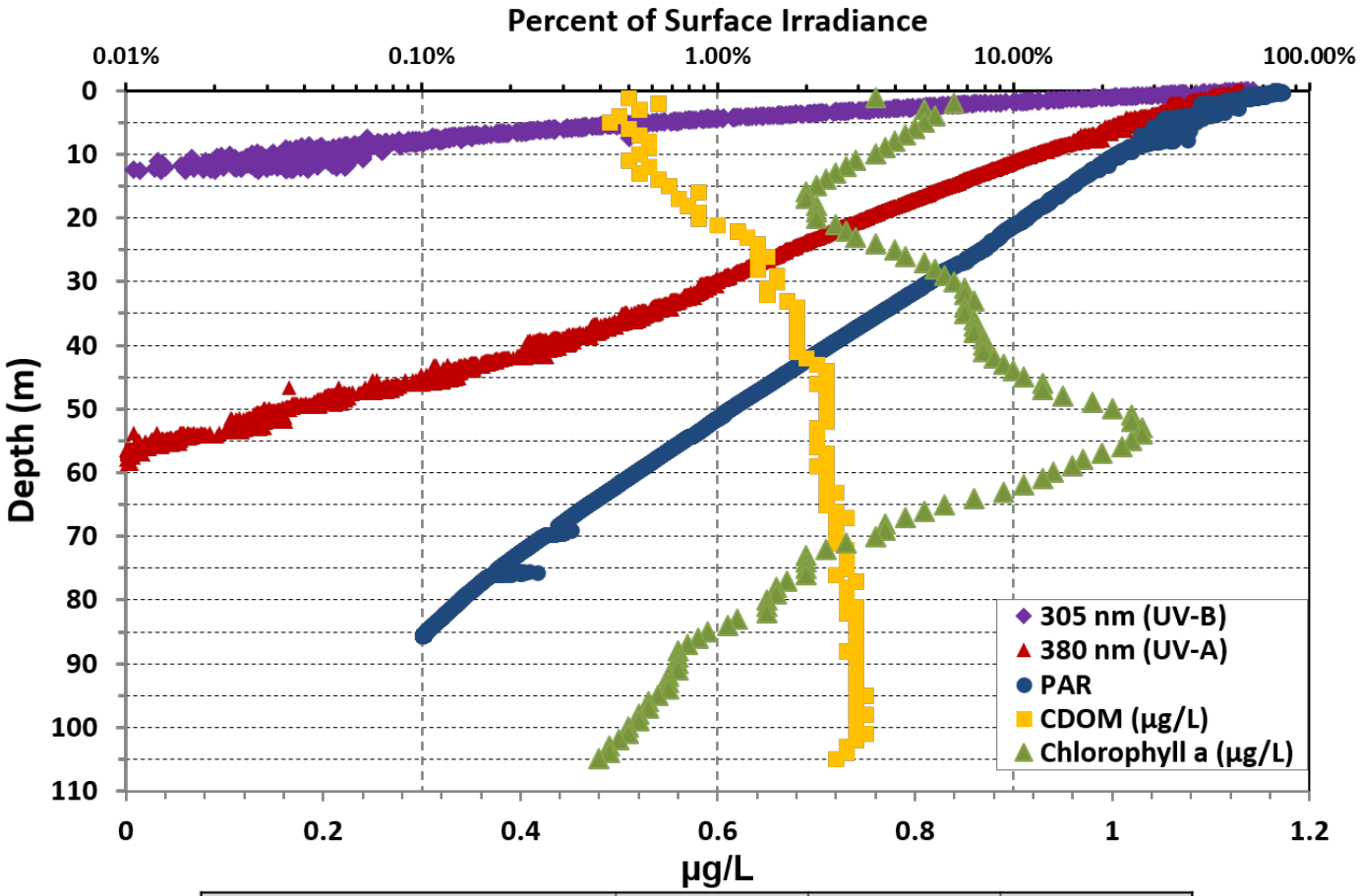

	305 nm	380 nm	PAR
1% Attenuation Depth (m)	4.5	30.8	52.2
K_d (/m)	0.94	0.13	0.08
Surface Irradiance	2.32 µW/(cm²nm)	43.86 µW/(cm²nm)	1100 µE/(m²sec)

Figure 18: UV Irradiance at M110 on July 25, 2015. UV-B (305 nm) radiation could have a potentially negative effect on some zooplankton and larval fish in the upper 5 m of the water column. UV-A (380 nm) and PAR levels penetrate much further and remain relatively high throughout the water column allowing visual predators such as *Bythotrephes* and planktivorous fishes to detect prey at greater depths.

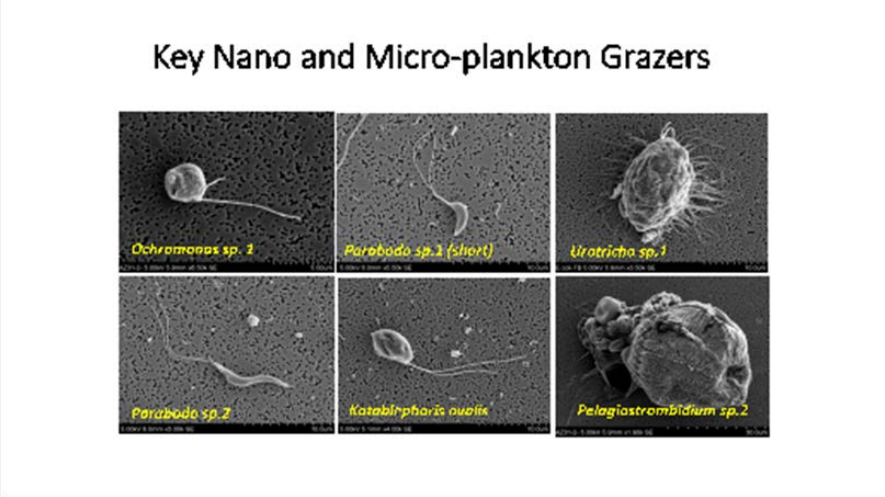

Figure 19: Dominant Nano and Micro-plankton grazers in Lake Michigan.

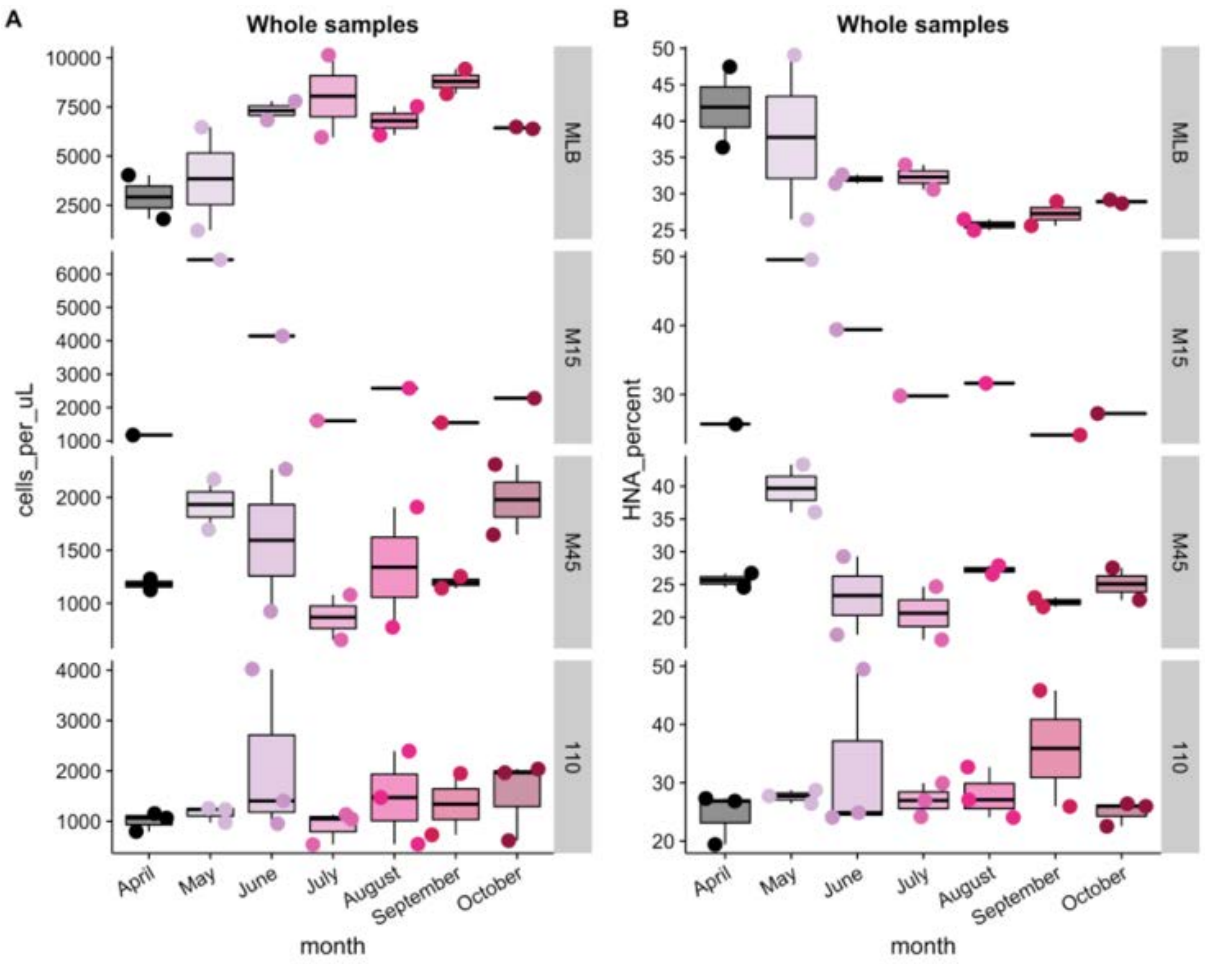

Figure 20: Flow cytometric analysis of the bacterial community across the transect. (A) total cell numbers per microliter of water sampled over time, and (B) the fraction of all cells that were in the High-nucleic acid content fraction (HNA). MLB = Muskegon Lake estuary, GVSU buoy location; M15, M45, M110 = Lake Michigan 15 m, 45 m, and 110 m depth stations.

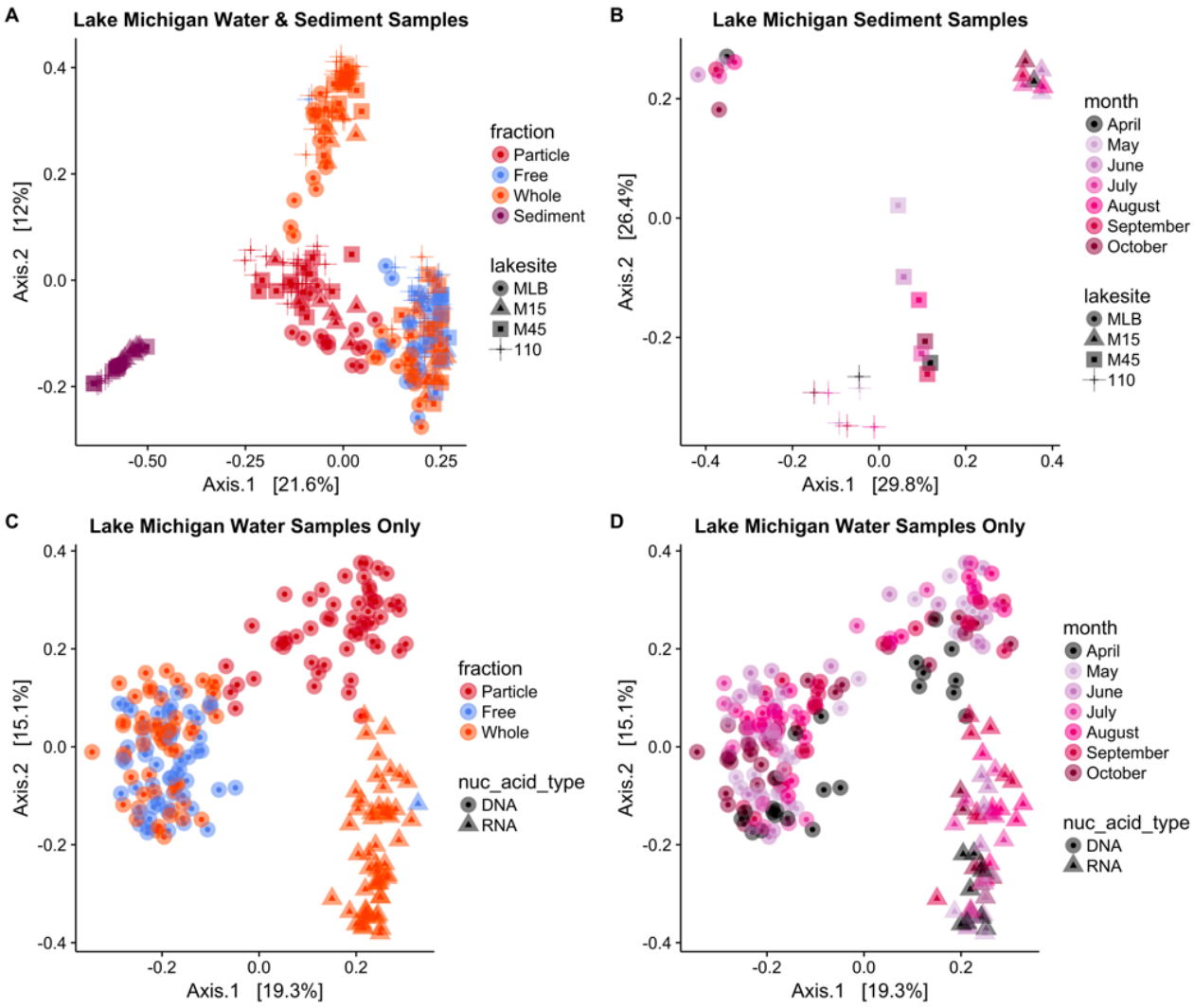

Figure 21: Abundance-weighted bacterial community composition dynamics. Principal coordinates ordination of (A) all columns samples, which were fractionated as 0.22-3 (free), 3-20 (particle), and 0.22-20 (whole) micrometer fractions during sampling, and detailed analyses for (B) sediment samples, and (C, D) water samples. The whole fraction was analyzed at the DNA and RNA level, while other fractions and the sediment was only analyzed at the DNA level.

Table 1: GLERL sampling activities during the 2015 Lake Michigan CSMI field season. X=M15, *=M45, += M110. PSS Long Transect sampling runs from sites M15 to M110 while passing through M45; Diel sampling in a short PSS run along the depth isobaths at either M45 or M110 during the day and night.

	April	May	June	July	August	September	October
Acoustics	x+*	x+*	x+*	x+*	x+*	x+	x+
Bottom Trawl	x+*	x+*	x+*	x+*	x+*		x+*
Chlorophyll	x+*	x+	x+	x+*	x+	x+	x+
CTD	x+*	x+*	x+*	x+*	x+*	x+*	x+*
Fluoroprobe		x+	x+*	x+*	x+*	x+*	x+*
Larval Fish	x+	x+*	x+*	x+*	x+*	x+	
Microbes	x+	x+*	x+*	x+*	x+*	x+*	x+*
Mysis	+*	+*	+*	+*	+*	+*	+*
Nutrients	x+*	x+	x+	x+*	x+	x+	x+
PSS:							
Long Transect	x+*	x+*	x+*	x+*	x+*	x+	x+
Diel		+	+	*			
UV Radiometer		+	+	*		+	
Zooplankton:							
Full	x+	x+	x+	x+*	x+*	x+	x+
Depth Stratified	+	+	+	+*		+	

Report: Major Findings from the CSMI Benthic Macroinvertebrate Survey in Lake Michigan in 2015 With an Emphasis on Temporal Trends

Authors:

Thomas F. Nalepa, University of Michigan
Lyubov E. Burlakova, SUNY Buffalo State
Ashley K. Elgin, NOAA Great Lakes Environmental Research Laboratory
Alexander Y. Karatayev, SUNY Buffalo State
Gregory A. Lang, NOAA Great Lakes Environmental Research Laboratory
Knut Mehler, SUNY Buffalo State

Contact:

Alexander Karatayev

Email: karataay@buffalostate.edu

Phone: 716-878-4329

Address:

Great Lakes Center

Buffalo State, The State University of New York

1300 Elmwood Avenue

Buffalo, NY 14222

Introduction

As part of the Coordinated Science and Monitoring Initiative (CSMI) in Lake Michigan in 2015, a lake-wide benthic survey was conducted to assess the status of the benthic macroinvertebrate community, with a primary focus on the invasive mussels *Dreissena rostriformis bugensis* and *Dreissena polymorpha*, and the native amphipod *Diporeia*. Similar lake wide surveys were conducted to assess the status of these three taxa beginning in 1994/1995 and repeated every five years through 2010 (Nalepa et al. 2014). Based on previous surveys, major changes in population abundances of all three taxa were observed over this 15-year period. *D. polymorpha* was first reported in Lake Michigan in 1989 (Marsden et al. 1993) and densities subsequently increased to reach a peak in 2000. Thereafter, densities declined to such an extent that by 2010 it was rarely found. Over the entire period, *D. polymorpha* was mainly found at depths < 50 m. After *D. r. bugensis* was first reported in the lake in 1997 (Nalepa et al. 2001), densities have mostly continued to increase at all depths through 2010, attaining densities that exceeded those of *D. polymorpha* even at depths < 50 m. Lastly, the amphipod *Diporeia* has been in a steady state of decline ever since *Dreissena* became established. Lower densities relative to those in pre- *Dreissena* years were first observed in the early 1990s (Nalepa et al. 1998), and declines continued at all depths from 1994/1995 through 2010. In 2010, it had mostly disappeared at depths < 50 m and had declined by 95% at > 50 m.

Both *Dreissena* and *Diporeia* play key roles in the ecosystem of Lake Michigan and the other Great Lakes. *Dreissena* has a great capacity to filter particulate material from the water column and excrete metabolic by-products (biodeposits, nutrients). As a result, *Dreissena* has dramatically restructured food webs and altered spatial patterns of energy and nutrient flow (Vanderploeg et al. 2002, Hecky et al. 2004). Specific impacts of *Dreissena* on the Lake Michigan ecosystem have been well-documented, including reduction of the spring phytoplankton bloom and alteration of benthic-pelagic processes (Fahnenstiel et al. 2010, Cuhel and Aguilar 2013, Vanderploeg et al. 2015). Before it declined, *Diporeia* was a keystone species in the offshore food web, accounting for over 70% of benthic biomass

and serving as an energy-rich food source for many fish species. As a detritivore that feeds on freshly-settled material in the upper sediments, *Diporeia* was an important pathway by which energy was cycled from the benthic to the pelagic region (Nalepa 1989, Nalepa et al. 2000, 2009). The decline of *Diporeia* has led to large changes in the relative health, growth, and community structure of fish communities in the lake (Pothoven et al. 2001, Hondorp et al. 2005, Bunnell et al. 2009). Because of these key ecosystem roles and population shifts through 2010, the current status of *Dreissena* and *Diporeia* were of particular interest in 2015.

For the first time since the lake-wide surveys were initiated in 1994/1995, the entire benthic community (i.e., all benthic taxa) was examined in 2015, which allowed an assessment of other taxa besides *Dreissena* and *Diporeia*, and provided a baseline to examine future changes of the entire benthic community in Lake Michigan. Lake-wide trends in the entire benthic community have recently been examined in Lake Huron (Nalepa et al. 2007), Lake Ontario (Birkett et al. 2015), and Lake Erie (Burlakova et al. 2014).

This report provides a summary of recent trends of *Dreissena*, *Diporeia*, and other major taxa based on results of the 2015 survey. In addition, it also gives a synopsis of other, ancillary data collected during the survey, such as length-weight relationships and size frequencies of the dreissenid population. The primary focus is to present major findings and to place these findings into a historic perspective. More detailed analyses and discussion of trends, spatial patterns, and community composition, including comparisons to lake-wide surveys in the other Great Lakes, will be provided in other publications.

Methods

Benthic samples were collected at 140 stations in Lake Michigan, July 20-29, 2015 (Table 1). Of these, 135 were located in the main basin of the lake, and 5 were located in the outer portion of Green Bay (Table 1, Fig. 1a, b, c). The number and location of stations have generally remained consistent since 2000. For the complete list and locations of stations sampled in all previous surveys see Nalepa et al. (2014).

Sampling procedures in 2015 were the same as in previous surveys. In brief, benthic samples were taken in triplicate at each site with a Ponar grab (area in 2015 = 0.048 m^2). Collected material was washed through an elutriation device fitted with a 0.5-mm mesh net, and retained residue was preserved in 5-10% buffered formalin containing rose bengal stain. Sample jars were labeled with the station designation, replicate number, and date. Sampling depth and a general description of the sediments at each station were recorded (Table 1).

As noted, only *Dreissena* and *Diporeia* were counted and identified in surveys prior to 2015, whereas all organisms were counted and identified in 2015. Details of laboratory procedures and protocols will not be provided here. Procedures prior to 2015 are given in Nalepa et al. (2014). Procedures in 2015 followed those in the EPA Standard Operating Procedure (SOP) LG407 "Standard Operating Procedure for Benthic Invertebrate Laboratory Analysis" (Revision 09, April 2015) as given in: https://www.epa.gov/sites/production/files/2017-01/documents/sop-for-benthic-invertebrate-lab-analysis-201504-13pp.pdf

Methods to determine densities were straight-forward and similar across all survey years. All organisms were picked and counted under low magnification, with dreissenids proportionally split when numbers were high. In 2015, biomass of *Dreissena* was determined as both ash-free dry weight (AFDW, soft tissue) and total wet weight (TWW, shell included). Surveys prior to 2015 reported dreissenid biomass as AFDW, which was calculated by first determining relationships between AFDW and shell length, and then applying these relationships to size frequencies (Nalepa et al. 2014). As given in EPA's SOP, dreissenid biomass is determined as TWW, which is determined directly by blotting dry all dreissenids in a sample and then weighing. For consistency, dreissenid biomass was determined by both methods in 2015.

Length-weight relationships were derived from individuals freshly-collected with a Ponar grab from 22 sites during the 2015 survey (Table 2). While priority was given to sites where individuals for length-weight relationships were collected in 2010, the ultimate criteria for site selection depended on the number of mussels found at the time of sampling, and by a visual estimate of the size range (shell lengths)

of the population. For the latter, a broad size range of individuals was a requirement (10 mm to > 20 mm) so that a representative relationship could be obtained. Also, an effort was made to collect at sites located throughout the lake and at various depths. Immediately after collection of mussels, soft tissues of about 25 individuals between 10 mm and > 20 mm were removed from the shells, placed individually into pre-weighed aluminum planchets, and dried at 60 C^o for at least 48 h. After drying, the planchets were placed and kept in a dessicator. Upon completion of the survey cruise and return to the laboratory, soft tissues were weighed, ashed at 550 C^o for 1 h, and then re-weighed. AFDW was then calculated as the difference between dry weight and post-ashed weight. Corresponding shell lengths were measured to the nearest 0.5 mm. Overall, a total of 569 individuals from the 22 sites were weighed and measured (Table 3). All individuals for length-weight determinations were *D. r. bugensis* since *D. polymorpha* was not found. Measured AFDWs and shell lengths (SL) were used to develop length-weight relationships according to the allometric equation: $\log_e$AFDW (mg) = b + a*$\log_e$SL (mm). Relationships were developed for pooled sites within four different depth intervals: $\leq$ 30 m, 31-50 m, 51-90 m, and > 90 m (Table 3, also see below). For size frequencies, shell lengths of all mussels in each replicate sample were measured and then binned into 1-mm size categories. In prior surveys, individuals < 5 mm were not individually measured and were therefore binned into one category (0-5 mm). In 2015, these small individuals were measured and binned into 1-mm size categories. Further, mussels < 1 mm were not included in biomass calculations.

To determine AFDW biomass, the number of individuals in each size category was multiplied by the AFDW of an individual in that category as derived from the length-weight regression (calculated from the mid-shell length of that category). All size-category weights were then summed.

For analysis of trends, sites in the main lake were divided into the same four depth intervals as in previous surveys: $\leq$ 30 m, 31-50 m, 51-90 m, and > 90 m. These intervals define distinct physical habitats that result in distinguishable benthic communities (Alley and Mozley 1975, Nalepa 1989). Because physicochemical conditions in Green Bay are so different than in the main lake, results for the 5

sites located in the bay are given separately. All values were $\log_e$ +1 transformed before any statistical tests.

Results and Discussion

The 2015 survey extended the assessment of lake-wide trends in *D. polymorpha*, *D. r. bugensis*, and *Diporeia* that were previously defined between 1994/1995 and 2010 (Nalepa et al. 2014). For *D. polymorpha*, no individuals were found in any of the samples collected in 2015 (Table 4, Fig. 2). This species peaked in 2000 at depths < 50 m and has steadily declined since. Only a few individuals were found at just one station in 2010, thus it is not surprising that no individuals were collected in 2015. The decline of *D. polymorpha* coincided with the rapid expansion of *D. r. bugensis* between 2000 and 2005 (Fig. 3). Both species are filter-feeders and compete for the same food resources. Because *D. r. bugensis* has a lower respiration rate and a higher assimilation rate than *D. polymorpha* (Baldwin et al. 2002, Stoeckmann 2003), it is more efficient in allocating resources to growth and reproduction and thus has a competitive advantage when available food resources are limited. Further, *D. r. bugensis* has a lower temperature threshold of reproduction compared to *D. polymorpha* and therefore is able to colonize to deeper depths (Karatayev et al. 2015).

For *D. r. bugensis*, some important temporal patterns emerged in 2015 that perhaps signaled a shift in population dynamics. Most notably, when compared to densities in 2010, densities in 2015 declined at all depth intervals except at the deepest (> 90 m) (Table 4, Fig. 3). In prior surveys through 2010, densities of *D. r. bugensis* have generally increased at all depth intervals. The exception was at the 31-50 m interval where densities peaked in 2005 and have declined since (Table 4). In 2015, mean densities declined by 79%, 56%, and 40% at the $\leq$ 30 m, 31-50 m, 51-90 m depth intervals, respectively. These declines were significant for each interval ($P < 0.05$, t-test). With these declines, densities of *D. r. bugensis* have seemingly peaked at depths < 90 m. The only depth interval where densities of *D. r.*

bugensis were not lower in 2015 compared to 2010 was > 90 m. Mean density at this interval increased from 2,037/m^2 to 2,797/m^2; this difference, however, was not significant ($P > 0.05$).

It is worth noting that the number of sites at $\leq$ 30 m was far lower in 2015 than in 2010 (n = 29 and 38, respectively; see Table 4). Many sites are located around 30 m, and in 2015 some sites were recorded as a few meters deeper than in 2010, placing them into the 31-50 m interval. Also, two sites in the $\leq$ 30 m interval were not sampled in 2015 but were sampled in 2010. To be certain that declines in *D. r. bugensis* in 2015 at the < 30 m and 31-50 m intervals were not a result of sites changing depth categories, means were again determined after placing these sites into the same category as in 2010. Mean densities in 2015 thus determined were 2,780 ± 661/m^2 for $\leq$ 30 m (n=36) and 5,817 ± 707/m^2 for 31-50 m (n=41). Both densities were still significantly lower than in 2010.

Trends in dreissenid AFDW biomass were similar to trends in density at $\leq$ 30 m and > 90 m. That is, mean biomass in 2015 declined at the former interval and increased at the latter interval when compared to 2010 (Fig. 4), and these year-to year differences were significant at both depth intervals ($P < 0.05$). Mean biomass at 31-50 m and 51-90 m did not decline like density (Fig. 4), and differences between 2010 and 2015 were not significant ($P > 0.05$). Considering biomass on a lake-wide basis, the mean, depth-weighted biomass for *Dreissena* in 2000, 2005, 2010, and 2015 was 0.30 g/m^2, 8.9 g/m^2, 13.7 g/m^2, and 16.5 g/m^2, respectively. Thus, total depth-weighted biomass was greater in 2015 than in 2010, which can mainly be attributed to increased biomass at > 90 m, a depth interval that comprises 41.5% of the main-lake area.

The divergence of trends in dreissenid density and AFDW biomass at the 31-50 and 51-90 m intervals between 2010 and 2015 can either be attributed to differences in length-weight, or to differences in size frequencies (or to both). With a decline in density in 2015, weight per unit shell length (AFDW/SL) must have increased, or the average size of individuals in the population must have increased. To assess differences in AFDW/SL, the AFDW of a standard 15-mm mussel was calculated and compared between the two years based on regressions given in Table 3. AFDW of a 15-mm mussel at 31-50 m was 5.46 mg and 5.17 mg in 2010 and 2015, respectively, and AFDW at 51-90 m was 6.07 mg

and 5.78 mg. Thus, AFDW/SL at both intervals was lower in 2015 than in 2010, and hence cannot account for mean biomass being higher in 2015. Size frequencies in the two years were examined by placing individuals into 5-mm size categories and then determining the proportion of all mussels in each category for each depth interval. At both the 31-50 m and 51-90 m intervals, the proportion of the population < 10 mm decreased, while the proportion > 10 mm increased in 2015 compared to 2010 (Table 5). Individuals > 10 mm increased from 30.4% to 58.4% at 31-50 m, and increased from 27.9% to 40.3% at 51-90 m. These increases in the proportion of larger-sized individuals in 2015 compared to 2010 appear to be the likely reason for biomass not declining despite significant declines in density. Since tissue weight increases exponentially with shell size, even a modest increase in the proportion of larger individuals greatly affects biomass. For the other two intervals, the proportion of individuals > 10 mm declined at $\leq$ 30 m (37.1% to 30.2%), but increased at > 90 m (26.5% to 45.6%). Increased biomass at > 90 m in 2015 relative to 2010 can thus be attributed to not only an increase in density in 2015, but also to a greater proportion of larger individuals. An increase in AFDW/SL may also have played a role (see below).

Besides using length-weight relationships to determine dreissenid biomass, these relationships are also useful to assess the relative health of the population. For *Dreissena*, the amount of tissue per unit shell length is directly related to food availability (Walz 1978, Sprung and Borchering 1991, Nalepa et al. 1995). This relationship holds true for molluscs in general (Russell-Hunter 1985). Given this, a lower AFDW/SL over time would indicate that tissue loss or tissue "degrowth" has occurred, a sign that individuals are catabolizing soft tissue while under nutritional stress. Ultimately, lower tissue weight can hinder survival (Karatayev et al. 2010) and lead to lower reproduction (Bielefeld 1991, Sprung 1995). Temporal trends in AFDW/SL can thus be a broader indicator of future population growth. As noted, the AFDW of a standard 15-mm mussel was lower in 2015 than in 2010 at 31-50 m and 51-90 m. To further explore trends at all depth intervals, AFDW of a standard 15-mm mussel was determined from regressions for *D. r. bugensis* in Lake Michigan going back to 2004 (see Table 3). Trends varied widely between the depth intervals (Fig. 5). AFDW of a 15-mm mussel was consistently greatest at the $\leq$ 30 m

interval over the 11-year period, but because of great variation between years a clear temporal trend was not readily discernable. On the other hand, the most defined temporal trend occurred at 31-50 m. At this interval, the AFDW of a 15-mm mussel steadily declined between 2004 and 2015; by 2015 it was 30.8% lower than in 2004. For the two deeper intervals, 51-90 m and > 90 m, regressions were only available in 2010 and 2015. At the 51-90 m interval, the AFDW of a 15-mm mussel declined by 4.8% over the 5-year period, while at the > 90 m interval it increased 6.0%. Based on these trends, and the fact that relative values in 2015 were lowest at 31-50 m and 51-90 m, it appears that *D. r. bugensis* populations at these two intervals may be under nutritional stress.

Biomass estimates of *Dreissena* populations in the Great Lakes have been reported in a number of different units including AFDW, dry weight (DW), and TWW. Of these, dried mass (AFDW or DW) of mussel tissue most accurately reflects functional mass, and hence estimates of dreissenid metabolic functions such as filtering, respiration, and excretion rates are generally provided as per unit AFDW or DW (Vanderpoeg et al. 2010, Johengen et al. 2014, Tyner et al. 2015). These metabolic rates along with population biomass provided as AFDW or DW have been used to estimate lake-wide ecosystem impacts (Nalepa et al. 2009, Vanderploeg et al. 2010, Rowe et al. 2015, Tyner et al. 2015). In 2015, dreissenid biomass was determined as both AFDW and TWW. To examine the relationship between AFDW and TWW, biomass estimated by both methods was plotted for each station (Fig. 6). A regression through the origin between the two values was significant ($R^2 = 0.92$) and defined by: TWW = 50.09*AFDW. Given this strong relationship between AFDW and TWW, the equation given above may be useful in converting from one biomass estimate to the other. One caveat, however, is the wide variation between the two estimates when values of AFDW are greater than about 40 g/m^2 (Fig. 6). Reasons for this variation are unclear. One potential reason is that at sites with a greater number/biomass of mussels, any differences between the TWW/SL relationship at that one site and the generalized depth-specific length-weight relationship used to calculate AFDW are compounded and therefore results in a greater discrepancy between the two methods. Also, at high mussel numbers/biomass, shell weight per unit shell length may be more inconsistent, the amount of water retained in the shell cavity may be more variable, or more

debris might be found on shells. Regardless, at high numbers/biomass AFDW is both lower and higher relative to TWW which complicates any potential theory.

Based on the 2015 survey, the amphipod *Diporeia* continued to decline (Table 4, Fig. 7). In 2015, *Diporeia* was collected at only one site that was < 90 m, and at 9 sites that were > 90 m. In comparison, in 2010 *Diporeia* was collected at 13 sites < 90 m and 11 sites > 90 m. This depth-defined pattern of decline, with densities declining first and most rapidly in nearshore, shallow regions and more slowly with increased depth, has been apparent since the decline of *Diporeia* was first reported in the lake in the early 1990s (Nalepa et al. 1998). Such a spatial pattern coincides directly with the depth-related expansion of *Dreissena*. *D. polymorpha* increased mostly in the nearshore region ($\leq$ 30 m) until 2000, and subsequently *D.r. bugensis* increased rapidly in nearshore regions and more slowly in deeper, offshore regions (> 90 m). The exact reason for the negative response of *Diporeia* to *Dreissena* has not been determined but, with the exception of Lake Superior where the *Dreissena* population is very limited, the decline of *Diporeia* has consistently occurred in all the Great Lakes within a few years after *Dreissena* became established (Nalepa et al. 2006).

Although mean density of *Diporeia* at > 90 m was not lower in 2015 than in 2010, the continued increase of *D. r. bugensis* at this depth interval would suggest that densities of *Diporeia* will most likely decrease, or the population will be completely gone, in future surveys. In 2015, not only were densities of *D. r. bugensis* greater at sites > 90 m compared to 2010, the spatial extent of the population had expanded. *D. r. bugensis* was present at 9 of 10 sites where *Diporeia* was collected in 2015. In Lake Ontario, *D.r. bugensis* expanded to deeper depths (> 90 m) sooner than in Lake Michigan, and in a lake-wide survey of Lake Ontario in 2013, only one *Diporeia* was collected at sites > 90 m, and no individuals were collected at sites < 90 m (Nalepa and Elgin unpublished). Mean density of *D. r. bugensis* at > 90 m was 2,044/m^2 in Lake Ontario in 2013, which is comparable to the mean density of 2,797/m^2 found in Lake Michigan at this depth interval in 2015. Thus, if such a density of *D. r. bugensis* nearly extirpated *Diporeia* at this depth interval in Lake Ontario, a similar outcome might be expected in Lake Michigan.

Since 2015 was the first survey year in which the entire benthic community was examined, lake-wide temporal trends in taxa other than *Dreissena* and *Diporeia* could not be assessed. However, a more limited assessment of changes in these other benthic taxa can be derived by comparing 2015 results to benthic data collected in the 1990s in just the southern basin. As part of a NOAA monitoring program, benthic samples have been collected at 40 sites in the southern basin for 2 consecutive years every 5 years beginning in 1980-1981 (Nalepa 1987, Nalepa et al. 1998). The two most recent years in which data are entirely available are in 1998-1999 (Nalepa and Elgin, unpublished). Since the same 40 sites were sampled in 2015 (see Table 1), densities of Oligochaeta, Sphaeriidae, and Chironomidae in 2015 were compared to densities in 1992-1993 and 1998-1999 at just these 40 sites. The 1992-1993 period was just after *D. polymorpha* became established in the southern basin, and the 1998-1999 period was about when *D. polymorpha* peaked and just before *D. r. bugensis* spread into the basin (about 2001). For oligochaetes, mean densities progressively increased in each of the three sampling periods (that is, 1992-1993, 1998-1999, and 2015) at the three depth intervals < 90 m (Table 6). These increases, particularly apparent at the $\leq$ 30 m and 31-50 m intervals, may be a result of a dreissenid impact known as the "nearshore shunt" (Hecky et al. 2004). In brief, this is the process by which organic material is retained for a longer period of time in nearshore regions by the activities of *Dreissena*. *Dreissena* filters particulate material (mainly phytoplankton) from the water column and subsequently deposits this organic material in the benthic zone in the form of feces and pseudofeces. These biodeposits would then serve as an added food source for benthic detritivores. Most all oligochaetes are detritivores and thus populations would benefit from these added food inputs. Benthic inputs of organic material are more pronounced in nearshore regions since primary production is greatest in this region, and because the water column is well-mixed giving *Dreissena* access to all phytoplankton present. Most chironomids are also detritivores but, although mean densities of chironomids were greater in 2015 than in the 1990s at the two shallowest intervals, variation was too great to state with certainty that densities increased. Oligochaetes did not increase at the deepest interval (> 90 m). Although *Dreissena* in deeper, offshore waters also deposit organic material, these biodeposits would have less of an impact on detritivores. Benthic food availability

in offshore regions is greatly diminished compared to nearshore regions not only because primary production in the upper water column is less, but also because this organic matter is fed upon by organisms (bacteria, protozoans, etc.) as it settles downward through a longer water column to ultimately reach the benthic region.

In contrast to increased densities of oligochaetes in the shallower depth intervals, densities of sphaeriids were lower at all depth intervals in 2015 compared to the 1990s (Table 6). A decline in sphaeriids at all depths was first observed soon after *Dreissena* became established in the southern basin (Nalepa et al. 1998). Reasons for the negative response of sphaeriids to *Dreissena* are not clear. Since sphaeriids are filter-feeders, it is presumed that they are being outcompeted by *Dreissena* for available food. Yet the dominant sphaeriid in the Great Lakes is *Pisidium* spp., a genus that filters bacteria in benthic interstitial waters and therefore should benefit from increased bacteria associated with dreissenid biodeposits.

The dominance of *Dreissena* in the benthic community of Lake Michigan and the other Great Lakes has clear implications for other benthic taxa. While detailed comparisons of benthic community trends between lakes will not be provided here, a general overview of between-lake trends in *Dreissena* puts Lake Michigan results into a broader perspective. A comparison of density trends of *Dreissena* in Lakes Michigan, Ontario, and Huron at the $\leq$ 30 m, 31-90 m, and > 90 m intervals is given in Fig. 8. To make this comparison, densities at 31-50 m and 51-90 m were combined (interval becomes 31-90 m) for Lakes Michigan and Huron since these two depth intervals were not reported separately for Lake Ontario in previous studies (Watkins et al. 2007, Birkett et al. 2015). Density trends at $\leq$ 30 m are difficult to compare between lakes since high variation in physical drivers (i. e., substrate heterogeneity, wave-induced disturbance) strongly influence dreissenid estimates. This is evident in the wide year-to-year variation at this depth interval in Lake Ontario (Fig. 8). Physical conditions become more stable as depth increases, and population trends at depths > 30 m are better suited for lake-to-lake comparisons. The decline of *D. r. bugensis* in Lake Michigan in 2015 at 31-90 m is similar to an ongoing decline in Lake Ontario that has been evident since 2008 (Fig. 8). If populations in both lakes have indeed peaked at this

depth, a greater peak density was attained in Lake Michigan. In both lakes, densities increased sharply and then gradually declined. In contrast, densities at 31-90 m in Lake Huron have increased gradually and, as of 2012, do not yet appear to have peaked. Densities at > 90 m are still increasing in all three lakes (Fig. 8). Similar comparisons of temporal trends in dreissenid biomass are not possible since biomass was not historically measured in each lake. However, the most recent lake-wide survey in each lake determined and reported biomass using the same methods, and values in the four depth intervals are given in Table 7. Again, considering biomass only at depths > 30 m, mean biomass in Lakes Michigan and Ontario were generally comparable at 31-50 m, 51-90 m, and > 90 m, whereas biomass in Lake Huron was about 50%, 78%, and 38% lower than in Lakes Michigan and Ontario at these three depth intervals, respectively.

Summary

A lake-wide benthic survey was conducted in Lake Michigan in 2015 to assess the current status of the macroinvertebrate community. Similar lake-wide surveys have been conducted in the lake at 5-year intervals beginning in 1994/1995. These previous surveys only examined populations of *Dreissena polymorpha*, *Dreissena r. bugensis*, and *Diporeia*, whereas the 2015 survey examined the entire benthic community. Perhaps the most significant finding in 2015 was the decline in densities of *D. r. bugensis* at depths < 90 m. Compared to densities in 2010, densities in 2015 declined 79%, 56%, and 40% at the $\leq$ 30 m, 31-50 m, 51-90 m intervals, respectively. In contrast, densities at > 90 m increased 37%. Because of a greater proportion of larger individuals in the population, biomass at 31-50 m and 51-90 m remained stable or slightly increased in 2015 compared to 2010. Overall, depth-weighted biomass increased from 13.7 g/m^2 in 2010 to 16.5 g/m^2 in 2015, largely due to increased biomass at sites > 90 m. The other dreissenid species, *D. polymorpha*, was not collected at any of the sites in 2015, indicating it has essentially been displaced by *D. r. bugensis*. Also, the amphipod *Diporeia* continued to disappear. It was collected at only one site < 90 m and at 9 sites > 90m. Lake-wide temporal trends in other major benthic taxa such as Oligochaeta, Sphaeriidae, and Chironomidae could not be assessed since 2015 was

the first year the entire benthic community was sampled. However, based on comparisons to data collected in just the southern basin in 1992-1993 and 1998-1999, oligochaetes have progressively increased in shallower and mid-depth regions between 1992-1993 and 2015. A likely reason is an increased amount of potential food resulting from the biodeposition of organic material by *Dreissena*. In contrast, sphaeriids progressively declined all depth intervals between 1992-1993 and 2015.

References

Alley, W. P. and S. C. Mozley. 1975. Seasonal abundance and spatial distribution of Lake Michigan macrobenthos, 1964-67. Great Lakes Res. Division Spec. Publ. 54, University of Michigan, Ann Arbor, MI.

Baldwin, B. S., M. S. Mayer, J. Dayton, N. Pau, J. Mendilla, M. Sullivan, M. Moore, A. Ma, and E. L. Mills. 2002. Comparative growth and feeding in zebra amd quagga mussels (*Dreissena polymorpha and Dreissena bugensis*): implications for North American lakes. Can. J. Fish. Aquat. Sci. 59: 680-694.

Bielefeld, U. 1991. Histological observation of gonads and digestive gland in starving *Dreissena polymorpha* (Bivalvia). Malacologia 33: 31-42.

Birkett, K., S. J. Lozano, and L. G. Rustram. 2015. Long-term trends in Lake Ontario's benthic macroinvertebrate community. Aquat. Ecosys. Health & Manag. 18: 78-88.

Burlakova, L. E., A. Y. Karatayev, C. Pennuto, and C. Mayer. 2014. Changes in Lake Erie benthos over the last 50 years: Historical perspectives, current status, and main drivers. J. Great Lakes Res. 40: 560-573.

Bunnell, D. B., S. R. David, C.P. Madenjian. 2009. Decline of bloater fecundity in southern Lake Michigan after decline of *Diporeia*. J. Great Lakes Res. 35: 45-49.

Cuhel, R. L. and C. Aguilar. 2013. Ecosystem transformations of the Laurentian Lake Michigan by nonidigenous biological invaders. Ann. Rev. Mar. Sci. 5: 289-320.

Fahnenstiel, G., T. Nalepa, S. Pothoven, H. Carrick, and D. Scavia. 2010. Lake Michigan lower food web: Long-term observations and *Dreissena* impact. J. Great Lakes Res. 36 Suppl. 3): 1- 4.

Hecky, R. E., R. E. H. Smith, D. R. Barton, et al. 2004. The nearshore phosphorus shunt: a consequence of ecosystem engineering by dreissenids in the Laurentian Great Lakes. Can. J. Fish. Aquat. Sci. 61:1285-1293.

Hondorp, D. W., S. A. Pothoven, and S. A. Brandt. 2005. Influence of *Diporeia* density on diet composition, relative abundance, and energy density of plantivorous fishes in southeast Lake Michigan. Trans. Am. Fish. Soc. 134: 588-601.

Johengen, T. H., H. A.Vanderploeg, and J. R. Liebig. 2014. Effects of algal composition, seston stoichiometry, and feeding rate on zebra mussel (*Dreissena polymorpha*) nutrient excretion in two Laurentian Great Lakes. In *Quagga and Zebra Mussels: Biology, Impacts, and Control*, Second Edition. T. F. Nalepa and D. W. Schloesser, eds., pp. 445-459. CRC Press: Boca Raton. Fl.

Karatayev, A. Y., S. E. Mastitsky, D. K. Padilla, L. B. Burlakova, and M. M. Hajduk. 2010. Differences in growth and survivorship in zebra and quagga mussels: size matters. Hydrobiologia 668: 183-194.

Karatayev, A. Y., L. E. Burlakova, and D. K. Padilla. 2015. Zebra versus guagga mussels: a review of their spread, population dynamics, and ecosystem impacts. Hydrobiologia 745: 97-112.

Marsden, J. E., N. Trudeau, and T. Keniry. 1993. Zebra mussels study in Lake Michigan. Aquat. Ecol. Rept 93/14. Illinois Natural History Survey.

Nalepa, T. F. 1987. Long term changes in the macrobenthos of southern Lake Michigan. Can. J. Fish. Aquat. Sci. 44:515-524.

Nalepa, T. F. 1989. Estimates of macroinvertebrate biomass in Lake Michigan. J. Great Lakes Res. 15: 437-443.

Nalepa, T. F., J. A. Wojcik, D. L. Fanslow, and G. A. Lang. 1995. Initial colonization of the zebra mussel (*Dreissena polymorpha*) in Saginaw Bay, Lake Huron: Population recruitment, density, and size structure. J. Great Lakes Res. 21: 417-434.

Nalepa, T. F., D. J. Hartson, D. L. Fanslow, G. A. Lang, and S. J. Lozano. 1998. Declines in benthic macroinvertebrate populations in southern Lake Michigan, 1980-1993. Can. J. Fish. Aquat. Sci. 55: 2402-2413.

Nalepa, T. F., D. J. Hartson, J. Buchanan, J. F. Cavaletto, G. A. Lang, and S. J. Lozano. 2000. Spatial variation in density, mean size and physiological condition of the holarctic amphipod *Diporeia* spp. in Lake Michigan. Freshwater Biology 43: 107-119.

Nalepa, T. F., D. W. Schloesser, S. A. Pothoven, D. W. Hondorp, D. L. Fanslow, M. L. Tuchman, and G. L. Fleischer. 2001. First finding of the amphipod *Echinogammarus ischnus* and the mussel *Dreisssena bugensis* in Lake Michigan. J. Great Lakes Res. 27: 384-391.

Nalepa, T. F., D. C. Rockwell, and D. W. Schloesser. 2006. Disappearance of the amphipod *Diporeia* spp. in the Great Lakes. Workshop Summary, Discussion, Recommendations. NOAA Technical Memorrandum GLERL-136. NOAA, Great Lakes Environmental Research Laboratory, Ann Arbor, MI.

Nalepa, T. F., D. L. Fanslow, S. A. Pothoven, A. J. Foley III, and G. A. Lang. 2007. Long-term trends in benthic macroinvertebrate populations in Lake Huron over the past four decades. J. Great Lakes Res. 33: 421-436.

Nalepa, T. F., D. L. Fanslow, G. A. Lang. 2009. Transformation of the offshore benthic community in Lake Michigan: recent shift from the native amphipod *Diporeia* spp. to the invasive mussel *Dreissena rostriformis bugensis*. Freshwater Biology 54:466-475.

Nalepa, T. F., D. L. Fanslow, and S. A. Pothoven. 2010. Recent changes in density, biomass, recruitment, size structure, and nutritional state of *Dreissena* populations in southern Lake Michigan. J. Great Lakes Res. 36 (Suppl.3): 5-19.

Nalepa, T. F., D. L. Fanslow, G. A. Lang, K. Mabrey, and M. Rowe. 2014. Lake-wide benthic surveys in Lake Michigan in 1994-1995, 2000, 2005, and 2010: abundances of the amphipod *Diporeia* spp and abundances and biomass of the mussels *Dreissena polymorpha* and *Dreissena rostriformis bugensis*. NOAA Technical Memorandum GLERL-164. NOAA Great Lakes Environmental Research Laboratory, Ann Arbor, MI.

Pothoven, S. A., T. F. Nalepa, P. J. Schneeberger, and S. B. Brandt. 2001. Changes in diet and body condition of lake whitefish in southern Lake Michigan associated with changes in benthos. N. Amer. J. Fish. Manag. 21: 876-883.

Russell-Hunter, W. D. 1985. Physiological, ecological, and evolutionary aspects of molluscan tissue degrowth. Amer. Malacol. Bull. 3: 213-221.

Rowe, M. D., D. R. Obenour, T. F. Nalepa, H. A. Vanderploeg, F. Yousef, and W. C. Kerfoot. 2015. Mapping the spatial distribution of the biomass and filter-feeding effect of invasive dreissenid mussels on the winter-spring phytoplankton bloom in Lake Michigan. Freshwater Biology 60: 2270-2285.

Sprung, M. 1995. Physiological energetic of the zebra mussel *Dreissena polymorpha* in lakes I. Growth and reproductive effort. Hydrobiologia 304: 117-132.

Sprung, M. and J. Borcherding. 1991. Physiological and morphometric changes in *Dreissena polymorpha* (Mollusca; Bivalvia) during a starvation period. Malacologia 33: 179-191.

Stoeckmann, A. 2003. Physiological energetics of Lake Erie dreissenid mussels: a basis for the displacement of *Dreissena polymo*rpha by *Dreissena bugensis*. Can. J. Fish. Aquat. Sci. 60:126-134.

Tyner, E. H., H. A. Bootsma, and B. M. Lafrancois. 2015. Dreissenid metabolism and ecosystem effects as revealed by oxygen consumption. J. Great Lakes Res. 41 (Suppl. 3): 27-47.

Vander ploeg, H. A., T. F. Nalepa, D. J. Jude, et al. 2002. Dispersal and emerging ecological impacts of Ponto-Caspian species in the Laurentian Great Lakes. Can. J. Fish. Aquat. Sci. 59: 1209-1228.

Vanderploeg, H. A., J. R. Liebig, T. F. Nalepa, G.. L. Fahnenstiel, and S. A. Pothoven. 2010. *Dreissena* and the disappearance of the spring phytoplankton bloom in Lake Michigan. J. Great Lakes Res. 36 (Suppl.3): 50-59.

Vanderploeg, H. A., D. B. Bunnell, H. J. Carrick, and T. O. Hook. 2015. Complex interactions in Lake Michigan's rapidly changing ecosystem. J. Great Lakes Res. 41 (Suppl. 3): 1-6.

Walz, N. 1978. The energy balance of the freshwater mussel *Dreissena polymorpha* Pallas in laboratory experiments and in Lake Constance. IV. Growth in Lake Constance. Arch. Hydrobiol./Suppl. 55: 142-156.

Watkins, J. M., R. Dermott, S. J. Lozano, E. L. Mills, L. R. Rudstram, and J. V. Scharold. 2007. Evidence for remote effects of dreissenid mussels on the amphipod *Diporeia*: Analysis of Lake Ontario benthic surveys, 1972-2003. J. Great Lakes Res. 33: 642-657.

Table 1. Location, depth, and described substrate of sites sampling in Lake Michigan in 2015. *Stations that were originally part of NOAA's benthic monitoring program in the southern basin in the 1990s (Nalepa et al. 1998). See text for details.

Region/Station	Depth	Latitude	Longitude	Substrate
South				
A-1*	17.3	42°06.5530	086°31.9709	sand
A-2*	29.9	42°06.0153	086°36.9776	silt and clay
A-4	72.4	42°03.4904	087°06.5073	100% mud
B-2*	49.6	42°23.9931	086°27.0413	100% mud
B-3*	62.0	42°23.9757	086°35.4838	100% mud
B-4*	126.0	42°23.5103	087°00.9441	silty clay
B-5*	102.7	42°22.5024	087°20.9581	silt and clay
B-6*	82.4	42°22.5274	087°29.9469	silt
B-7*	43.7	42°21.9742	087°39.9606	silty sand
C-1*	17.7	42°49.6624	086°14.8867	sand
C-2	45.0	42°49.6581	086°18.1607	silt, clay
C-3*	77.3	42°49.1494	086°28.4125	silt
C-45	45.2	42°09.5638	087°30.1969	silty sand
C-5*	129.0	42°48.9918	086°49.9923	silty clay
C-6*	98	42°47.6759	087°26.7942	95% silt over loam, 5% sand
C-7*	58.5	42°47.5263	087°34.4815	90% sand, 10% mud
EG-12*	54.0	42°20.8597	087°36.9207	sandy silt
EG-14*	93.3	42°22.6546	086°46.4204	100% silt
EG-18*	55.3	42°17.6162	086°38.5844	100% silt
EG-22*	46.4	43°06.1985	086°21.9813	silt
F-2	44.3	42°30.0489	086°21.8592	100% mud
F-3	71.6	42°30.1042	086°31.4951	silty mud
G-45	43.3	41°56.9564	087°13.4598	variable, mostly sand, some gravel & mud
H-8*	17.8	42°23.9597	087°46.2676	silt over loam, no *Dreissena*
H-9*	39.8	42°26.7390	087°42.3416	80% silt, some loam and sand
H-11*	69.9	42°33.2505	087°35.8191	80% silt, 20% sand
H-13*	17.9	41°55.5694	087°29.4711	90% sand, 10% shells
H-14*	34.9	42°04.3359	087°27.2110	sand
H-15*	56.2	42°09.5212	087°26.0221	silty sand
H-18*	19.8	41°58.9774	086°36.0354	silty sand
H-19*	34.8	42°00.0033	086°41.0855	silty ooze
H-20*	53.6	42°00.8410	086°45.1599	silty mud, ooze
H-21*	72.0	42°02.4175	086°53.0036	silty fine sediment, ooze like
H-22*	51.3	42°08.3490	086°39.8233	silt, soft
H-24*	19.0	42°23.2856	086°20.0614	100% sand
H-28*	22.3	42°37.7982	086°15.9440	100% sand
H-29*	37.1	42°37.8117	086°18.3111	silty sand

H-30*	73.5	42°37.8048	086°25.9938	black silt
H-31*	43.0	43°02.4984	086°19.9544	silty clay
M-25	26.0	43°12.0097	086°22.6710	sand
M-45	42.5	43°11.4208	086°25.7241	50% sand, 50% mud
N-2	37.0	41°53.5031	086°52.0062	silt
N-3	60.1	41°57.9916	086°59.0004	silt
Q-13	14.2	42°50.6140	087°47.9134	sand
Q-30	31.0	42°50.5888	087°39.2398	90%clay, 10% sand
R-20	22.4	42°45.0562	087°41.7560	100% sand
R-45	47.3	42°45.0205	087°36.3117	90% sand, rest dressenid shells
S-2*	10.3	41°45.9239	087°23.4838	100% fine sand
S-3*	26.5	41°50.9822	087°19.2111	90% fine sand, 10% siltS
S-4*	40.2	41°56.0843	087°15.1277	sand and gravel
SAU-45	43.5	42°41.1347	086°18.8971	silty ooze
T-3	71.6	42°10.0378	086°43.0227	silt, some sand
V-1*	17.5	41°41.7981	087°00.7974	variable, clay, sandy silt
V-2*	28.4	41°48.9911	087°02.9051	thick silt
X-1*	35.6	43°08.2531	086°21.6891	variable, silt/clay, some sand
X-2*	100.6	43°11.9988	086°31.0275	85% silt, 15% sand
Central				
E-1	44.9	44°37.5016	086°18.2152	85% sand, 15% mud
K-2	46.8	43°20.2260	086°30.0222	80% mud, 20% sand
KE-1	22.4	44°23.3271	087°27.6720	80%sand, 10% silt, 10% dreissenid shells
KE-2	31.7	44°23.3271	087°27.6720	Variable, mostly sand, some silt
KE-3	48.1	44°23.3037	087°26.2201	80% sand, 20% silt
KE-5	78.5	44°23.3123	087°24.0022	50% sand, 50% silt
L-220	21.2	43°30.0506	086°30.1907	sand
L-230	33.4	43°30.0446	086°31.1570	50% mud, 50% sand
L-245	44.0	43°30.0491	086°31.8934	85% mud, 15% sand
L-260	60.4	43°30.0629	086°33.3126	100% dark mud
L-280	80.5	43°30.0621	086°36.1907	100% dark mud
LU-1	22.0	43°56.6498	086°32.1102	sand
LU-3	44.0	43°56.6455	086°36.4846	silty sand
LU-4	62.5	43°56.6250	086°37.6144	silty sand
LU-5	78.0	43°56.6410	086°39.0196	70% silt, 30% sand
MAN-1	20.9	44°24.7956	086°16.8948	100% sand
MAN-2	35.9	44°24.7813	086°17.1189	80% mud, 20% sand
MAN-3	44.8	44°24.7729	086°19.8942	silty clay, sand
MAN-4	58.6	44°24.8098	086°20.3585	silty sand, clay
MAN-5	74.0	44°24.7721	086°20.8248	sandy silt, clay
PW-2	32.0	43°26.8258	087°46.9135	80% silt, 20% fine sand
PW-3	44.9	43°26.8217	087°46.1627	80% silt, 20% fine sand
PW-4	59.5	43°26.8348	087°43.9985	silty clay, sand

PW-5	79.0	43°26.8325	087°41.8609	silty clay, sand
SY-1	22.5	43°55.0747	087°39.8279	silty sand
SY-2	31.0	43°55.0780	087°38.8513	silt
SY-4	59.0	43°55.0786	087°30.2854	sand
SY-5	77.0	43°55.1038	087°22.5379	85% sand, 15% silt
9552	83.3	43°11.1025	087°12.5799	mud over loam
9554	109.0	43°14.2628	086°53.1725	100% mud
9556	72.9	43°18.3335	087°46.3070	silty sand
9561	130.0	43°28.2513	086°47.0433	100% mud
9562	123.0	43°29.9922	087°37.0272	silt
9564	133.0	43°36.0367	087°20.4315	silty clay
9570	165.0	43°53.1746	086°54.4904	silty mud
9574	139.0	44°04.1020	087°08.8314	tin layer mud over loam
9576	164.0	44°09.0855	086°37.2796	70% silt , 30% clay
9577	78.1	44°14.6051	087°22.4592	silty sand
9582	120.0	44°24.5028	086°22.1030	silt, detritus
9587	196.0	44°37.2816	086°21.1621	100% mud
78110	33.0	43°56.6170	086°34.7150	sand, some silt
82882	58.6	44°23.3560	087°25.3558	89% fine sand, 20% silt
82902	40.0	43 55.0900	087 37.4400	silt, fine sand
82922	17.7	43°26.8127	087°47.7663	50% fine sand, 50% silt
North				
EA-7	40.0	45°16.8126	085°26.1806	silty, clay, sand
FR-1	20.0	44°48.9956	086°08.3822	mostly *Dreissena* druses, some sand
FR-2	32.0	44°49.0038	086°09.3452	sand
FR-3	44.0	44°49.0065	086°10.1009	mostly silt, some sand
FR-4	56.4	44°48.9911	086°11.1107	60% silt, 40% sand
FR-5	78.8	44°48.9811	086°11.7992	70% mud, 30% sand
PET-2	38.5	45°26.7409	085°04.5516	silty sand
PET-3	39.0	45°26.7319	085°11.1409	silt, clay, sand
SB-2	35.0	44°51.7024	087°09.7100	sand
SB-3	47.6	44°51.4571	087°09.0359	sand, some clay
SB-4	60.0	44°51.4272	087°08.1949	70% sand, 30% silt
SB-5	79.9	44°51.4479	087°05.1681	silt, mud
SB-6	154.0	44°51.4508	086°55.3928	80% clay, 20% silt
SC-2	29.0	45°50.4724	086°06.3233	coarse sand
SC-3	43.5	45°49.0404	086°06.3392	silt, dreissenid shells
SC-4	60.0	45°47.3931	086°06.3204	silt
SC-5	83.0	45°45.3760	086°06.3413	silty ooze
WI-1	17.4	45°14.8408	086°54.2876	sand
WI-2	31.3	45°14.8303	086°52.5656	sand
WI-3	45.4	45°14.8570	086°49.8001	sand
WI-5	85.0	45°14.8361	086°38.2513	60% silt, 40% sand

9597	162.0	44°58.3213	086°22.1965	silt with clay
74880	24.0	45°54.5117	085°01.4952	90% mud, 10% fine sand
74900	54.3	45°26.7280	085°13.2994	silty sand, some clay
76442	19.3	46°00.0540	085°24.5721	dark silt
76462	64.0	45°32.0863	085°38.1520	variable, mostly silt, some and rock
76471	31.5	45°14.5004	085°33.3449	silty sand
76482	28.6	45°04.1289	085°51.4266	sand
78030	33.5	45°48.7051	085°43.0632	70% silt, 30% sand
79612	20.5	45°54.0042	086°06.3019	coarse sand
81220	37.0	45°42.6096	086°24.5279	sand
81240	56.0	45°14.8459	086°40.1503	60% sand, 40% silt
82851	80.0	45°03.0013	086°55.3601	60% clay, 40% silt
82862	13.3	44°51.4530	087°11.3734	sand
95120	134.0	44°58.3213	086°22.1965	silt
Green Bay				
BBN-1	11.8	45°41.9760	086°44.5177	rock and sand
BBN-2	25.0	45°37.2398	086°44.5132	silt
BBN-3	28.6	45°32.5008	086°44.5119	silt, alga present
LBDN-3	23.3	45°30.0167	087°05.7984	90% sand, 10% silt
84450	10.2	45°36.1817	087°05.7656	sand

Table 2. Sites where additional *Dreissena* was collected for determination of length-weight relationships in 2010 and 2015.

Depth Interval	Year	Stations
≤ 30 m	2010	H-18, MAN-2, PW-2, SB-2, SC-2
	2015	FR-1, H-28, M-25
31-50 m	2010	B-7, H-19, MAN-3, PW-3, SB-3, SC-3
	2015	82902, B-2, B-7, FR-3, LU-3, M-45,SB-3, SC-3
51-90 m	2010	EG-12, H-20, H-21, MAN-4, MAN-5, PW-4, PW-5, SB-4, SB-5, SC-4, SC-5, 82851
	2015	FR-5, H-21, LU-5, SB-5, SC-5, SY-5
> 90 m	2010	9582
	2015	9561, 9582, B-5, EG-14, X-2

Table 3. Relationship between shell length (SL in mm) and tissue ash-free dry weight (AFDW in mg) for *D. polymorpha* and *D. r. bugensis* at various depth intervals in Lake Michigan in 2004, 2008, 2010, and 2015. Regression constants (a, b) derived from the linear regression: $Log_e AFDW = a + b*Log_e SL$; n = total number of mussels used to derive the relationship. Also given is the AFDW of a standard 15-mm individual as derived from the given regression. Regressions in 2004 and 2008 were from Nalepa et al. (2010), and regressions in 2010 were from Nalepa et al. (2014). [#]AFDWs in 2010 were likely underestimated by 15 % (Nalepa et al. 2014).

Year/Depth Interval (m)	No. of Stations	Species	a	b	n	R^2	15 mm
2004							
≤ 30	2	*D. polymorpha*	-5.256	2.672	242	0.76	7.24
31-50	2	*D. polymorpha*	-5.255	2.652	242	0.80	6.87
≤ 30	2	*D. r. bugensis*	-6.095	2.968	244	0.85	6.98
31-50	2	*D. r. bugensis*	-6.969	3.316	247	0.90	7.47
2008							
≤ 30	1	*D. r. bugensis*	-6.299	3.193	199	0.92	10.46
31-50	1	*D. r. bugensis*	-5.469	2.659	193	0.93	5.65
2010[#]							
≤ 30	5	*D. r. bugensis*	-5.857	2.814	122	0.63	5.83 (6.70)
31-50	6	*D. r. bugensis*	-5.528	2.617	172	0.85	4.75 (5.46)
51-90	12	*D. r. bugensis*	-5.601	2.683	269	0.87	5.28 (6.07)
> 90	1	*D. r. bugensis*	-5.993	2.854	24	0.98	5.67 (6.52)
2015							
≤ 30	3	*D. r. bugensis*	-5.608	2.879	77	0.92	8.92
31-50	8	*D. r. bugensis*	-5.793	2.746	211	0.88	5.17
51-90	6	*D. r. bugensis*	-5.392	2.639	153	0.91	5.78
> 90	5	*D. r. bugensis*	-5.259	2.656	128	0.85	6.91

Table 4. Mean (± SE) density (no./ m^2) of *Diporeia*, *Dreissena polymorpha*, and *Dreissena r. bugensis* at four depth intervals (≤ 30 m, 31-50 m, 51-90 m, and > 90 m) in each survey year. n = number of stations sampled. t-tests were used to determine differences between 2010 and 2015: * significant at P< 0.05, ** significant at P < 0.01. Note: Values for 2010 are slightly different than values given in Table 5 of Nalepa et al. (2014) as some stations in Table 5 were placed into the wrong depth interval.

	Year				
Depth Interval/Taxa	1994-95	2000	2005	2010	2015
≤ 30 m	n = 16	n = 38	n = 41	n = 38	n = 29[1]
Diporeia	3,907 ± 1,005	853 ± 315	104 ± 88	1 ± 1	0 ± 0
D. polymorpha	730 ± 509	2,113 ± 539	258 ± 86	0 ± 0	0 ± 0
D. r. bugensis	0 ± 0	51 ± 26	7,547 ± 1,566	9,254 ± 1,689	2,052 ± 697**
31-50 m	n = 11	n = 36	n = 36	n = 41	n = 46[2]
Diporeia	6,111 ± 1,377	2,116 ± 563	24 ± 16	<1 ± <1	0 ± 0
D. polymorpha	252 ± 239	1,021 ± 511	427 ± 109	1 ± 1	0 ± 0
D. r. bugensis	0 ± 0	11 ± 9	15,838 ± 2,860	13,133 ± 1,086	5,800 ± 640**
51-90 m	n = 32	n = 41	n = 41	n = 39	n = 42[3]
Diporeia	6,521 ± 562	3,469 ± 464	548 ± 131	103 ± 51	1 ± <1
D. polymorpha	< 1 ± <1	16 ± 8	38 ± 29	0 ± 0	0 ± 0
D. r. bugensis	0 ± 0	0 ± 0	6,472 ± 1,704	14,846 ± 1,335	8,955 ± 762*
>90 m	n = 25	n = 13	n = 13	n = 19	n = 18
Diporeia	4,547 ± 385	2,804 ± 453	1,244 ± 217	406 ± 117	528 ± 186
D. polymorpha	0 ± 0	0 ± 0	<1 ± <1	0 ± 0	0 ± 0
D. r. bugensis	0 ± 0	0 ± 0	12 ± 7	2,037 ± 872	2,797 ± 824
Green Bay (≤ 30 m)				n = 6	n = 5
Diporeia		26 ± 25	0 ± 0	0 ± 0	0 ± 0
D. polymorpha		820 ± 444	80 ± 53	0 ± 0	0 ± 0
D. r. bugensis		1 ± 1	6,640 ± 3,637	5,990 ± 2,140	3,797 ± 1,270

[1]n=26 for *Diporeia*
[2]n=38 for *Diporeia*
[3]n=37 for *Diporeia*

Table 5. Percentage of measured *D. r. bugensis* within various size categories at four depth intervals (≤ 30 m, 31-50 m, 51-90 m, and > 90 m) in 2010 and 2015. Categories based on shell length (mm). All collected mussels were measured in 2015. In 2010, mussels were measured from representative sites (details for 2010 are given in Nalepa et al. 2014).

	Shell Length (mm)						
Interval/Year	< 5	5-10	10-15	15-20	20-25	25-30	> 30
≤ 30 m							
2010	62.0	19.4	12.4	5.1	1.0	<0.1	0.0
2015	69.7	6.7	6.3	10.2	5.6	0.8	<0.1
31-50 m							
2010	41.1	29.6	16.8	8.9	3.3	0.3	<0.1
2015	21.1	21.1	24.8	21.3	9.8	1.7	0.2
51-90 m							
2010	55.1	17.0	17.2	8.5	1.9	0.2	<0.1
2015	38.6	21.6	18.7	15.5	4.9	0.7	<0.1
> 90 m							
2010	73.5	13.9	7.7	4.5	0.3	<0.1	0.0
2015	54.4	21.1	12.2	7.9	3.8	0.7	<0.1

Table 6. Mean (± SE) density (no./ m^2) of major macroinvertebrate taxa at four depth intervals (≤ 30 m, 31-50 m, 51-90 m, and > 90 m) at 40 sites in the southern basin of Lake Michigan. n= 12, 10, 12, and 6 for the four intervals, respectively.

	Year		
Depth Interval/Taxa	1992-1993	1998-1999	2015
≤ 30 m			
Diporeia	2,624 ± 568	183 ± 125	0 ± 0
Dreissena	1,159 ± 855	1,521 ± 524	627 ± 284
Oligochaeta	1,684 ± 430	1,965 ± 355	4,087 ± 1,265
Chironomidae	187 ± 29	297 ± 46	531 ± 431
Sphaeriidae	900 ± 287	330 ± 139	87 ± 45
31-50 m			
Diporeia	7,857 ± 852	1,425 ± 450	0 ± 0
Dreissena	16 ± 6	955 ± 333	7,076 ± 1,639
Oligochaeta	3,050 ± 315	4,077 ± 762	6,031 ± 1,248
Chironomidae	100 ± 18	52 ± 12	202 ± 156
Sphaeriidae	1,677 ± 304	1,069 ± 181	7 ± 7
51-90 m			
Diporeia	5,911 ± 385	3,487 ± 616	0 ± 0
Dreissena	1 ± <1	3 ± 1	8,753 ± 1,591
Oligochaeta	1,693 ± 125	2,019 ± 244	2,924 ± 650
Chironomidae	66 ± 12	28 ± 7	6 ± 3
Sphaeriidae	597 ± 139	620 ± 68	12 ± 8
>90 m			
Diporeia	3,201 ± 477	3,314 ± 597	207 ± 207
Dreissena	0 ± 0	2 ± 2	5,644 ± 1,712
Oligochaeta	1,124 ± 141	996 ± 131	887 ± 196
Chironomidae	45 ± 10	26 ± 7	7 ± 6
Sphaeriidae	106 ± 36	175 ± 62	15 ± 8

Table 7. Mean (± SE) biomass (gAFDW/m^2) of *Dreissena* at ≤ 30 m, 31-50 m, 51-90 m, and > 90 m depth intervals based on the latest lake-wide surveys in Lake Michigan, Lake Ontario, and Lake Huron. Given in parenthesis is the number of stations sampled.

	Dreissena Biomass (gAFDW/m^2)		
Depth Interval	Lake Michigan in 2015	Lake Ontario in 2013	Lake Huron in 2012
≤ 30 m	7.93 ± 3.30 (29)	21.53 ± 7.92 (8)	2.65 ± 1.77 (19)
31-50 m	26.44 ± 3.05 (46)	28.79 ± 9.63 (8)	13.91 ± 4.43 (30)
51-90 m	28.39 ± 1.98 (42)	20.86 ± 1.82 (8)	5.43 ± 2.45 (26)
> 90 m	6.81 ± 2.23 (18)	7.08 ± 2.16 (21)	4.32 ± 3.97 (8)

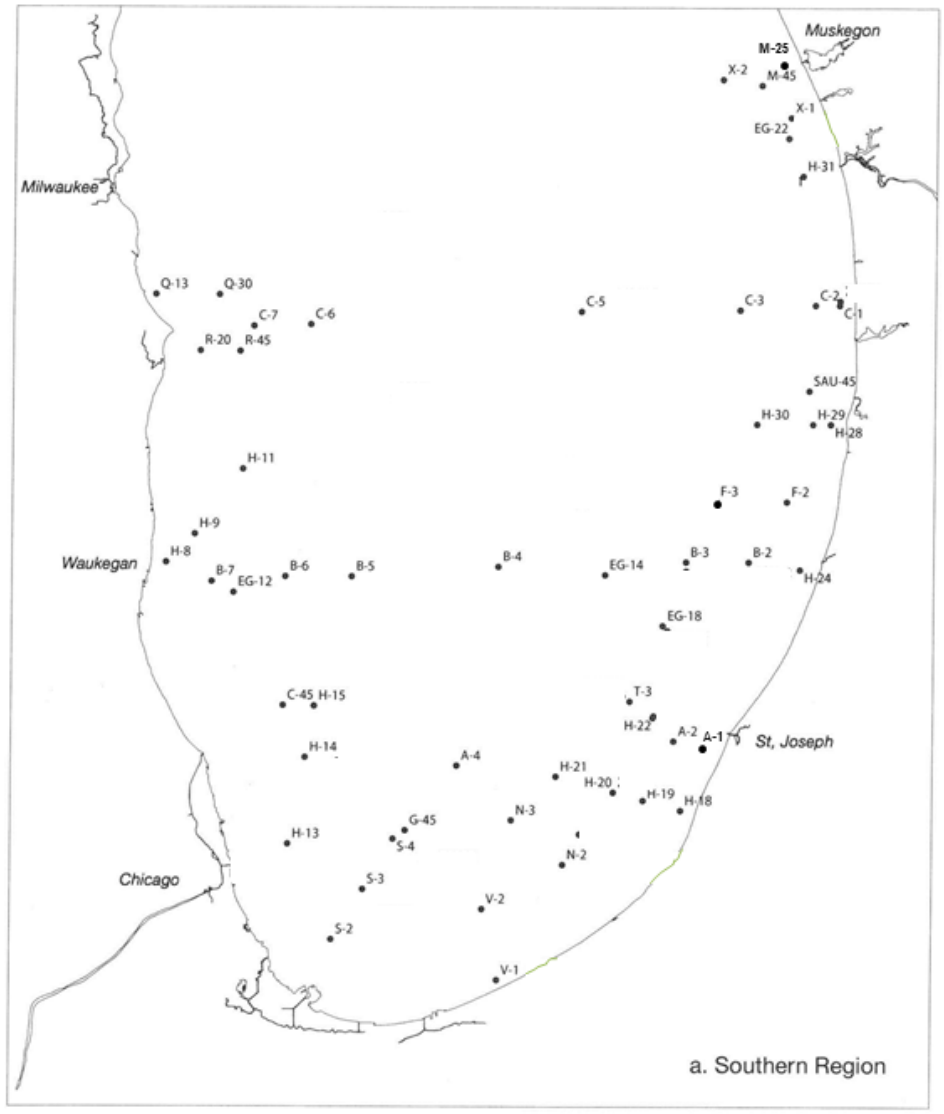

Figure 1a. Location of sampling sites in the southern region of Lake Michigan in 2015.

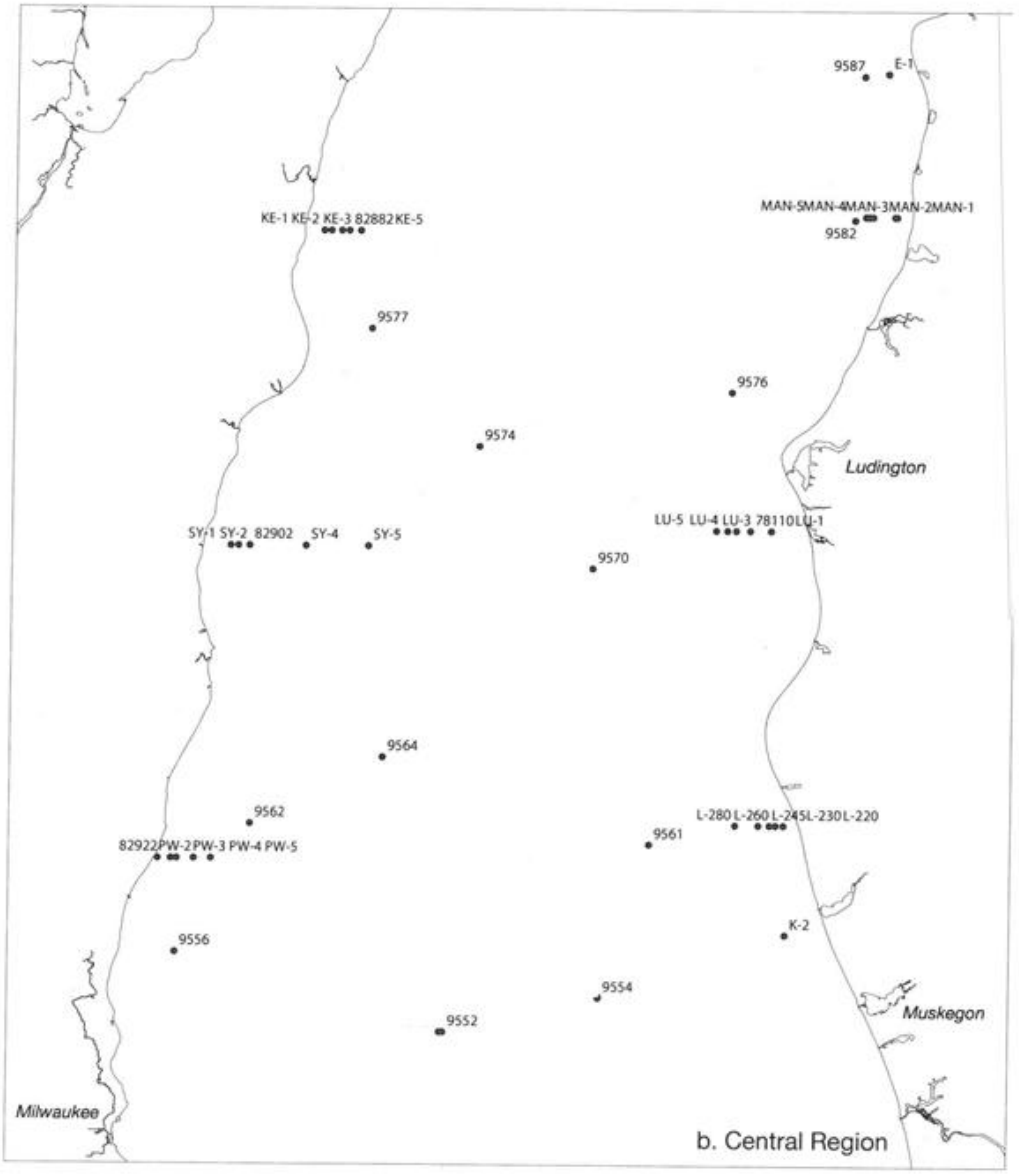

Figure 1b. Location of sampling sites in the central region of Lake Michigan in 2015.

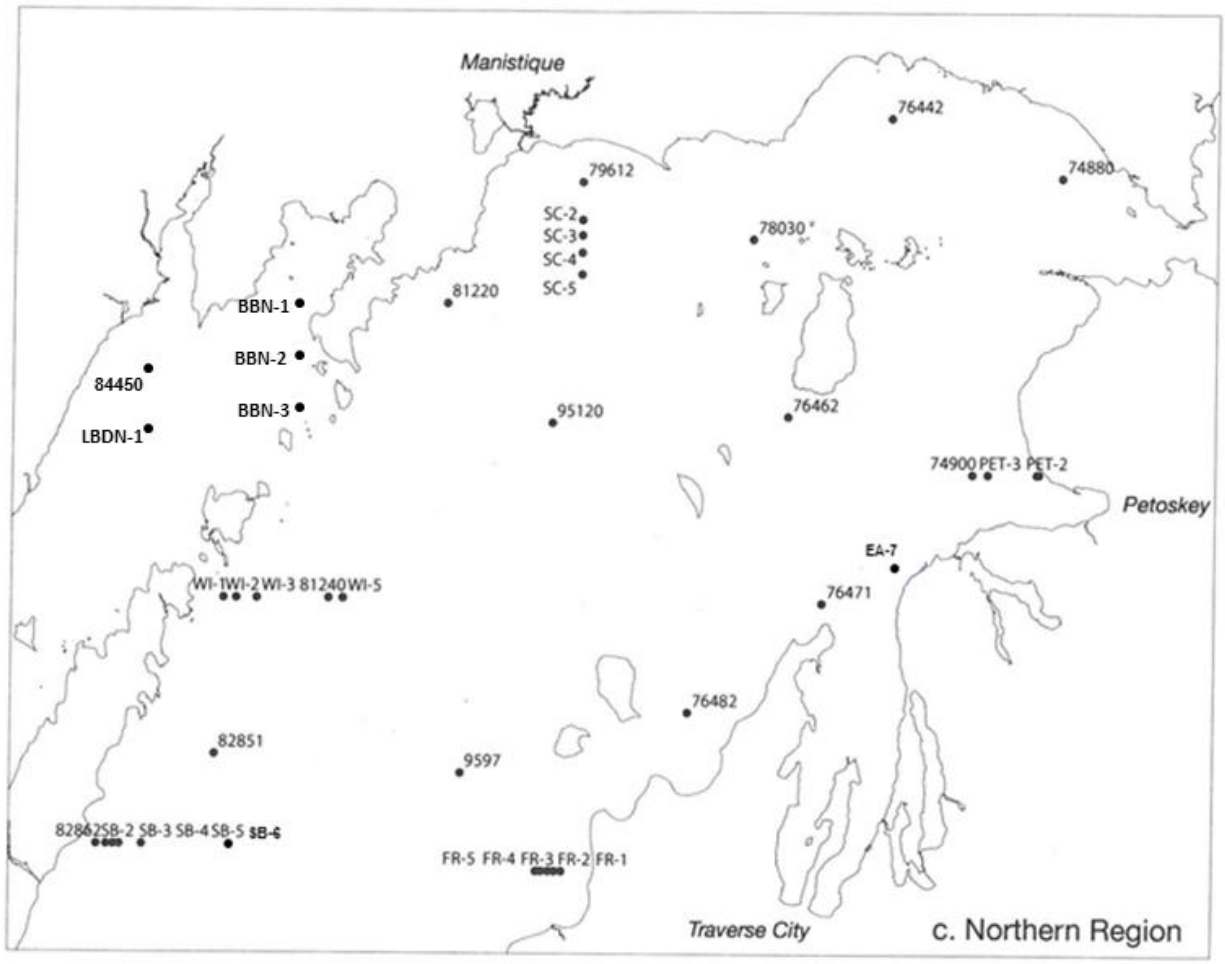

Figure 1c. Location of sampling sites in the northern region of Lake Michigan in 2015.

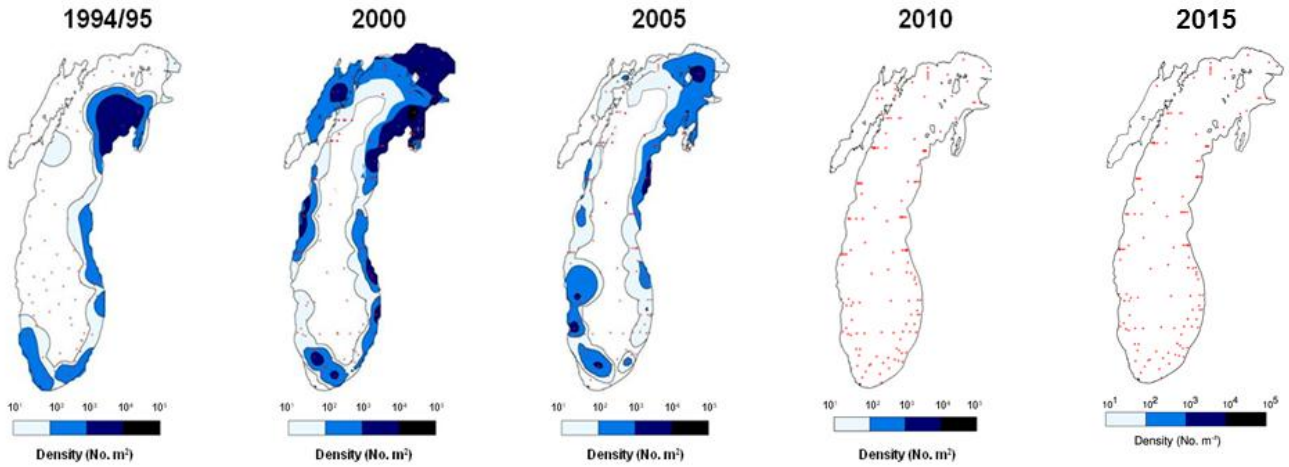

Figure 2. Density (no. per m^2) of *Dreissena polymorpha* in Lake Michigan based on lake-wide surveys in 1994/1995, 2000, 2005, 2010, and 2015. Small red dots indicate location of sampling sites.

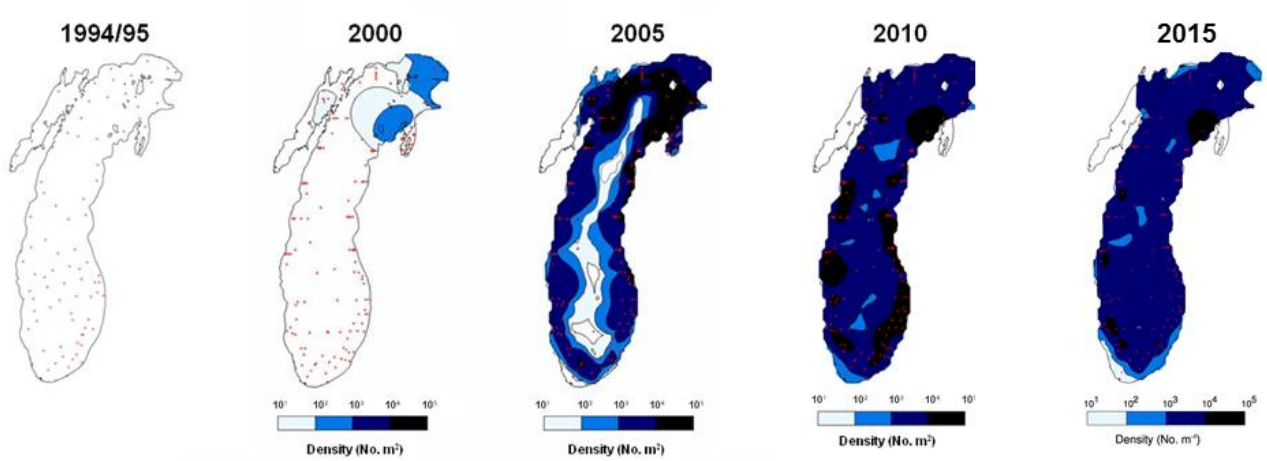

Figure 3. Density (no. per m^2) of *Dreissena r. bugensis* in Lake Michigan based on lake-wide surveys in 1994/1995, 2000, 2005, 2010, and 2015. Small red dots indicate location of sampling sites.

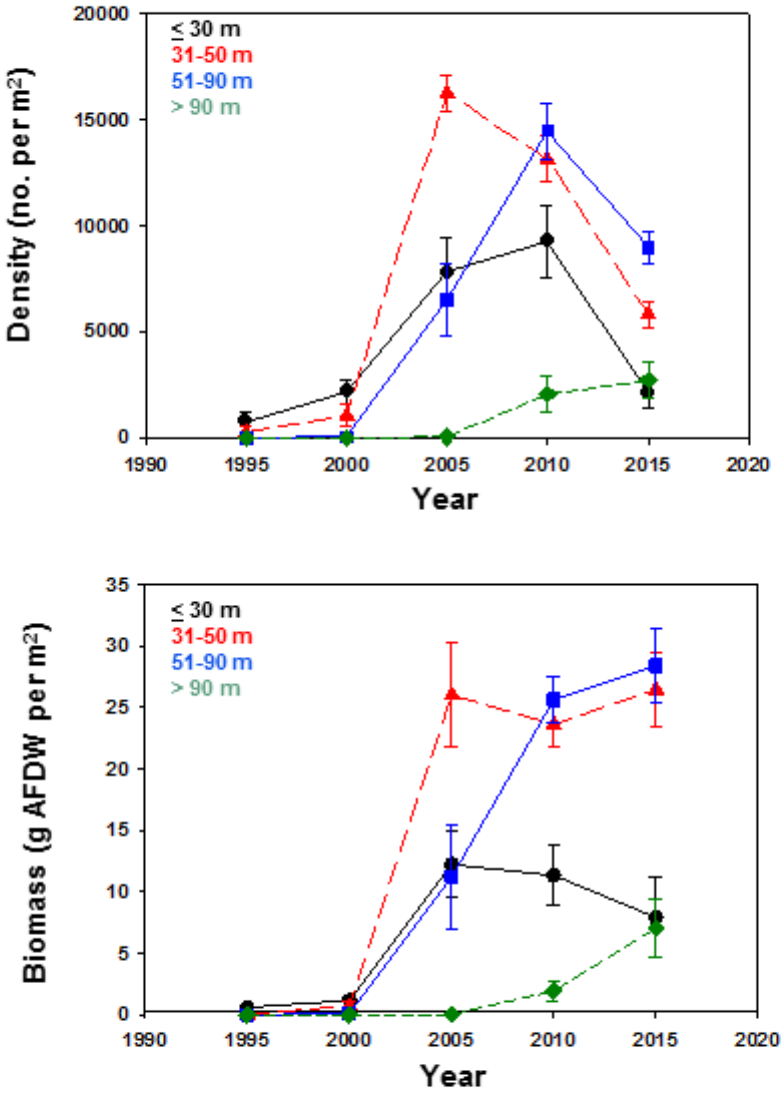

Figure 4. Long-term trends of total *Dreissena* in Lake Michigan in 1994/1995, 2000, 2005, 2010, and 2015. Values given are lake-wide means (± SE) at four depth intervals: ≤ 30 m (black, circles), 31-50 m (red, triangles), 51-90 m (blue, squares), and > 90 m (green, diamonds). Upper panel = density; lower panel = biomass.

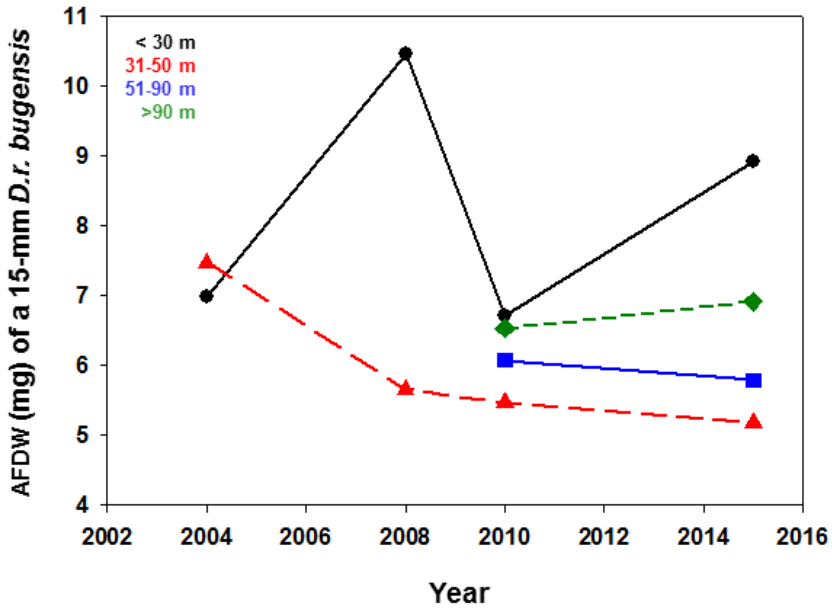

Figure 5. Ash free dry weight (AFDW, mg) of a standard 15-mm *D. r. bugensis* at four depth intervals intervals in Lake Michigan between 2004 and 2015. Values derived from regressions given in Table 4. Depth intervals: ≤ 30 m (black, circles), 31-50 m (red, triangles), 51-90 m (blue, squares), and > 90 m (green, diamonds).

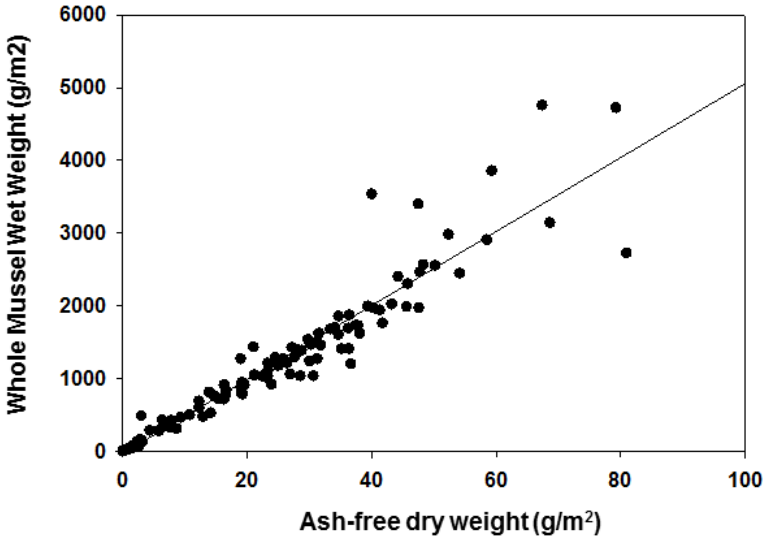

Figure 6. Relationship between ash free dry weight (AFDW) and total wet weight (TWW, whole mussel, tissue and shell) of *D. r. bugenisis* at each sampling site in the main basin of Lake Michigan in 2015 (n=135). The regression through the origin was defined as: TWW = 50.09*AFDW (R^2 = 0.92)

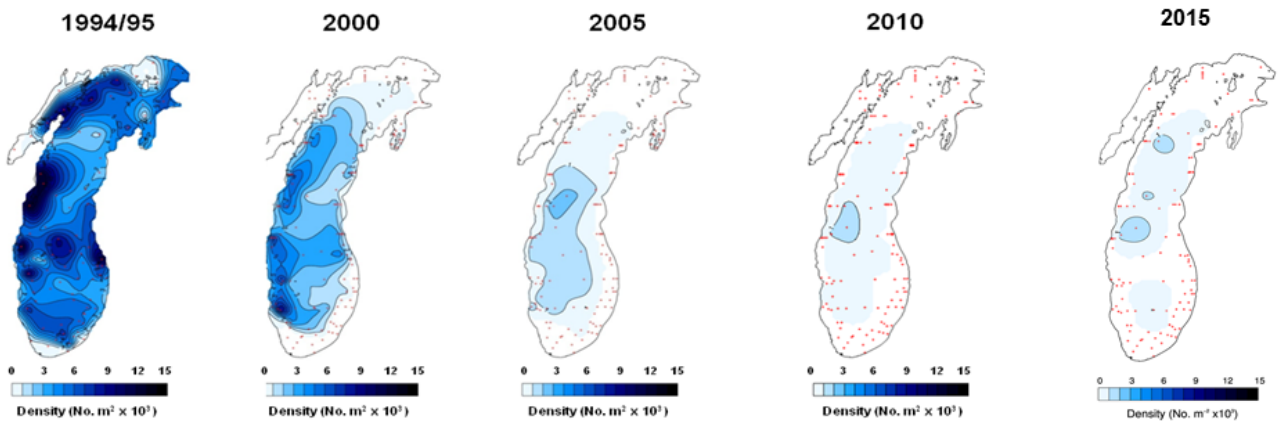

Figure 7 Density (no. per m^2) of *Diporeia spp.*in Lake Michigan based on lake-wide surveys in 1994/1995, 2000, 2005, 2010, and 2015. Small red dots indicate location of sampling sites.

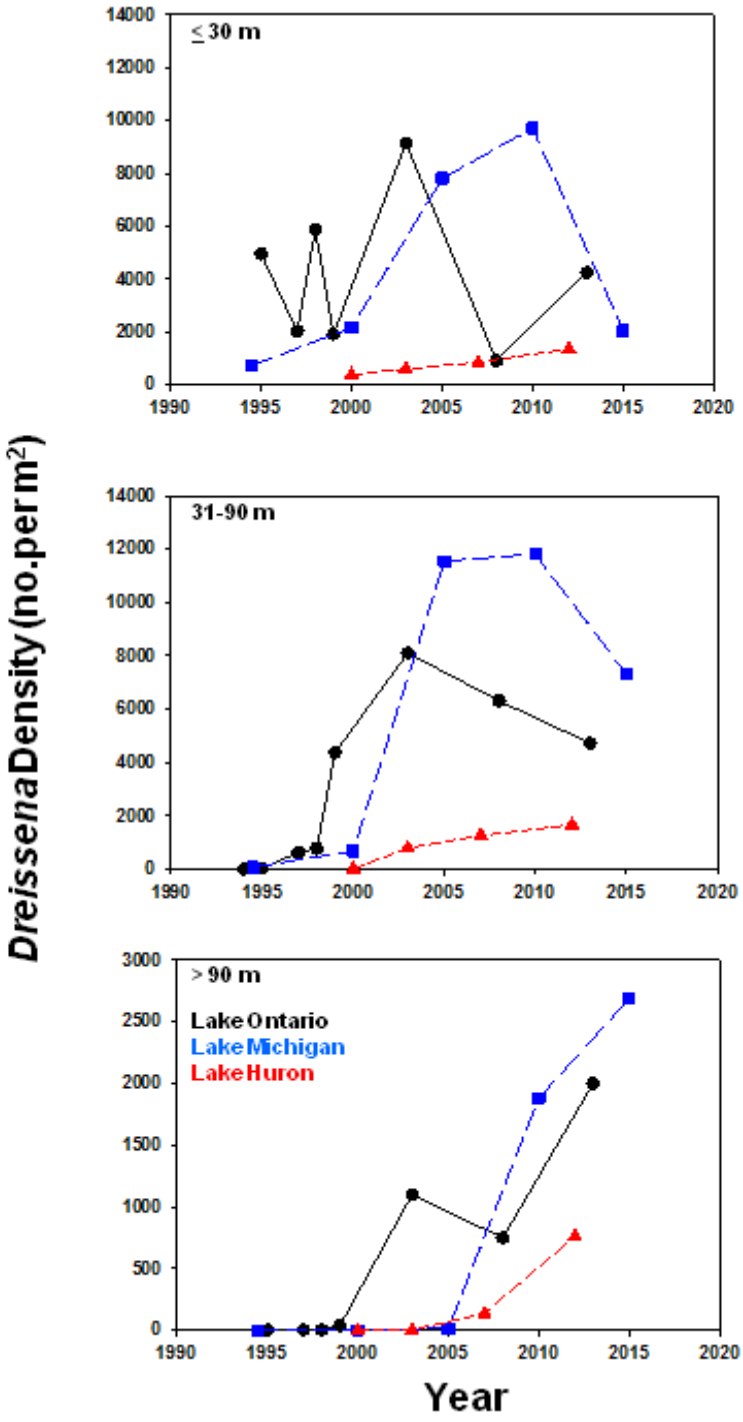

Figure 8. Density (no. per m^2) of total *Dreissena* at ≤ 30 m (upper panel), 31-90 m (middle panel), and > 90 m (lower panel) in Lake Ontario (black, circle), Lake Michigan (blue, square), and Lake Huron (red, triangle). Values taken from the following sources: Lake Ontario (Birkett et al. 2015, Nalepa and Elgin unpublished), Lake Michigan (Nalepa et al. 2014, this study); Lake Huron (Nalepa et al. 2007, Nalepa unpublished). Note the different scale for the > 90 m interval.

A summary of Mid-Continent Ecology Division Efforts Associated With the 2015 Lake Michigan Cooperative Science Monitoring Initiative (CSMI)

- **Water Quality and Lower Trophic Level Summary from the 2015 Lake Michigan CSMI -** Anett Trebitz, Anne Cotter, Joel Hoffman
  USEPA Mid-Continent Ecology Lab, Duluth, MN

- **Application of a Nutrient Model to Address Nearshore Phosphorus Levels in Lake Michigan -** James Pauer, Terry Brown, Tom Hollenhorst
  USEPA Mid-Continent Ecology Lab, Duluth, MN

- **"Data in Motion" - Continuous Water Sensor Data Collection for the 2015 Lake Michigan CSMI -** Tom Hollenhorst[1], Laura Fiorentino[2], Paul McKinney[1], Terry Brown[1], Anett Trebitz[1], Joel Hoffman[1]
  [1]USEPA Mid-Continent Ecology Lab, Duluth, MN
  [2]NOAA - Center for Operational Oceanographic Products and Services, Chesapeake, VA

Water quality and lower trophic level summary from the 2015 Lake Michigan CSMI

Anett Trebitz, Anne Cotter, Joel Hoffman,

U.S. EPA Office of Research and Development, Mid-Continent Ecology Division, Duluth MN.

Background

Among the major research questions identified for the 2015 Lake Michigan Cooperative Science Monitoring Initiative (CSMI) was to better understand the distribution, abundance, and movement of nutrients and biota across nearshore-offshore gradients. To address this question, a comprehensive suite of biota and water quality data were collected according to a sampling design that consisted of eight onshore-offshore transects representing a gradient in nutrient loading (Fig. 1). Three of the transects were placed away from tributaries (e.g., "no load"), two were positioned at "low load" tributaries, and three were positioned at "high load" tributaries. The loads were determined by averaging, across 2002 through 2004, the annual total phosphorus loading estimates generated by Dolan and Chapra (2012). To resolve spatial and temporal dimensions of this nearshore-offshore gradient, each transect was sampled at a shallow (~18m) mid (~46m) and deep (~110m) station with sampling repeated in each of three seasons (May, July, September). Sampling was accomplished via an interagency collaboration that included U.S. Environmental Protection Agency (EPA), National Oceanic and Atmospheric Administration (NOAA0, and the United States Geological Survey (USGS) as well as various academic partners.

Data collection under CSMI included both traditional station-based sampling (e.g., for water and biota) as well as continuous transect-based sampling (e.g., with towed sensor arrays or glider technology). Here, we examine station-based data from the 2015 Lake Michigan CSMI with respect to water quality patterns (e.g., nutrients, planktonic chlorophyll) and lower trophic level patterns (carbon and nitrogen stable isotopes as food-web tracers). For context, we also draw on long-term monitoring data from Lake Michigan that is collected annually by the EPA Great Lakes National Program Office ("GLNPO monitoring data", hereafter). This long-term monitoring focuses on mid-lake locations, in contrast to the CSMI 2015 effort which sought specifically to elucidate the nearshore-to-offshore pattern.

Spatial patterns and temporal trends in water quality

The 2015 CSMI sampling design was intended to contrast nearshore vs. further offshore water quality across transects, and permit examining the influence of differing tributary loading (including absence of tributaries) on open-lake water quality. Since watershed landuse is a major driver of nutrient loading to the Great Lakes (Han et al. 2011, Robertson and Saad 2011) and since hydrodynamic features such as shore-parallel thermal bars and longshore currents tend to "trap" watershed-derived inputs relatively close to shore (e.g., Bolgrien and Brooks 1992, Beletsky and Schwab 2008, Yurista et al. 2015), we had expected to find among-transect differences in productivity (e.g., nutrients and planktonic chlorophyll) to be associated with tributary loading, and to find an onshore-offshore gradient in which shallow stations had higher nutrient and chlorophyll concentrations than deeper stations.

There was a suggestion of a positive relationship across transects between tributary phosphorus load and in-lake surface water total phosphorus (TP) concentration in spring (May data, Fig 2a) but none of the lines had significant linear regression slope (see Fig. 2 caption), and in summer (July) TP showed no relationship to tributary TP load at any station depth (Fig. 2b). In contrast, the slope of chlorophyll a (CHLA) in spring relative to tributary load was flat for all stations except the shallow one (Fig. 3a), but in summer CHLA had a positive relationship to tributary load at all station depths (Fig. 3b). The 2015 CSMI data did not support the expectation that TP would be higher at nearshore relative to deeper stations; rather the shallowest stations (in green in Fig. 2) had slightly lower TP levels than the deep station in both May and July. However, CHLA concentrations were slightly higher at shallow compared to mid-depth and deep stations, and the slope of the relationship to tributary loading was steeper at the shallow vs. the mid-depth or deep stations in both spring and summer (Fig. 3).

We did not present data for September in Figures 2 and 3 because occurrence of wind-driven upwellings complicate the interpretation of nearshore to offshore gradients (and because logistic constraints prevented sampling of two transects). Four of the six transects that were sampled in September had substantially colder surface water at the shallow than at the deep station, indicating cold benthic water being "pulled" up-slope behind surface waters that is being driven away from shore by strong lateral winds. Such upwelling events can be frequent and prolonged in Lake Michigan (Plattner et al. 2006), and the September CSMI data, in which three of the four transects affected by upwelling are on the western side, is consistent with the Plattner et al. finding upwelling more prevalent along the western than eastern shoreline.

As mentioned above, EPA's GLNPO collects data annually for a set of offshore Lake Michigan stations, comparable to the deep CSMI stations but not to the mid-depth and shallow CSMI stations. Publications to date summarize these data only through 2012 (e.g., Barbiero et al. 2012, Dove and Chapra 2015, Mida et al. 2010), so for context to the 2015 CSMI we include plots here that extend the GLNPO station timeseries through 2015. For TP, the plots (Fig. 4) continuance confirm patterns already noted in the above publications, namely that concentrations remain low relative to the 1980s and early 1990s, that summer concentrations remain slightly lower than spring concentrations, and that differences between deep (~100m stations) and extra-deep stations (~150m) early in the time series are no longer evident. For CHLA, the extended the time series (Fig. 5) confirms that concentrations have remained approximately level over the last decade, that intra-annual variability remains lower now than during the 1980s and early 1990s, that marked differences between spring and summer CHLA early in the time series no longer exist, and that concentrations at deep stations remain slightly less than at extra-deep stations.

In contrast to the strong data record for offshore station, very little nearshore data is archived in the GLNPO long-term dataset. Spatially well-distributed data for regions of Lake Michigan shallower than 100 m are available only for the early 1980s. The 2015 CSMI thus provides a picture of nearshore spatial patterns in Lake Michigan that has been unavailable for many years. For TP (Fig. 6 left-hand panels), boxplots show no indication of levels being higher at shallower relative to deeper stations in either spring or summer and in either 1983 (GLNPO monitoring data) or 2015 (CSMI data). In other words, the TP data show no evidence for the expectation that nutrient levels would be highest closest to the shoreline from which the loading presumably emanates. In contrast, patterns among nearshore depths are quite different between 1983 and 2015 and between seasons for CHLA (Fig. 6 right-hand panels). In 1983 (GLNPO monitoring data), box-plots for both spring and summer show a steadily increasing level of

CHLA from the deep to mid-depth to shallow stations, with the CHLA magnitude and the difference among depths being largest in spring. In 2015 (CSMI data), box-plots do not show CHLA differences among depths in spring and the pattern of differences among depths in summer is the opposite of the pattern seen in 1983.

Taken together, the water quality spatial and temporal patterns presented here are consistent with previous findings (e.g., Fahnenstiel et al. 2010, Rowe et al. 2017, Yousef et al. 2017) of long-term declines in TP and CHLA and temporal (spring vs. summer) decoupling of nutrients to plankton production coincident with the arrival of dreissenid mussels. The results also provide support for the prediction that dreissenid mussels would substantially alter spatial patterns of water quality across the nearshore-offshore gradient (Hecky et al. 2004, Nalepa et al. 2010, Yousef et al. 2017). However rather than increasing nearshore CHLA as might be expected were dreissenids increasingly retaining and cycling nutrients in the nearshore (the "nearshore shunt" hypothesis), our findings suggest that dreissenid action is instead producing a homogenization of conditions horizontally (i.e., across depth gradients) in Lake Michigan – which may also be responsible for the quite muted tributary loading response we observed.

Spatial patterns and temporal trends in biota stable isotopes

We also examined spatial patterns of the carbon and nitrogen stable isotope composition in zooplankton, quagga mussel (*Dreissena bugensis*), and other benthic invertebrates (oligochaetes). The carbon stable isotope composition (i.e., its $\delta^{13}C$ value) is a diet tracer; the $\delta^{13}C$ value of an organism reflects the isotopic composition of its prey ("you are what you eat"; Peterson and Fry 1987). If organisms have different $\delta^{13}C$ values, this reveals they are eating different prey. In contrast, the nitrogen stable isotope composition ($\delta^{15}N$ value) traces both nitrogen source and trophic level. Previous studies in the Great Lakes demonstrated that an enrichment of ^{15}N in the food web (as measured by tissue samples of invertebrates, fish, or both) in either coastal wetlands or nearshore waters (<10 m depth) was related to increased dissolved nutrients in coastal waters, as well as increased urban and agricultural activity in the watershed (Peterson et al. 2007, Hoffman et al. 2012). If these human sources of nitrogen strongly influence the food web, then we expect higher $\delta^{15}N$ values in organisms captured in the nearshore compared to the offshore, with the highest $\delta^{15}N$ values associated with high N concentrations near rivers with relatively large nutrient loads to Lake Michigan (e.g,. St. Joseph River). Moreover, there is a consistent enrichment with ^{15}N with trophic level, such that consumers that feed higher in a food web will have higher $\delta^{15}N$ values than those feeding lower on the food web (Vander Zanden and Rasmussen 2001).

Here, we focus on large zooplankton (those that were retained by a filter with a 153 μm nominal pore size) and adult quagga (those with a shell length >15 mm), which were generally captured at most or all stations sampled. Oligochaetes were also found in sediment dredge samples, though at only a few stations. Among taxa, we observed substantial isotopic variation associated with depth, with a shift from relatively low $\delta^{15}N$ values and high $\delta^{13}C$ values in shallow, nearshore waters (18 m depth) to higher $\delta^{15}N$ values and lower $\delta^{13}C$ values in offshore waters (110 m depth; Fig. 7). For both zooplankton and quagga mussel, there was a statistically significant different among depths in both $\delta^{13}C$ and $\delta^{15}N$ values (ANOVA; $\delta^{13}C$ zooplankton: $p=0.003$, $\delta^{13}C$ quagga: $p=0.048$, $\delta^{15}N$ zooplankton: $p=0.030$, $\delta^{15}N$ quagga: $p<0.001$;

data generally met assumption of normality except quagga $\delta^{13}C$ values, for which a Kruskal-Wallis test was used). The magnitude of the shift in $\delta^{15}N$ values is much larger than that in $\delta^{13}C$ values. These $\delta^{15}N$ patterns are consistent with previous observations regarding nitrogen cycling in Lake Michigan, where offshore enrichment in ^{15}N reflects is likely caused by relatively high denitrification rates in sediment (Gardner et al. 1987). The shift in $\delta^{13}C$ is consistent with either a greater contribution of nearshore carbon sources to the food web (benthic algae) or higher production compared to offshore waters (or both; Sierszen et al. 2014). The relatively low $\delta^{15}N$ values in nearshore water suggests that sampling at this depth (18 m) was not sensitive to inputs of anthropogenic nitrogen. Among taxa, zooplankton and quagga mussel were much more isotopically similar to each other than to the oligochaetes, which were relatively ^{15}N- and ^{13}C-enriched (Fig. 7). The oligochaete we sampled were embedded among the byssal threads of the quagga mussels. The enriched isotopic composition implies they were feeding in a microbial food web, consuming either particles colonized and processed by sediment bacteria, the bacteria itself, or both. This is a distinct food web pathway from zooplankton and quagga mussel.

Comparing the zooplankton and quagga mussel, the question arises as to whether they are consuming the same food items, as indicated by their isotopic composition. We found a seasonal shift in the difference between zooplankton and quagga mussel (Fig. 8). In May, their isotopic composition was well-differentiated, indicating they were not feeding on the same algae or particles during the winter and spring. However, as summer progressed, they become increasingly isotopically similar, such that they were not different from each other by September. The observation that zooplankton and quagga mussel have relatively similar $\delta^{13}C$ and $\delta^{15}N$ values indicates they are potentially in competition for the exact same food source, presumably phytoplankton and sinking organic material largely composed of phytoplankton. Based on paired net samples, the zooplankton samples were largely composed of calanoid copepods (89.%, 75.5%, and 63.2% of biomass on average for the May, July, and September sampling events). The calanoids were mostly large species, including the grazer *Leptodiaptomus sicilis* and the omnivorous consumers *Senecella calanoides* and *Limnocalanus macrurus*. If they are in competition (i.e., particle density is limiting to growth), this implies that quagga mussel could exert a direct effect on the entire lake food web via competition with zooplankton. That is, quagga have the potential to reduce the energy available to the pelagic food web, which includes zooplankton, alewives, bloater, and Pacific salmon. The finding is notable because we would expect that quagga mussel and zooplankton are most likely to compete for food in the winter and spring when particle resuspension and mixing is occurring (Eadie et al. 1984), rather than in the summer when the lake is stratified.

References

Barbiero R.P., Lesht B.M. and Warren G.J. 2012. Convergence of trophic state and the lower food webs of lakes Huron, Michigan, and Superior. J. Great Lakes Res. 38: 368–380.

Beletsky, D., and Schwab, D. 2008. Climatological circulation in Lake Michigan, Geophys. Res. Lett., 35, L21604, doi:10.1029/2008GL035773.

Bolgrien, D.W. and Brooks, A.S. 1992. Analysis of thermal features of Lake Michigan from AVHRR satellite images. J. Great Lakes Res. 18: 259-266.

Dolan, D.N., and Chapra, S.C. 2012. Great Lakes total phosphorus revisited: 1. Loading analysis and update (1994-2008). J. Great Lakes Res. 38: 730-740.

Dove, A., and Chapra, S. C. 2015. Long-term trends of nutrients and trophic response variables for the Great Lakes. Limn. Ocean. 60(2): 696-721.

Eadie, B.J., Chambers, R.L., Gardner, W.S., and Bell, G.L. 1984. Sediment trap studies in Lake Michigan: resuspension and chemical fluxes in the southern basin. J. Great Lakes Res. 10:307-321.

Fahnenstiel, G. L., S. Pothoven, H. Vanderploeg, D. Klarer, T. Nalepa, and D. Scavia. 2010. Recent changes in primary production and phytoplankton in the offshore region of southeastern Lake Michigan. J. Great Lakes Res. 36(s3): 20–29.

Gardner, W.S., Nalepa, T.F., and Malczyk, J.M. 1987. Nitrogen mineralization and denitrification in Lake Michigan sediments. Limnol. Oceanogr. 32:1226-1238.

Han, H., Bosch, N. and Allan, J.D., 2011. Spatial and temporal variation in phosphorus budgets for 24 watersheds in the Lake Erie and Lake Michigan basins. Biogeochemistry, 102: 45-58.

Hecky, R. E., R. EH Smith, D. R. Barton, S. J. Guildford, W. D. Taylor, M. N. Charlton, and T. Howell. 2004. The nearshore phosphorus shunt: a consequence of ecosystem engineering by dreissenids in the Laurentian Great Lakes. Canadian J. Fish. Aquatic Sci. 61: 1285-1293.

Hoffman, J.C., Kelly, J.R., Peterson, G.S., Cotter, A.M., Starry, M., and Sierszen, M.E. 2012. Using $\delta^{15}N$ in fish as an indicator of watershed sources of anthropogenic nitrogen: response at multiple spatial scales. Estuaries and Coasts. 35:1453-1467.

Mida, J. L., Scavia, D., Fahnenstiel, G. L., Pothoven, S. A., Vanderploeg, H. A., & Dolan, D. M. 2010. Long-term and recent changes in southern Lake Michigan water quality with implications for present trophic status. J. Great Lakes Res. 36(s3): 42-49.

Nalepa, T. F., Fanslow, D. L., & Pothoven, S. A. 2010. Recent changes in density, biomass, recruitment, size structure, and nutritional state of Dreissena populations in southern Lake Michigan. J. Great Lakes Res. 36(s3): 5-19.

Peterson, B.J., and Fry, B. 1987. Stable isotopes in ecosystem studies. Ann. Rev. Ecol. Syst. 18: 293–320.

Peterson, G.S., Sierszen, M.E., Yurista, P.M., and Kelly, J.R. 2007. Stable nitrogen isotopes of plankton and benthos reflect a landscape-level influences on Great Lakes coastal ecosystems. J. Great Lakes Res. 33(s3): 27–41.

Plattner S., Mason D.M., Leshkevich G.A., Schwab D.J., Rutherford E.S. (2006), Classifying and forecasting coastal upwellings in Lake Michigan using satellite derived temperature images and buoy data, J. Great Lakes Res. 32: 63–76.

Robertson, D.M. and D.A. Saad, 2011. Nutrient Inputs to the Laurentian Great Lakes by Source and Watershed Estimated Using SPARROW Watershed Models. J. Am. Water Resources Assoc. 47: 1011-1033.

Rowe, M. D., Anderson, E. J., Vanderploeg, H. A., Pothoven, S. A., Elgin, A. K., Wang, J., and Yousef, F. 2017. Influence of invasive quagga mussels, phosphorus loads, and climate on spatial and temporal patterns of productivity in Lake Michigan: A biophysical modeling study. Limn. Ocean. 62: 2629-2649.

Sierszen. M.E., Hrabik, T.R., Stockwell, J.D., Cotter, A.M., Hoffman, J.C., and Yule, D.L. 2014. Depth gradients in food-web processes linking habitats in large lakes: Lake Superior as an exemplar ecosystem. Freshwater Biol. 59:2122-2136.

Vander Zanden, M.J., and Rasmussen, J.B. 2001. Variation in $\delta 1^{5}N$ and $\delta^{13}C$ trophic fractionation: Implications for aquatic food web studies. Limnol. Oceanogr. 46: 2061–2066.

Yousef, F., Shuchman, R., Sayers, M., Fahnenstiel, G., and Henareh, A. 2017. Water clarity of the Upper Great Lakes: Tracking changes between 1998–2012. J. Great Lakes Res. 43: 239-247.

Yurista, P. M., Kelly, J. R., Cotter, A. M., Miller, S. E., and Van Alstine, J. D. 2015. Lake Michigan: Nearshore variability and a nearshore–offshore distinction in water quality. J. Great Lakes Res. 41: 111-122.

Figure 1. Transects sampled by CSMI in 2015 and associated rivers and loading categories, overlain on a map of TP loading differences among shoreline locations. The map is excerpted from the Great Lakes Environmental Assessment Mapping Project website (http://data.glos.us/gleam/lake-stressors/nonpoint-pollution/phosphorus-loading.html), and is based on TP tributary loading data compiled over 1994-2008. and propagated into the lake assuming distance-based decay.

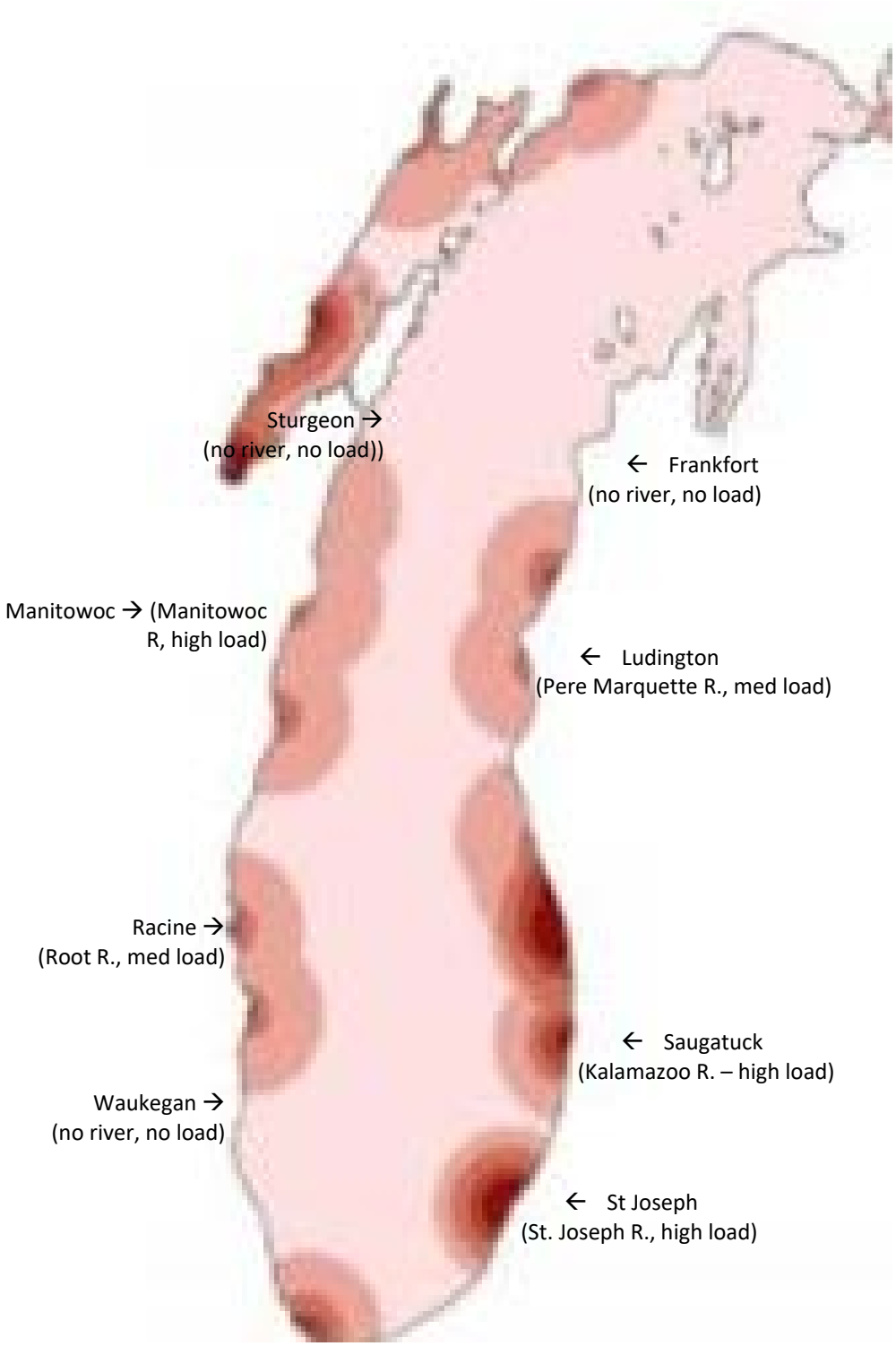

Figure 2. Graph showing relationship between surface-water TP measured on the May or July 2015 CSMI cruises vs. 2002-2008 avg annual TP loading from the adjacent tributary (the three no-tributary transects were assigned to zero load). The slopes of the lines in panel a) are not significantly different from zero in a linear least-squares regression.

.

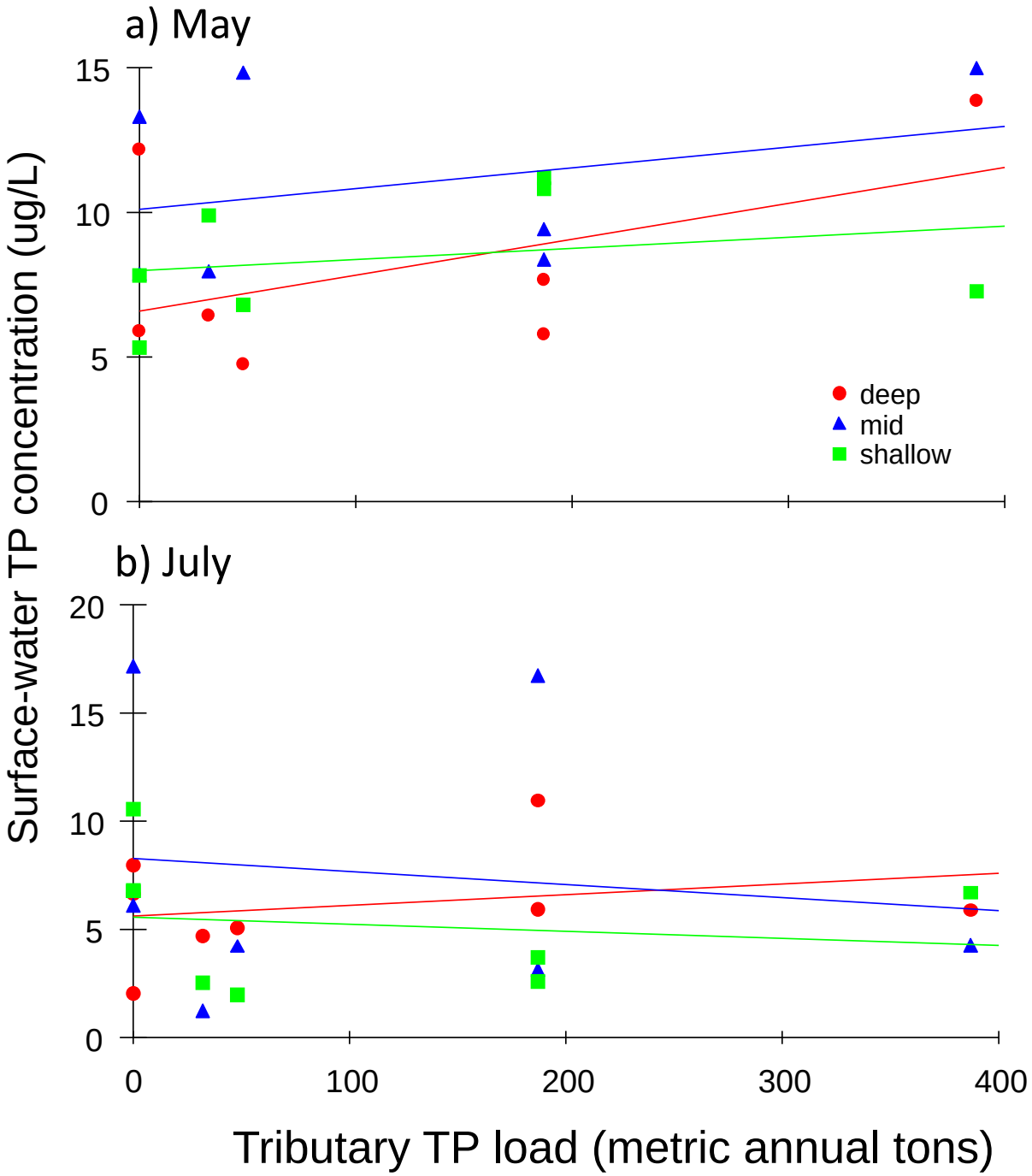

Figure 3. Graph showing relationship between surface-water planktonic CHLA measured on the May or July 2015 CSMI cruises vs. 2002-2008 avg annual TP loading from the adjacent tributary (the three no-tributary transects were assigned to zero load). The slopes of the shallow-depth line in panel a) is significantly different from zero in a linear least-squares regression (p=0.048) and the deep and shallow lines in panel b) have slopes significantly different from zero (<0.001 and 0.018, respectively) whereas the mid-depth line slope is not quite significant (p=0.071).

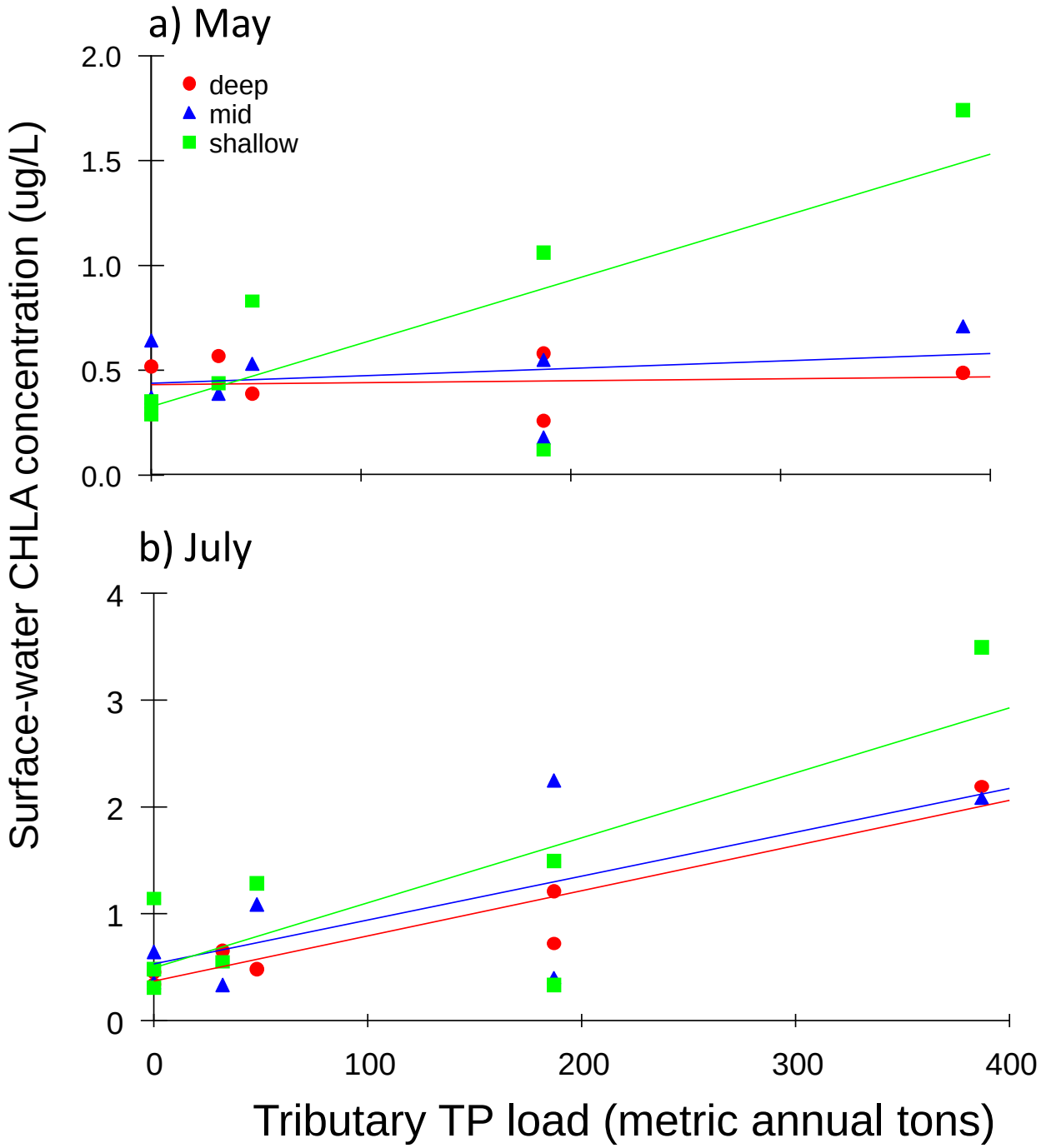

Figure 4. 1982-2015 time-series of upper-water column total phosphorous concentrations (mean ± 1 standard deviation) from a set of long-term monitoring stations (i.e., GLNPO monitoring data) measured in either spring (top panel; April or May) or summer (bottom panel; August or September). Stations were classified by lake depth as either deep (~100 m) or extra deep (<150 m). Plotted data meet the criteria of being from stations sampled 10+ years, from the epilimnion or upper water column layers, and from either late-spring (April or May) or late-summer (Aug/Sep).

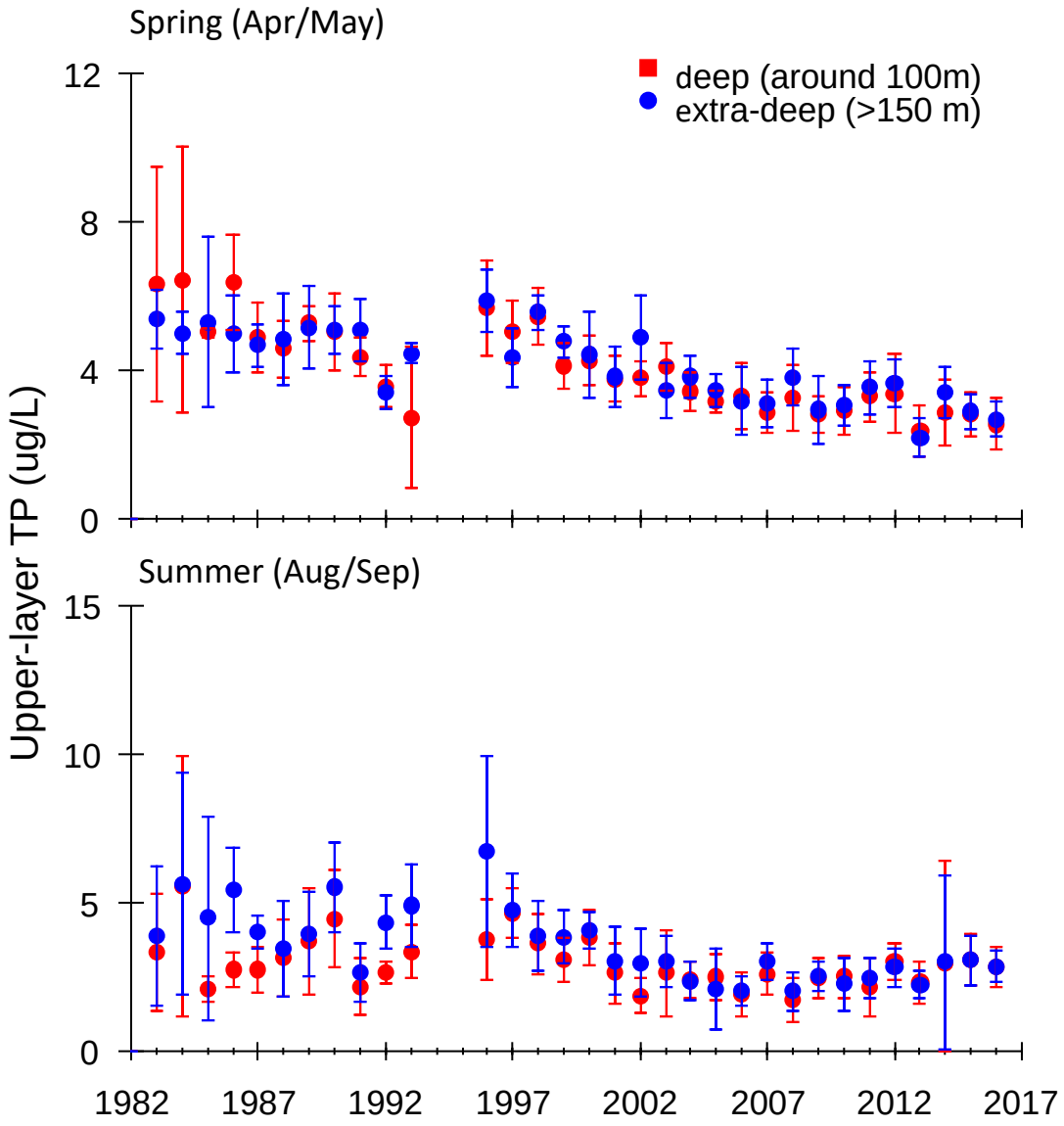

Figure 5. 1982 to 2015 time-series of upper-water column chlorophyll a (CHLA) concentration (mean ± 1 standard deviation) from a set of long-term monitoring stations (i.e., GLNPO monitoring data) measured in either spring (top panel; April or May) or summer (bottom panel; August or September). Stations were classified by lake depth as either deep (~100 m) or extra deep (<150 m). Plotted data meet the criteria of being from stations sampled 10+ years, from the epilimnion or upper water column layers, and from either late-spring (April or May) or late-summer (Aug/Sep).

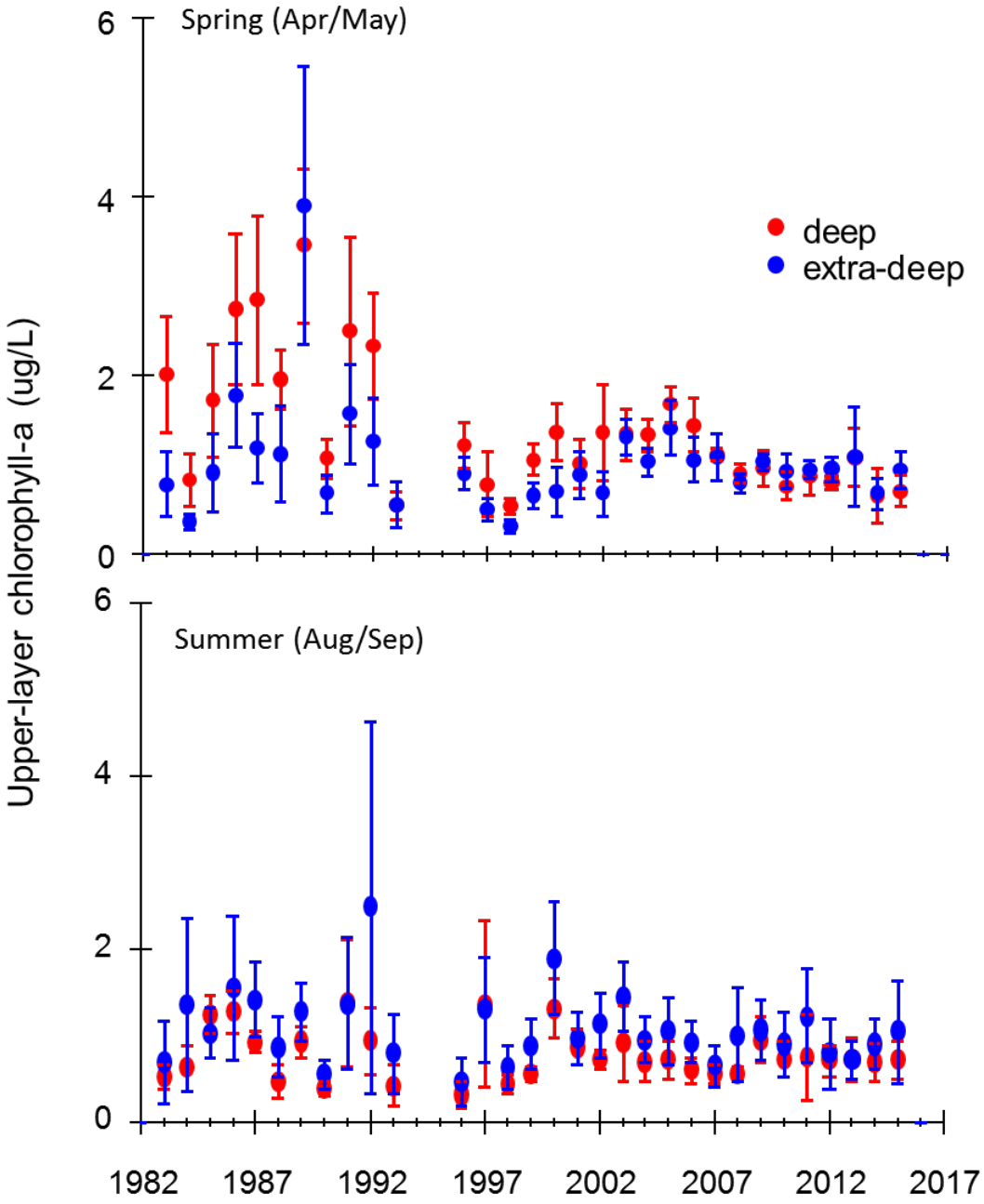

Figure 6. Box plots comparing levels of TP (left panels) and CHLA (right panels) across depths in 1983 (GLNPO monitoring data) relative to 2015 CSMI stations. Stations were classified as shallow if bottom depth was <30m, mid-depth if 30-60m, and deep if 70-120m. Top panels are for spring, bottom panels for summer. Data for multiple sampling depths (e.g., upper water-column as well as near-bottom) are included. Because the GLNPO database has historic data for mid-depth and shallow stations only in 1983, this comparison is not possible for intervening years.

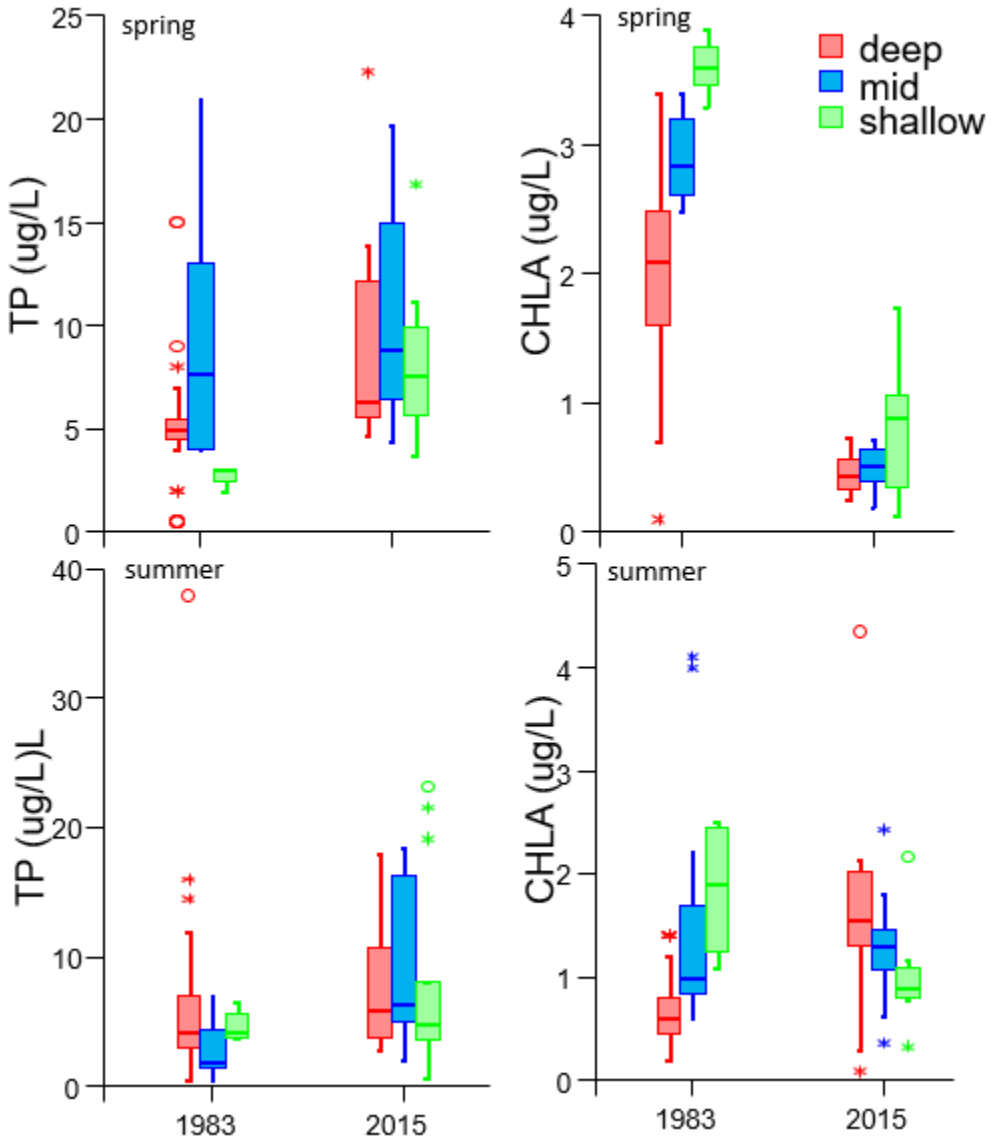

Figure 7. Carbon (A) and nitrogen (B) stable isotope ratios of quagga mussel, zooplankton (Zoop.), and oligochaetes (Oligo.) at the 18 m (left), 46 m (center), and 110 m (right) stations. Sample sizes are given in italics (same for $\delta^{13}C$ and $\delta^{15}N$ values). Box plots show median, quartiles, and outliers.

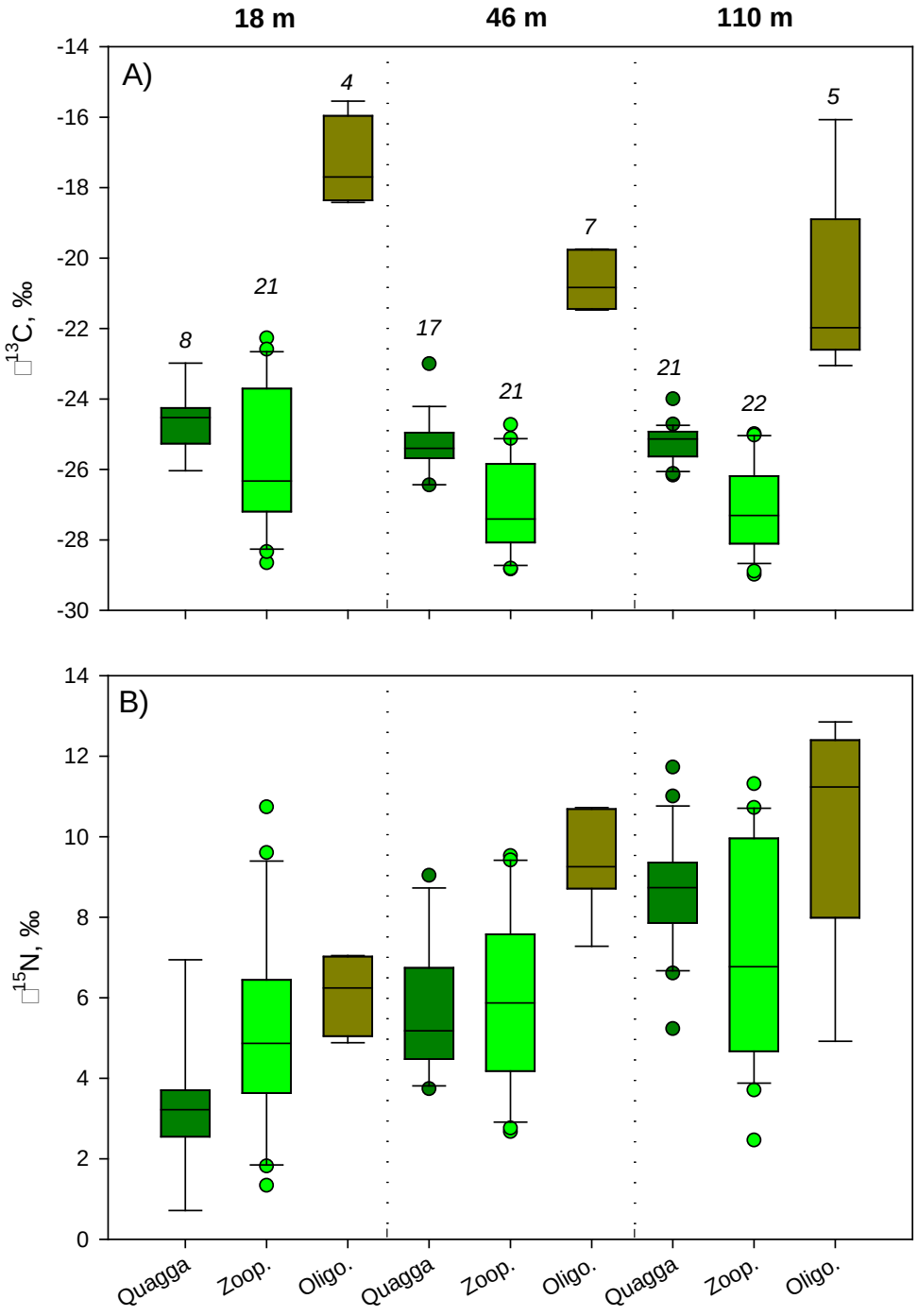

Figure 8. The difference between zooplankton and quagga mussel carbon (A) and nitrogen (B) stable isotope ratios by month (May, July, September). Values below the line indicate zooplankton have a lower $\delta^{13}C$ or $\delta^{15}N$ value than quagga mussel, and vice versa for values above the line. Box plots show median, quartiles, and outliers.

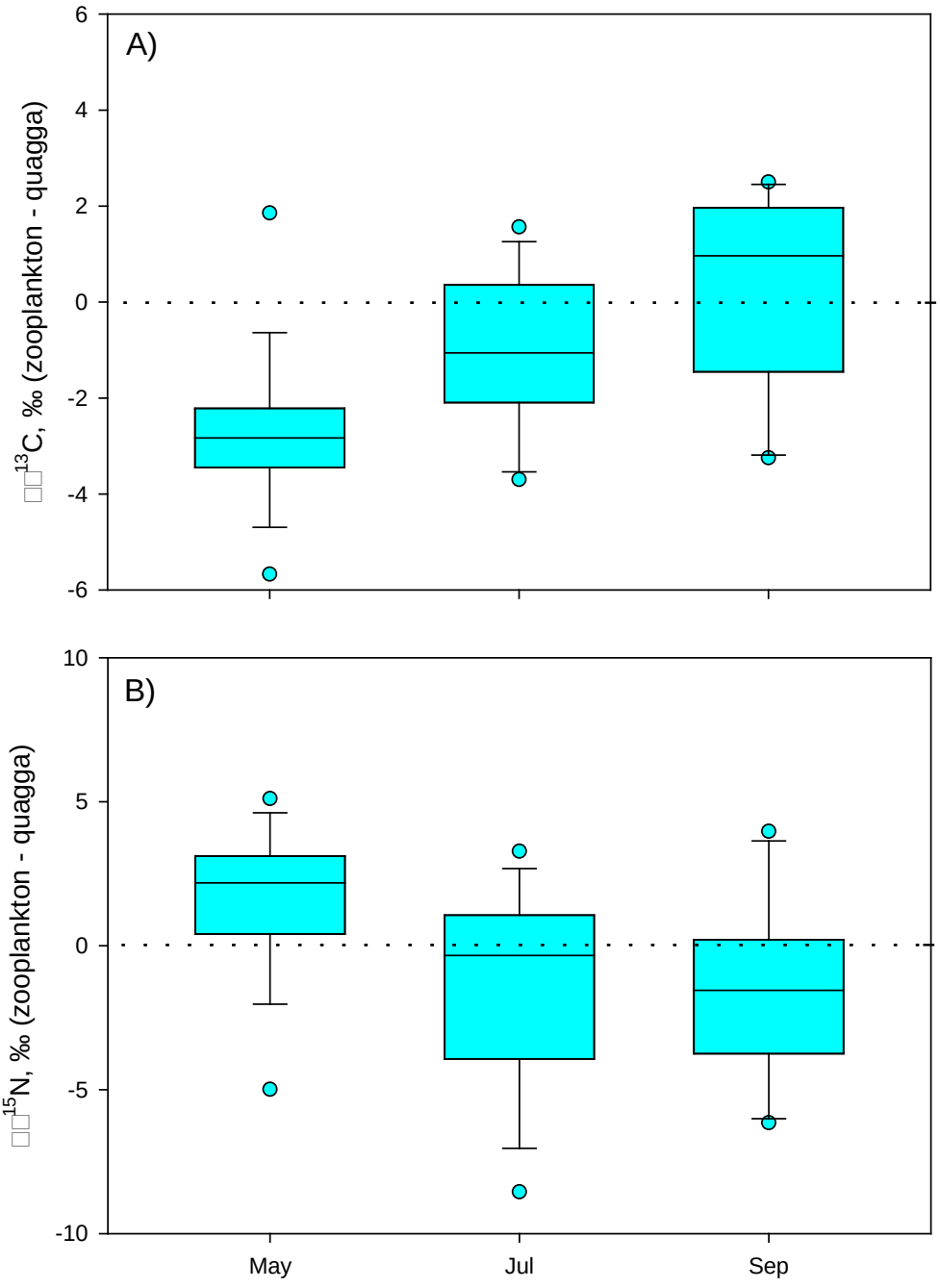

Application of a Nutrient Model to Address Nearshore Phosphorus Levels in Lake Michigan

James Pauer, Terry Brown, Tom Hollenhorst,
U.S. EPA Office of Research and Development, Mid-Continent Ecology Division, Duluth MN.

Introduction

Concerns with the nearshore water quality of the Laurentian Great Lakes, such as excessive eutrophication and harmful algal blooms, called for establishing a nearshore monitoring program and an improved understanding of the watershed-nearshore link (Great Lakes Water Quality Agreement, 2012). This is challenging, as sporadic runoff events and varying circulation patterns cause the nearshore to be dynamic and exhibit large spatial and temporal gradients. The Grand River is the largest discharger of phosphorus directly into Lake Michigan with the potential of causing high levels of nutrient and phytoplankton at the discharge point which is close the Grand Haven, Michigan (Figure 1). Mathematical models are powerful tools to understand nearshore nutrient circulation, identify the main drivers of phosphorus in the nearshore, and to assist stakeholders with management options to improve or maintain water quality. The objective of this study is to investigate the impact of tributary phosphorus loadings and lake circulation on the nearshore areas of southeastern Lake Michigan using a mathematical model and observational data. This study will explore how these drivers influence the nearshore phosphorus levels temporally and spatially. This work will be expanded in the future to address nearshore algal dynamics. A second study objective is to develop a simple, transparent and transportable tool to be easily applied in other ecological sensitive areas in Lake Michigan and the other Great Lakes.

Methods

A study area on the southeastern side of Lake Michigan was selected around the Grand and Muskegon rivers, two tributaries that contribute substantial phosphorus loadings to the eastern shore of the lake. The study area focuses on the nearshore within approximately 25 miles from the coast. The model has a computational grid of 5476 small (1km x 1km) completely mixed cells (Figure 1). The nearshore circulation (hydrodynamics) was provided by the US Naval Research Lab (Stennis, MS). The model used simple phosphorus kinetic equations similar to the lakewide phosphorus model developed by Chapra and Dolan (2012). The Cooperative Science Monitoring Initiative (CSMI) results were used to estimate boundary and initial conditions, and to ground-truth the model. No tributary loadings measurements were available beyond 2008, and therefore loadings were estimated looking at historical loading trends (Dolan and Chapra, 2012, Rossmann, 2006) and limited tributary measurements from the 2015 Lake Michigan CSMI. Due to the uncertainty with these loading estimates, we also investigating the impact of alternative tributary loads on model results.

Results and Discussion

Using the estimated (base) total phosphorus (TP) loadings, this relatively simple model somewhat over-predicts the 2015 TP observations. (Figure 2). The model prediction was higher than the observations at a number of locations very close to the Grand River. Model prediction that were much higher than the corresponding observations were also much more variable, intimating how dynamic and variable the nearshore can be (top-left of Figure 2). A possible reason for this discrepancy is a too high TP loading estimate for 2015, although the timing of the loading and the accuracy of the circulations might also contribute to the high model predictions. Running the model with lower TP loads (30% reduction of the base loads), the results has a tighter fit to the observations, although it still over-predicts the same observations close to the Grand River (Figure 3). We will further investigate the sensitivity of the loading estimate, timing of the loads, and lake circulation on the model results using the 2015 CSMI dataset, as well as data from other, previous sampling efforts.

Figure 4 shows spatial patterns of phosphorus in the nearshore of Lake Michigan at two dates in summer of 2015. The model results show that the nearshore close to the river discharges and within 1-3 km of the shore is often strongly impacted by the river's loads, but the nearshore phosphorus pattern can also change significantly. Phosphorus at deeper areas of the nearshore and further away from the discharge locations were much lower and approaching off-shore TP concentrations. Future analyses will investigate how TP loadings and circulation patterns impact the nearshore concentrations spatially and temporally.

This model, with limitations such as using simple phosphorus kinetic formulations and estimated rather than measured phosphorus loadings, demonstrates that Lake Michigan tributaries (watershed loading) can cause high phosphorus concentrations in the nearshore, but that it is limited to zones of impact that can change relatively rapidly depending on the nearshore circulation. We believe values from the model summarized spatially and temporally have potential to help guide future nutrient criteria development efforts for the near shore. This work also demonstrate that a simple model can be useful in guiding managers in making water quality decisions, and such a model can easily be applied to other locations in Lake Michigan and the Great Lakes. However, these models need to be thoroughly tested at these locations before any model predictions should be made.

References

Chapra, S.C., Dolan, D.M., 2012. Great Lakes total phosphorus revisited: 2. Mass balance modeling. J. Great Lakes Res. 38 (4), 741–754.

Dolan, D.M., Chapra, S.C. 2012. Great Lakes total phosphorus revisited: 1. Loading analysis and update (1994–2008). J. Great Lakes Res. 38 (4), 730–740.

Great Lakes Water Quality Agreement. Protocol Amending the Agreement between Canada and the United States of America on Great Lakes Water Quality, 1978, as Amended on October 16, 1983, and on November 18, 1987, Signed September 7, 2012, Entered into force February 12, 2013. http://ijc.org/files/tinymce/uploaded/GLWQA%202012.pdf (2012)

Rossmann, R., 2006. Results of the Lake Michigan Mass Balance Project: Polychlorinated Biphenyls Modeling Report. USEPA, Large Lakes Research Station, Grosse Ile, MI (2006), p. 621

LMMB Project, 2006. Results of the Lake Michigan Mass Balance Project: Polychlorinated Biphenyls. (Ed. Ronald Rossmann), pp579, Grosse Ile, MI

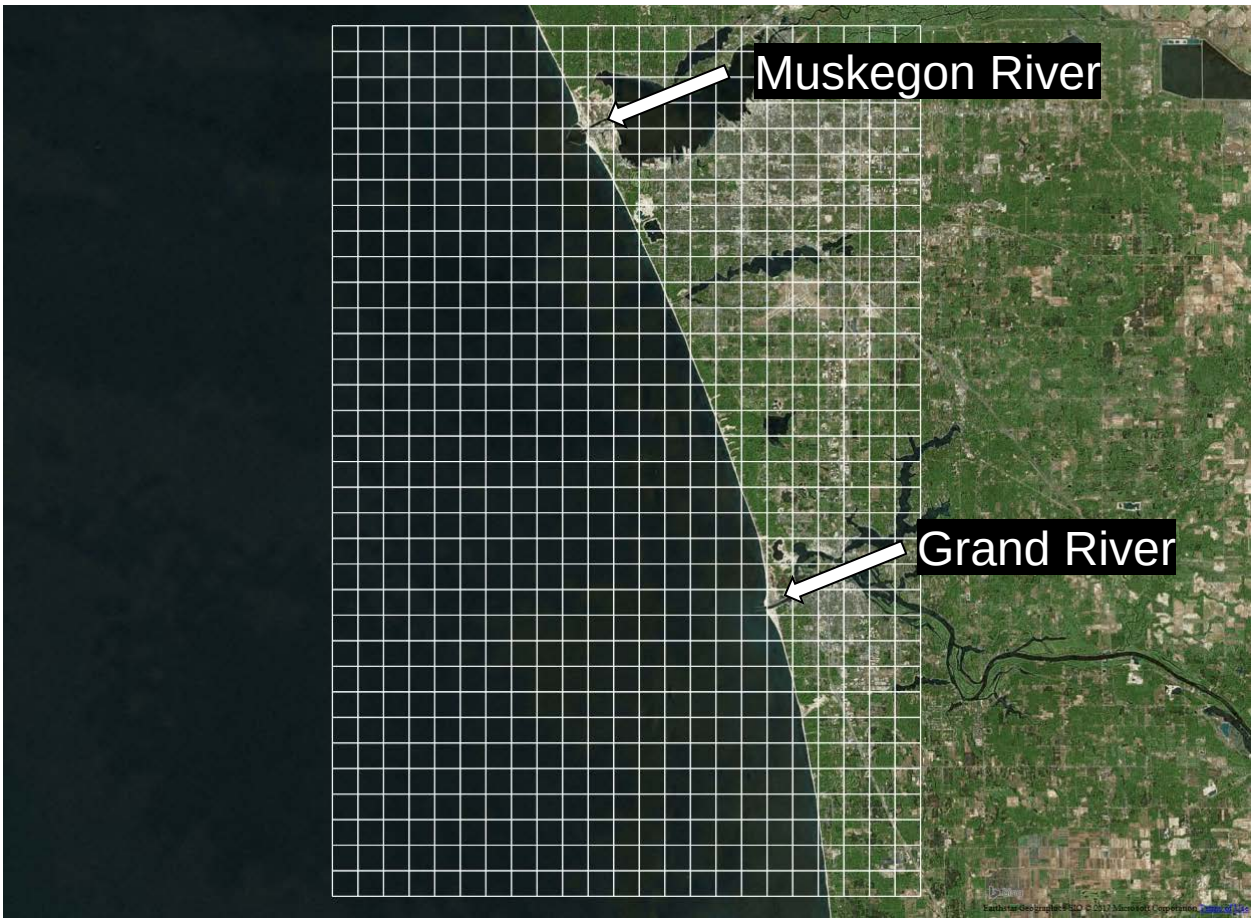

Figure 1: Computational grid (1km x 1km) of the study area. The area is southeast Lake Michigan adjacent to the Muskegon and Grand Rivers.

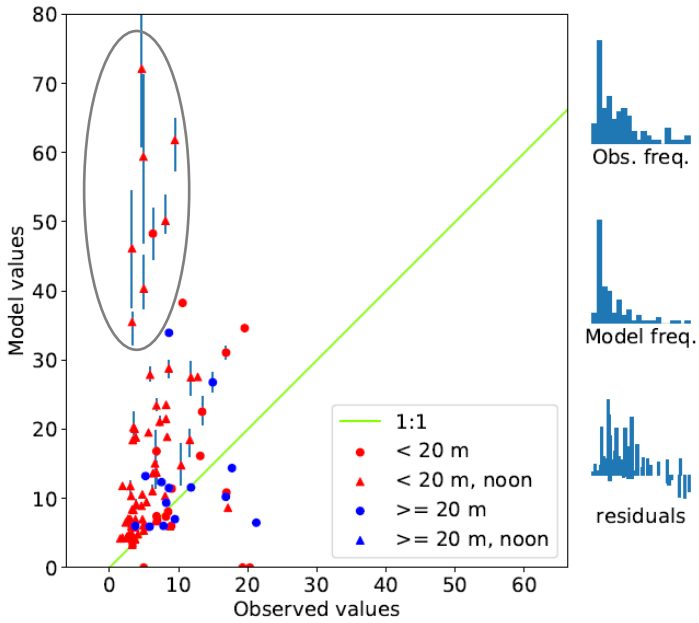

Figure 2: Model phosphorus results versus observational data (in µg/L): Base TP load. The circled area highlights areas where model prediction was much higher and variable than the observations.

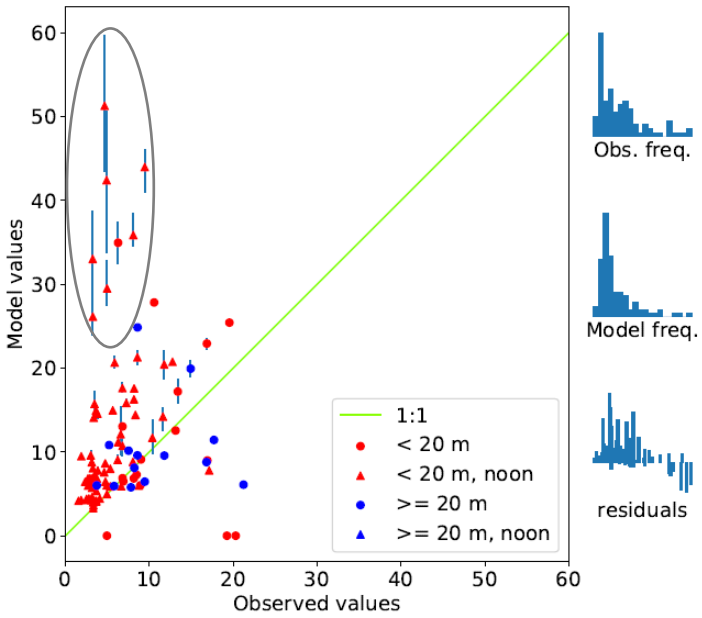

Figure 3: Model phosphorus results versus observational data (in µg/L): 30% reduction of the base TP load. The circled area highlights areas where model prediction was much higher and variable than the observations.

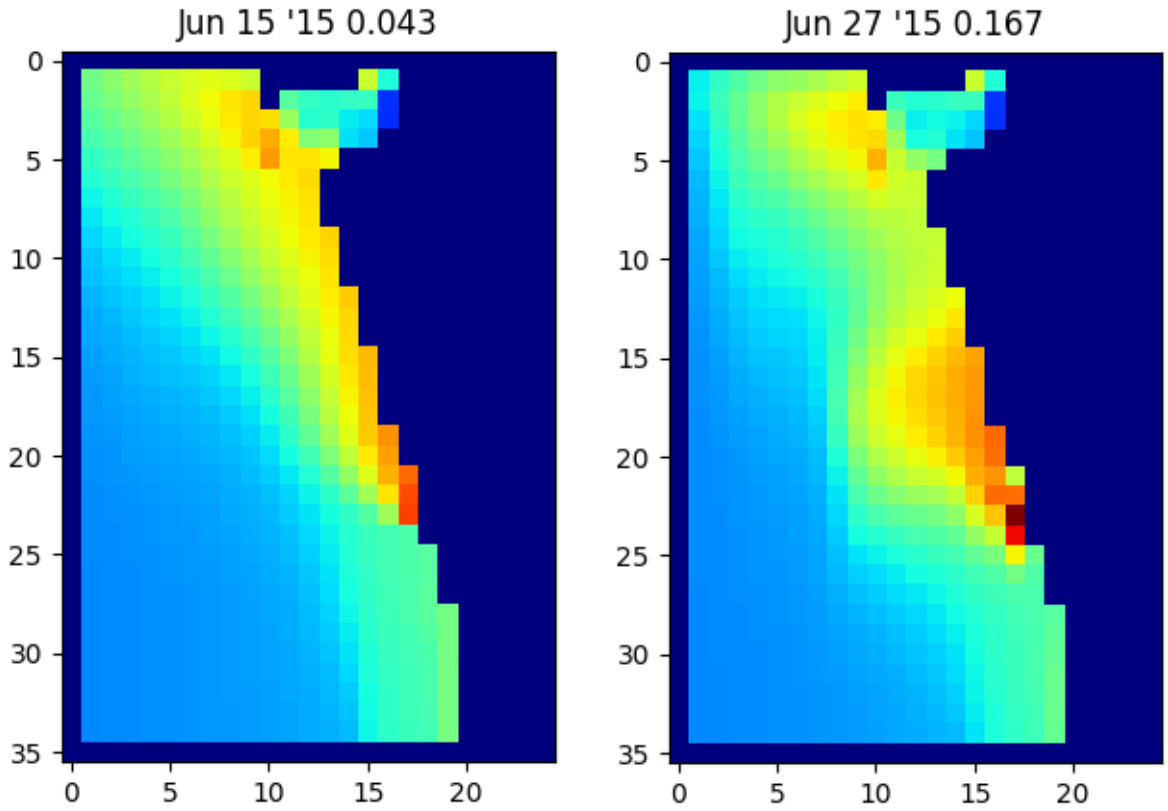

Figure 4: Nearshore spatial patterns of TP in the Lake Michigan for two dates in summer (2015). Hot colors represent high TP concentrations and cold colors reflect low concentrations.

"Data in Motion" - Continuous Water Sensor Data Collection for the 2015 Lake Michigan CSMI

Tom Hollenhorst[1], Laura Fiorentino[2], Paul McKinney[1,] Terry Brown, Anett Trebitz[1] and Joel Hoffman[1]
U.S. EPA Office of Research and Development, Mid-Continent Ecology Division, Duluth MN.
[2]NOAA - Center for Operational Oceanographic Products and Services, Chesapeake, VA

Introduction

The 2015 Cooperative Science Monitoring Initiative (CSMI) coordinated investigations linking Lake Michigan nearshore and offshore habitats and environments. Particularly, we were interested in understanding the distribution and abundance of nutrients and other water quality components at a high spatial resolution across the nearshore to offshore gradient. These investigations will help inform the implementation of the nearshore framework as envisioned by the Great Lakes Water Quality Agreement of 2012 (IJC 2016). To support this effort, during the 2015 Lake Michigan CSMI we collected continuous, undulating tow and autonomous glider data, including conductivity, temperature, pressure, fluorescence, and optical backscatter across survey tracks crossing the northern half of Lake Michigan. During the same period, we also collected discrete vertical water column profiles from our research vessel the Lake Explorer II at locations spread along four spatially coincident transects. Although the discrete vertical profiles are informative, we found the continuously collected data to be much more so, particularly when identifying wind and weather-related upwelling and their effect on lake thermal stratification. Researchers have long recognized the need for high resolution, detailed information about the variability and patchiness of limnological phenomena like upwellings (Megard et al. 1997). This is particularly true with transport processes along the nearshore where conditions are especially variable and episodic due to the contributions of tributaries after large rain events and the mixing that occurs in areas exposed to high amounts of wind and wave energy. A better understanding of nearshore transport processes will support a better understanding of several issues including nutrient loads, lower food web productivity, linkages with harmful algal blooms, and movements of sediments. This is especially important since stressors usually occur first and are felt the most strongly in the nearshore areas (Jetoo and Krantsberge, 2014 and Bails et al. 2005). Because the nearshore is so dynamic we need advanced technology to monitor and assess nearshore condition as well as long term trends along the nearshore of the Great Lakes. The 2015 Lake Michigan CSMI provide an opportunity to explore and compare some available technologies as applied to nearshore – offshore gradients.

Methods

Data Collection

We collected undulating tow data, as described by Yurista and Kelly (2007), combined with discrete vertical water column profiles from the research vessel the Lake Explorer II along four transects across northern Lake Michigan. The transects began in the nearshore at approximately 18 meters depth and extended offshore to approximately 110 meters' depth. The transects initiated near Sturgeon Bay, WI, Frankfort, MI, Ludington, MI and Manitowoc, WI (Figure 1 - map of transects). After collecting the tow data, we sampled at point locations starting at the deepest depth (110 m), then at 46 m and then at 18 m. At these stations we collected a vertical conductivity, temperature and depth (CTD) profile and water samples from at 2 m above the bottom, the mid-hypolimnion layer, at the depth of maximum fluorescence and from the mid-epilimnion as interpreted from the downward CTD temperature profile. Data were collected at each of three visits in June, July and September of 2015. During this time, we also flew two extended Slocum glider across-lake transect missions partially coincident with the ship transects, during July through August, and again from September through October. Dates for the CTD casts, tow transects and glider missions are listed in Table 1. Sensors on the Slocum glider, tow body and CTD Rosette (Figure 2 -photos of tow body, CTD Rosette glider) are listed in Table 2.

Data processing and visualization

The glider data was imported and initial plots of the data were processed in MatLab. The tow data was processed with a series of scripts with initial plots processed in ArcGIS 10.3. CTD casts were processed with SeaBird Scientific SeaSoft-Win32 software (www.seabird.com), binned into depths and trimmed to down cast only data and imported into a common Microsoft Access database and plotted with R. We also used ESRI story maps (http://storymaps.arcgis.com) to visualize the tow and glider data as an interactive map. A user can select points along the transects and visualize interpolated vertical profiles for the different sensors on board the tow body and glider at those locations. We also used Cesium, an open-source JavaScript library for developing dynamic animated map displays on 3D globes and maps.

Results and Discussion

Data visualization and analysis

The tools and techniques available for data visualization and analysis have greatly increased in just the last few years, as have the available platforms for sharing this type of data. For example, Xu et al (2017) recently came out with a tool for near-real time visualization and analysis of undulating tow data (which we have only begun to explore). In addition, the manufacturers of the Slocum glider (www.teledynemarine.com/webb-research) have recently released new mission control software for their gliders with more refined data visualization tools. And more and more so, platforms like ESRI Story Maps, Google Earth, Qlik Sense, Tableau, and other open source platforms like Cesium are being used to display and

disseminate complex geo-spatial data sets like we've collected as part of the Lake Michigan CSMI efforts.

We've visualized and analyzed our data using a variety of tools including MatLab, Cesium and ESRI Story maps. Each application has advantages and strengths depending on the data and visualization type. Figure 3 is a screen shot of a visualization of the glider-collected data created using Cesium. Cesium can be used to either create interactive web interfaces to the data or to record videos animating data through time, which helps to visually analyze the data. Figure 4 is a screen shot of an ESRI story map for Lake Superior glider data to illustrate what we hope to develop for the Lake Michigan 2015 glider and tow data. Figure 5 illustrates the dates and locations of the segments associated with the two glider missions. Managing these large complex data sets is extra challenging in terms of file sizes and complexity. Working with these large continuous data sets has helped us increase our understanding of the capabilities and usefulness of these processing and visualization tools, as we also develop workflows and techniques for automating the process.

Comparisons across seasons and sensor platforms

Comparisons across seasons and sensor platforms revealed some interesting features and differences in how each platform detected them. Although the discrete vertical profiles are informative we found the continuously collected data to be much more informative especially in terms of identifying wind and weather-related upwelling events, and their effect on lake thermal stratification. In one case an upwelling noticeable in the glider data didn't seem to be noticeable in the tow data (Figure 6), although the temperature stratification did seem weaker at the times the tows were conducted. Unfortunately, except for the very first glider segment of the first deployment, the tow and CTD data were collected days apart from when the glider was in the same area making comparisons difficult (see Table 1 and Figure 5 for dates and locations). That said, data collected by the glider did provide us with very high-resolution observations of the conditions following a major upwelling event. The horizontal and vertical resolution provided by the glider of the upwelling front are unprecedented in the Great Lakes. The event occurred during the second deployment (segment 7, Oct. 4-7), and affected water temperatures on the east side of the lake, near Ludington, MI. The glider passed through this area starting in the nearshore near Ludington and travelled west across the lake towards Sturgeon Bay, WI. The upwelling is apparent on the east side of the lake in the nearshore and appears to extend about 25 kilometers off shore (Figure 6). We also considered wind data leading up to this upwelling event as well as satellite imagery before and after the event. The wind data from the National Data Buoy Center (NDBC) (Figure 7) shows strong winds blew from the north and northeast during the four days before October 4th leading to the upwelling observed along the eastern shore near Ludington. The surficial extent of the upwelling is apparent in Advanced Very High Resolution Radiometry (AVHRR) satellite data collected on Oct. 10 (Figure 8). Although AVHRR satellite images are available daily, cloud cover over this part of the lake didn't allow for a useful image until October 10th. The Great Lakes Aquatic Habitat Framework (Wang et al 2015) developed a useful framework for mapping and classifying ecosystems and their key driving variables for the Great Lakes (Riseng et al 2018). As part of

that effort they modeled upwelling events from 1994 through 2013 using methods established by Plattner et al. (2006). From that we see these events affect nearshore water temperatures most frequently on the western side of Lake Michigan, but they do still frequently occur on the east side near Ludington (Figure 9)

It's not surprising that discrete vertical CTD casts (Figure 10) are not effective for capturing episodic, ephemeral phenomena like upwelling. The casts themselves represent a very discreet temporal sample limited only to the time it takes to lower and raise the CTD rosette. Also, they only represent a very limited spatial extent, represented only by a point location and the vertical data associated with it. The tow data is clearly an improvement in that vertical undulating tows are collected along a line, yet are still somewhat limited due to available ship time and staffing. In this study our tows were integrated with the point sampling so that only about half of each day was dedicated to the actual towing. We did detect a strong thermocline in the September tow data, particularly on the eastern side of Lake Michigan (fig. 11). Unfortunately, due to the short time available for towing we were not on site to capture the upwelling we observed in early October with the glider.

The data collected by the glider, although still a relatively small sample when compared the total volume and surface area of Lake Michigan across an entire season, has the best potential for capturing ephemeral events like upwelling. This is especially true when glider missions are integrated with near real-time satellite data and wind and weather data. That way glider missions can be adapted and redirected repeatedly across the gradients (temperature, fluorescence, etc.) associated with phenomena like upwelling, thermal bars, and tributary inputs after storm events. In addition, the glider can remain deployed during storm events when conditions are unfavorable for ship-based data collection.

Conclusions

Each of the Great Lake Cooperative Monitoring Initiatives collect exceedingly large amounts of complex data spanning a wide range of geographies and time spans. This is necessary to gain the knowledge and understanding of complex ecosystem processes in the Great Lakes. We've demonstrated here the application of three different data collection systems that range from discreet point orientated samples of the water column and relatively short continuous undulating tow transects that were visited three times over the spring, summer and fall of 2015, compared with 2 relatively long continuous glider missions that collected continuous data over a 28-day July-August mission, and a 27-day Sept.-Oct. mission. Each system has value due to the specific capabilities of each (e.g. different sensors, sampling limitations etc.), but it seems the successful integration of the data systems in time and space will prove the most useful. To do that we will need well established data frames for storing these large complex data sets and additional tools and algorithms for their analyses. That will further facilitate combining these data collection systems with effective visualization and analysis tools along with available remotely sensed imagery, weather data and modeled data like the upwelling index to provide for adaptive sampling in near real time. We anticipate that these continuous autonomous

sampling platforms combined with some or our more traditional techniques (CTD cast, plankton nets etc.) and leveraged with innovative and adaptive sampling designs will be key factors in recording and better understanding important physical and biological processes in the future.

References

Bails, J., Beeton, A., Bulkley, J., DePhillip, M., Gannon, J., Murray, M., Regier, H., Scavia, D., 2005. Prescription for Great Lakes Ecosystem Protection and Restoration: Avoiding the Tipping Point of Irreversible Changes. Wege Foundation and Joyce Foundation.

Great Lakes Water Quality Agreement. Protocol Amending the Agreement between Canada and the United States of America on Great Lakes Water Quality, 1978, as Amended on October 16, 1983, and on November 18, 1987, Signed September 7, 2012, Entered into force February 12, 2013. http://ijc.org/files/tinymce/uploaded/GLWQA%202012.pdf (2012)

IJC, 2016 The Great Lakes Nearshore Framework. https://binational.net/wp-content/uploads/2016/09/Nearshore-Framework-EN.pdf

Jetoo, S. and Krantzberg, G. 2014. Donning our thinking hats for the development of the Great Lakes nearshore governance framework. Journal of Great Lakes Research 40 (2014) 463–465.

Megard R. O., Kuns M. M., Whiteside M. C., Downing J. A. 1997. Spatial distributions of zooplankton during coastal upwelling in western Lake Superior, Limnology and Oceanography, 42, doi: 10.4319/lo.1997.42.5.0827.

Plattner, S., Mason, D. M., Leshkevich, G. A., Schwab, D. J., & Rutherford, E. S. 2006. Classifying and forecasting coastal upwellings in Lake Michigan using satellite derived temperature images and buoy data. Journal of Great Lakes Research, 32, 63−76.

Riseng, CM, KE Wehrly, L Wang, ES Rutherford, JE McKenna, Jr., LB Johnson, LA Mason, C Castiglione, TP Hollenhorst, BL Sparks-Jackson, SP Sowa (2018) Ecosystem classification and mapping of the Laurentian Great Lakes. *Candian Journal of Fisheries and Aquatic Sciences*, https://doi.org/10.1139/cjfas-2017-0242

Yurista, P.M., and Kelly, J.R. 2007. Spatial patterns of water quality and plankton from high-resolution continuous in situ sensing along a 537-km nearshore transect of western Lake Superior, 2004. M. Munawar, I.F. Munawar (Eds.), State of Lake Superior, M. & R. Heath, Ecovision World Monograph Series, Aquatic Ecosystem Health and Management Society, Canada (2007), pp. 439-471

Wang, L, CM Riseng, LA Mason, KE Wehrly, ES Rutherford, JE McKenna, Jr., C Castiglione, LB Johnson, DM Infante, S Sowa, M Robertson, J Schaeffer, M Khoury, J Gaiot, T Hollenhorst, C Brooks, M Coscarelli (2015) A spatial classification and database for management, research, and policy making: The Great Lakes aquatic habitat framework. *Journal of Great Lakes Research,* 41(2): 584-596. http://dx.doi.org/10.1016/j.jglr.2015.03.017

Xu, W., Collingsworth, P., Bailey, B., Mazur, M. C., Schaeffer, J., & Minsker, B. (2017). Detecting spatial patterns of rivermouth processes using a geostatistical framework for near-real-time analysis. Environmental Modelling & Software, 97, 72–85.

Tables

Table 1. Data collection dates for 2015 Lake Michigan CSMI

Transects	**Spring**	**Summer**	**Fall**
Sturgeon Bay, WI	May 30, 2015	July 14, 2015	Sept. 19, 2015
Frankfort, MI	May 31, 2015	July 15, 2015	Sept. 20, 2015
Ludington, MI	June 1, 2015	July 16, 2015	Sept. 21, 2015
Manitowoc, WI	June 3, 2015	July 19, 2015	Sept. 22, 2015
Glider Missions	**Start**	**Stop**	
Mission 1	July 14, 2015	Aug. 10, 2015	
Mission 2	Sept. 22, 2015	Oct. 18, 2015	

Table 2. Sensors on various sampling platforms used for CSMI

CTD Rosette	**Tow Body**	**Slocum Glider**
CTD	CTD	CTD
Transmissometer 1	Transmissometer 1	Backscatter
Transmissometer 2	Transmissometer 2	
Fluorometer	Fluorometer	Fluorometer/Chlorophyll -A
Dissolved Oxygen	Dissolved Oxygen	Dissolved Oxygen
pH	pH	
PARS	PARS	
	LOPC	
		CDOM

Figures

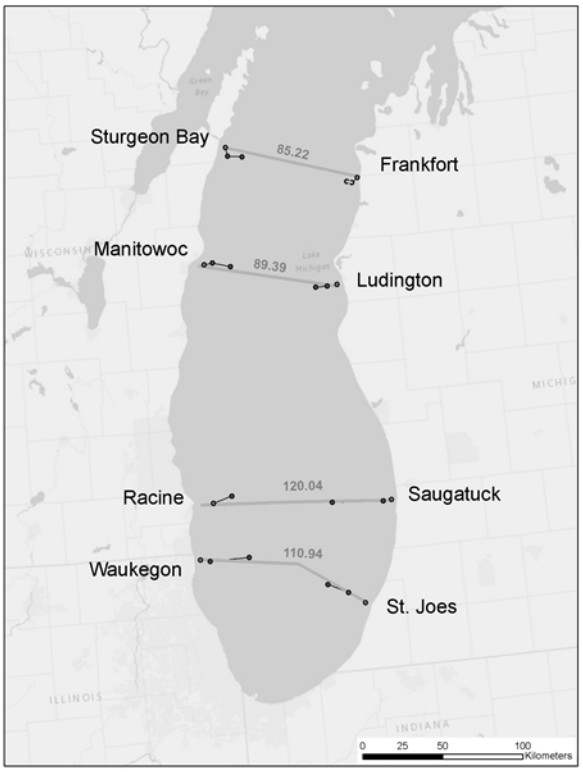

Figure 1. Lake Michigan 2015 CSMI transects with dots indicating vertical CTD casts. Light gray lines represent cross lake transects and distances.

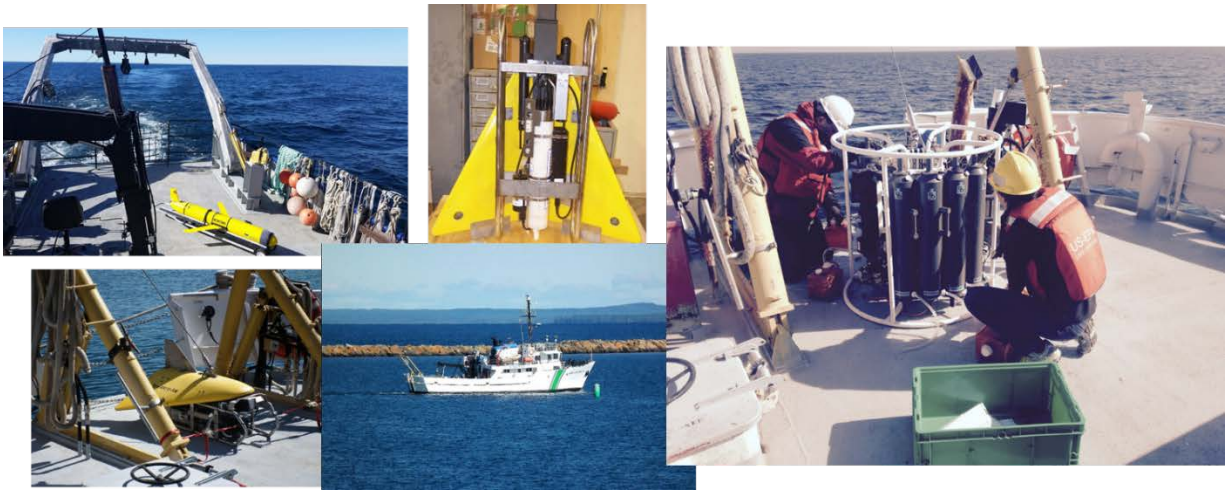

Figure 2. Clockwise from top left: Photos of Slocum Glider, tow body, CTD Rosette glider, Research Vessel the Lake Explorer II and tow body ready to be deployed.

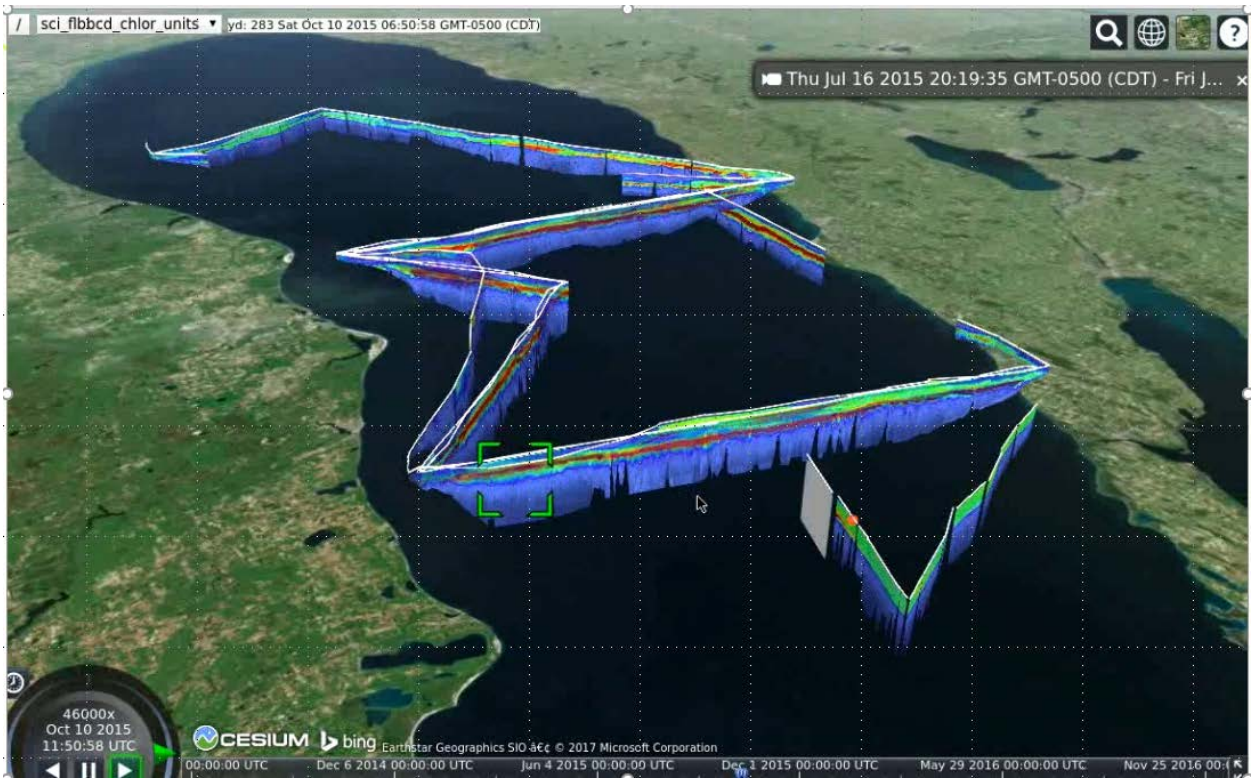

Figure 3. Screen shot of Cesium software animation of glider mission track displaying chlorophyll sensor data (red highest, blue lowest values).

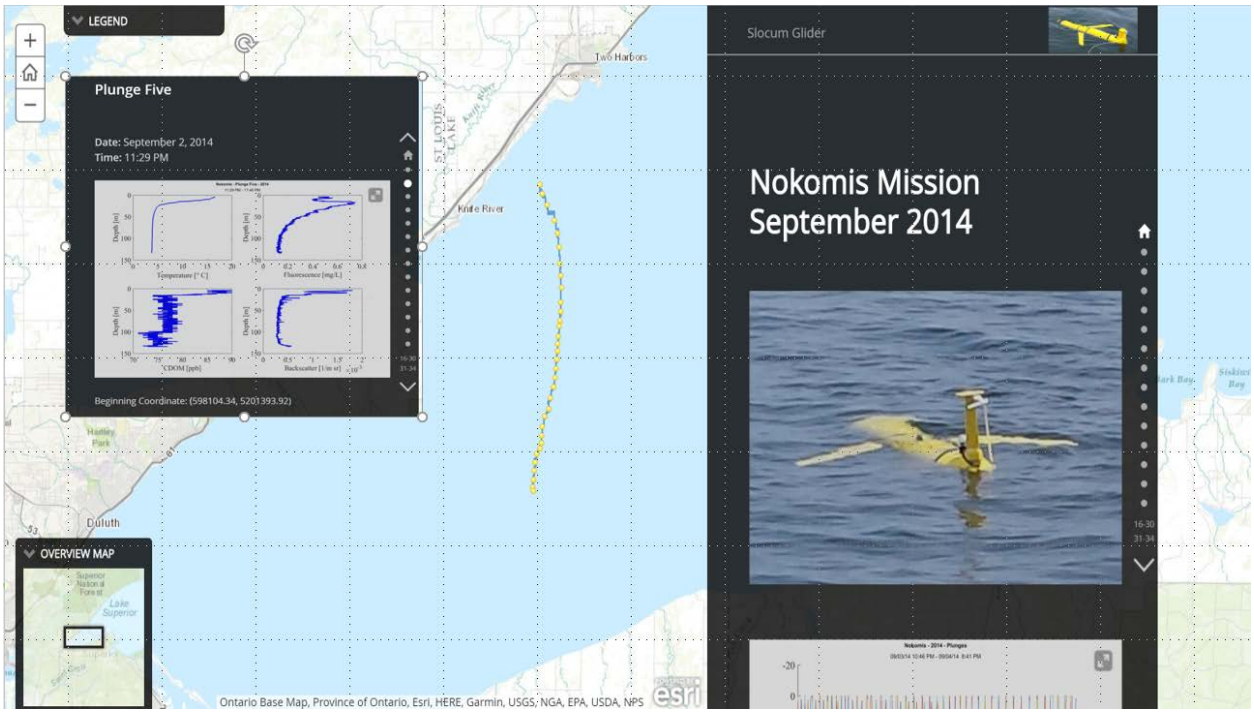

Figure 4. Screen shot of ESRI Story Map developed for Lake Superior glider data. Template could be used also for Lake Michigan 2015 CSMI glider and tow data.

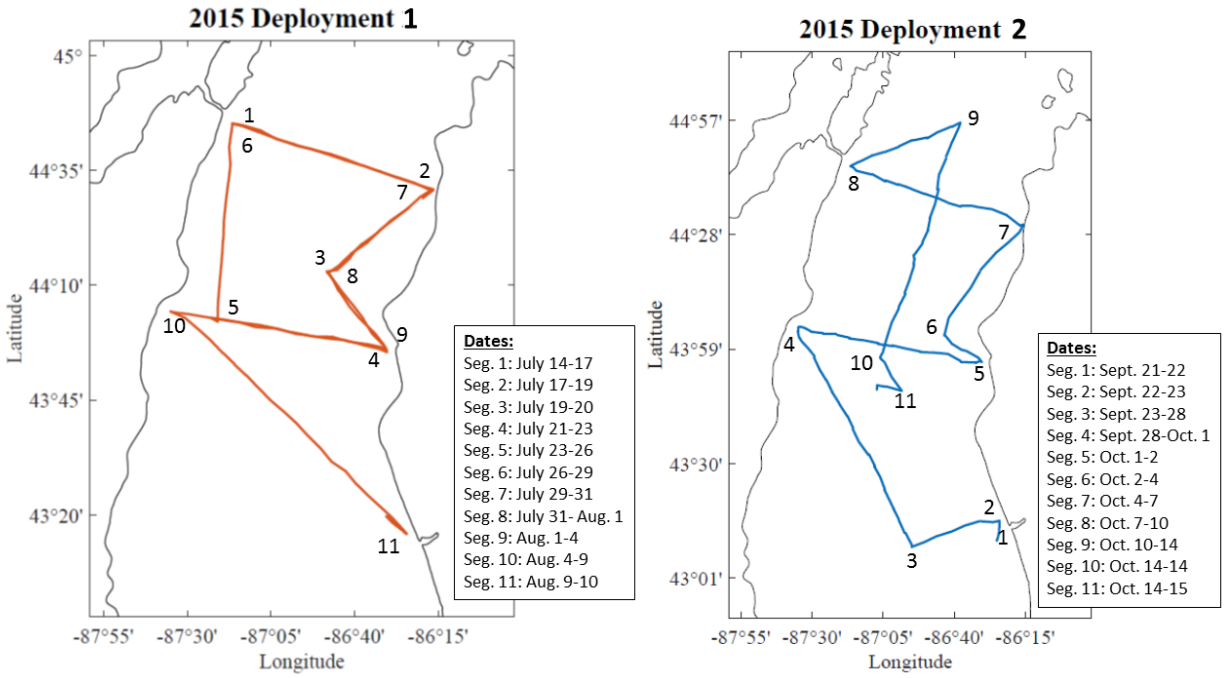

Figure 5. Dates of glider deployment segments.

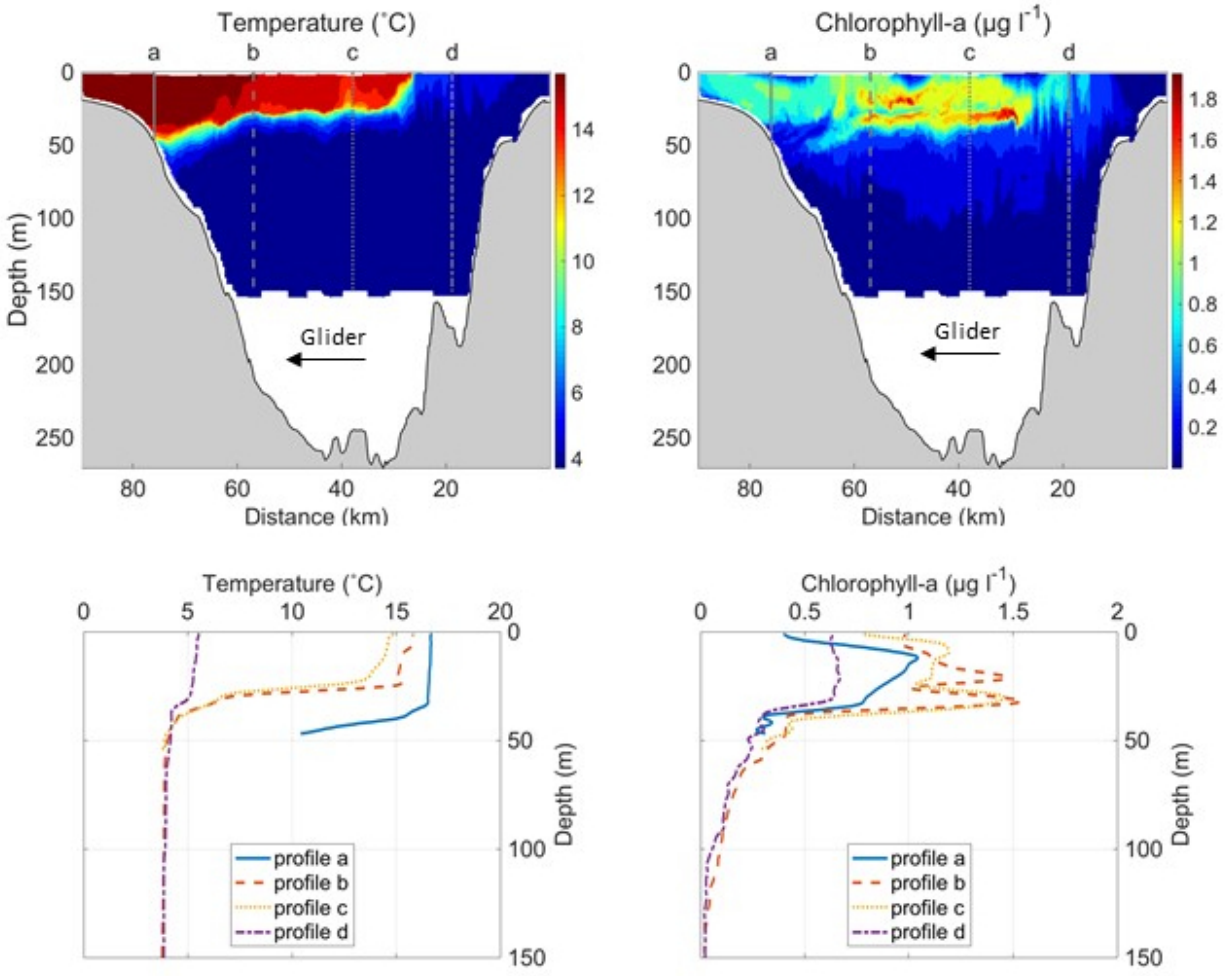

Figure 6. (top) Cross section of Lake Michigan temperature and chlorophyll-a from 2015 Deployment 2, segment 7 (for dates and location see Figure 5). The glider transited the lake from east to west, completing 480 profiles. The maximum dive depth for the glider is 150 m, and white area is no-data. (bottom) Representative profiles of temperature and chlorophyll-a from different distances (locations are indicated in top images) along the segment. Low values of Chlorophyll at the surface at 30 km, 50 km and 75 km are due to daytime quenching effects.

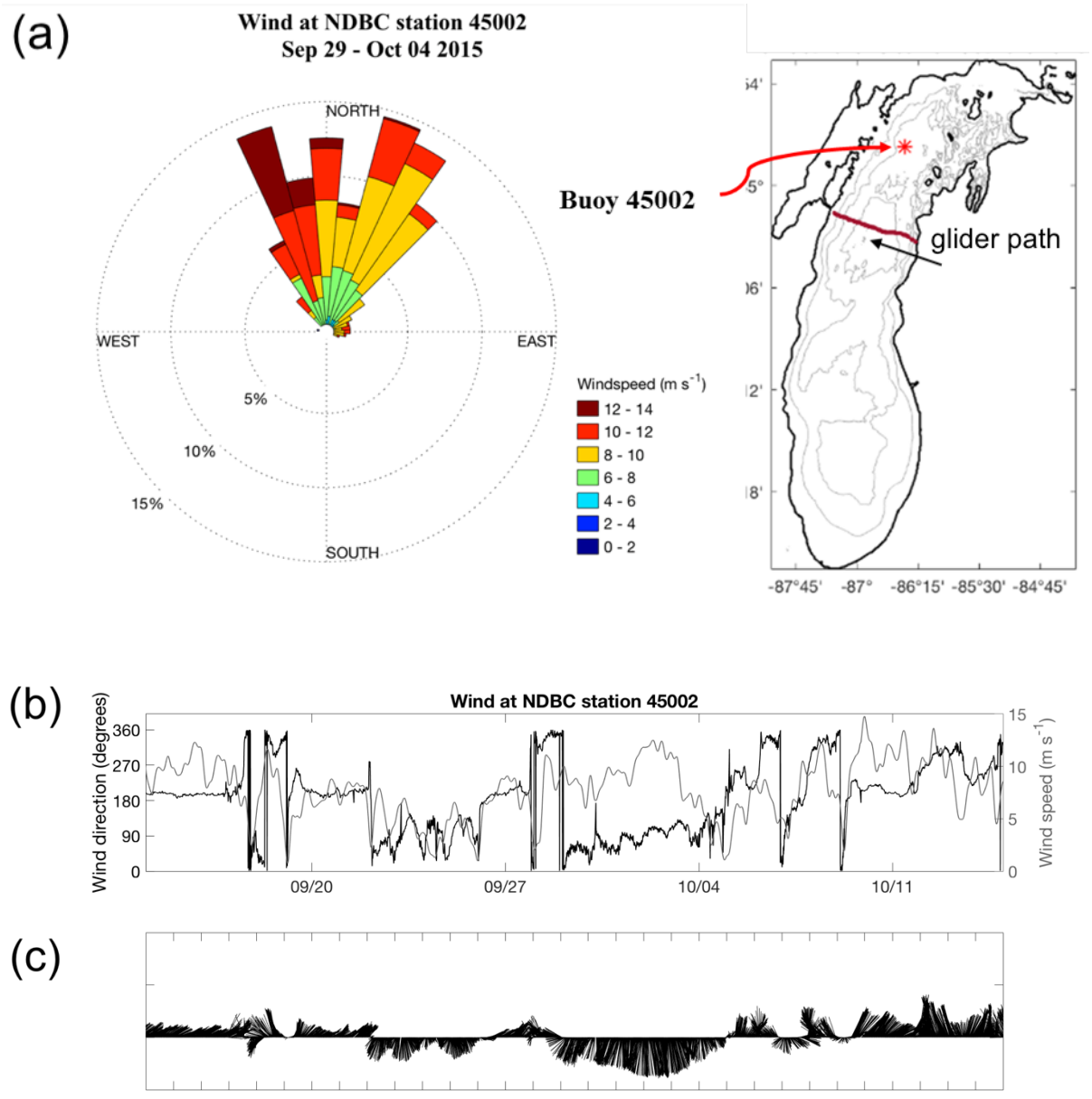

Figure 7. (a) Wind rose from data acquired at National Data Buoy Center (NDBC) buoy 45002, for the period covering the wind event discussed in the text. (b) Graph of wind direction (left axis) and wind speed (right axis) including 10 days before and after the event. (c) Quiver plot covering the same period as in (b); barbs point in direction of the wind.

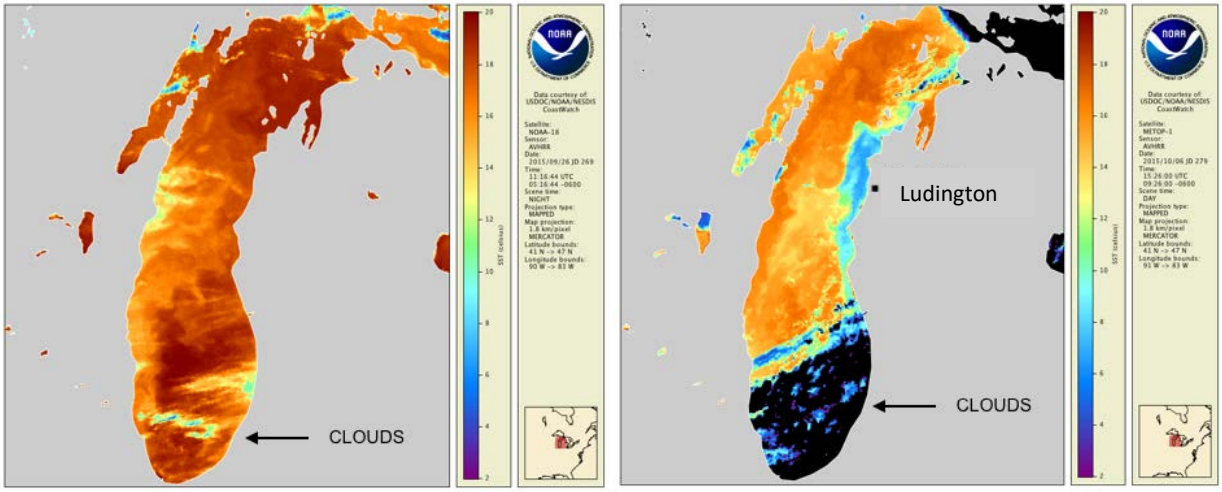

Figure 8. Lake Michigan surface temperature on Sept. 26, 2015 (left) and Oct. 10, 2015 (right). The left hand image, acquired prior to the wind event discussed in the text, shows warm surface temperature across most of the lake. In the right hand image, acquired after the wind event, cooler temperatures on the east side of the lake, near Ludington, MI., are the result of wind-driven upwelling of colder deep water to the surface.

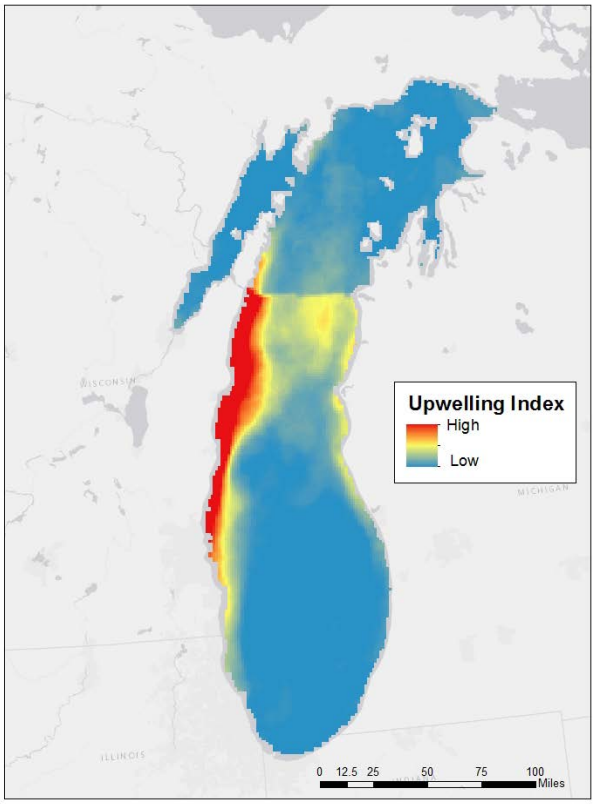

Figure 9. Lake Michigan Upwelling index summed from 1994 through 2013 using methods developed by Plattner et al 2006. Data acquired from www.glahf.org.

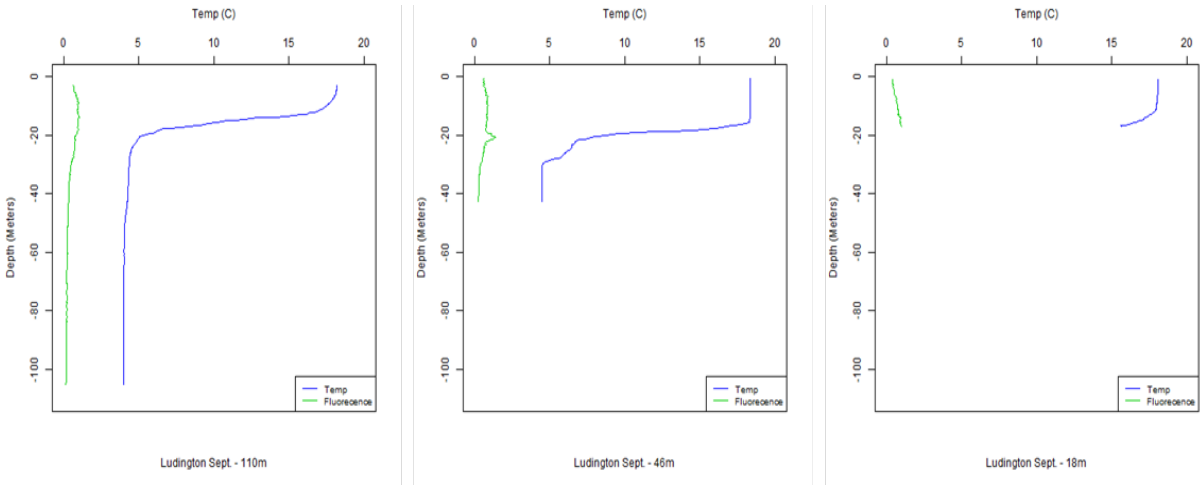

Figure 10. Vertical CTD Cast for the Ludington, MI transect at depths of 110, 46 and 18 meters collected on Sept. 21, 2015 (before the upwelling event).

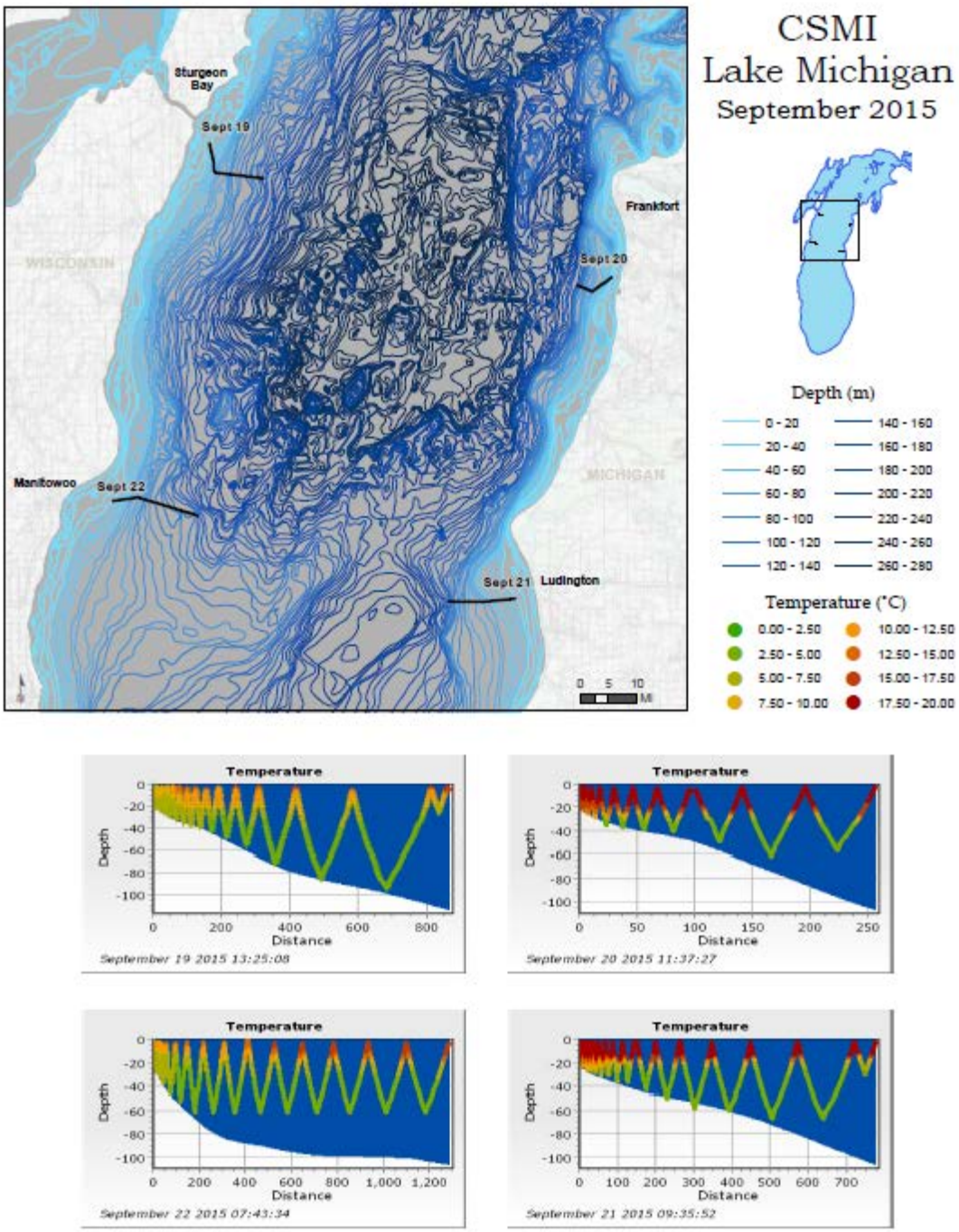

Figure 11. Tow temperature data from all four transects during September 2015. Note the strong thermal stratification occurring at this time.

Report: Atrazine Concentrations in Lake Michigan: Investigating Causes of the Recent Decline

Authors:

Kathryn A. Meyer, USEPA Great Lakes National Program Office (ORISE Fellow)

Russell G. Kreis, Jr., USEPA ORD/NHEERL/MED (Retired)

Kenneth R. Rygwelski, USEPA ORD/NHEERL/MED

Todd G. Nettesheim, USEPA Great Lakes National Program Office

Glenn J. Warren, USEPA Great Lakes National Program Office

Contact:

Glenn Warren

Email: Warren.glenn@epa.gov

Phone:

Address:

USEPA Great Lakes National Program Office

77 W. Jackson

Chicago, IL 60604

Project Summary

The 1994-1995 Michigan Mass Balance Study (MMBS) observed and forecasted whole lake, volume-weighted average atrazine concentrations for Lake Michigan. The atrazine concentrations were well below the U.S. Environmental Protection Agency (EPA) biological thresholds. But, with a decay estimated at less than 1% per year in the lake and knowing that atrazine acts similarly to a conservative substance, concentrations were expected to increase under current atrazine loadings. Ken Rygwelski and Russ Kreis developed a model to predict future atrazine concentrations in Lake Michigan for a variety of different scenarios (Figure 1).

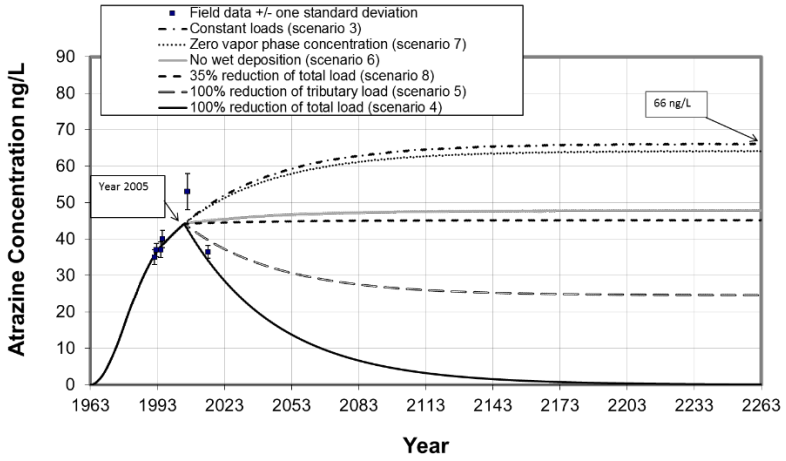

Figure 1: Lake Michigan atrazine concentration prediction modeling (Kreiss, Rygwelski)

Lake Michigan atrazine sampling was done again in 2015. Water samples were taken at the EPA Great Lakes National Program Office's Lake Michigan open water stations in August 2015 at both the mid-epilimnion and mid-hypolimnion depths. These samples were analyzed using gas chromatography – mass spectrometry by the U.S. Geological Survey National Water Quality Laboratory in Lakewood, Colorado. The average atrazine concentration for Lake Michigan in 2015 was 36 ng/L. This concentration fell between the model predictions for the 100% reduction of tributary loading and 100% reduction of total loading scenarios of the prediction model (Figure 1).

Three hypotheses were investigated regarding why the Lake Michigan atrazine concentration in 2015 was less than forecasted.

1) Atrazine is degrading more rapidly than predicted in the model
2) A decline in atrazine usage has significantly reduced atrazine input to Lake Michigan
3) Sedimentation processes are removing atrazine from the water column

The first hypothesis was addressed through a literature review. Studies have found that atrazine degradation may be occurring in soils, as atrazine degradation genes have evolved in many bacteria species, so less atrazine may be reaching the lake. Faster biodegradation rates were found in soils already treated with atrazine, too. The influence of photolysis in atrazine

degradation, which could also be stimulated by deeper light penetration (supported by increasing secchi depths) was also suggested. Atrazine-degrading bacteria have not yet specifically been found in Lake Michigan.

To address the second hypothesis, atrazine use data in the Lake Michigan basin from the USGS National Water-Quality Assessment (NAWQA) and the USDA National Agricultural Statistical Service (NASS) were evaluated. There was an estimated 34% decline in annual atrazine use from 1992-2015 in Lake Michigan counties (USGS NAWQA) and an estimated 18% decline in annual atrazine application from 1990-2014 in Lake Michigan states (USDA NASS). Annual atrazine use in the United States, which was assessed because atmospheric transport may also affect atrazine concentrations, had an estimated 15% decline from 1992-2015 (USGS NAWQA). Overall, the declines potentially contributed to lower atrazine concentrations.

The third hypothesis was address through another literature review. The prediction model assumed sedimentation was negligible. A recent study by Guo et al. (2016) found annual atrazine loadings to Lake Michigan sediments to be 44.4 +/- 25.6 kg/year; and that atrazine did not easily desorb from particles. Although atrazine sedimentation in Lake Michigan has been recorded, the amount of atrazine fluxing to the sediment is likely negligible compared to the large amount of atrazine entering the lake through other pathways.

The overall general conclusions for this investigation were that decreased atrazine usage is having an influence on the atrazine concentration in Lake Michigan, and that increased atrazine degradation is also having an influence on atrazine concentrations in the lake.

Relevant Literature Sources

Cessna, A.J. Nonbiological degradation of triazine herbicides: photolysis and hydrolysis. “The Triazine Herbicides.” Ch. 23. 2008. 329.

Fenner, K., et al. Relating atrazine degradation rate in soil to environmental conditions: Implications for global fate modeling. *Environ. Sci. Technol.* 2007, 41, 2840-2846.

Giardi, M.T., et al. Chemical and biological degradation of primary metabolism of atrazine by a Nocardia strain. *Agriculture Biology and Chemistry.* 1985, 49, 1551-1558.

Guo, J., et al. Occurrence of atrazine and related compounds in sediments of Upper Great Lakes. *Environ. Sci. Technol.* 2016, 50, 7335-7343.

Kurt-Karakus, P.B., et al. Metolachlor and atrazine in the Great Lakes. *Environ. Sci. Technol*. 2010. 44 (12), 4678-4684.

Mandelbaum, R.T., et al. Isolation and characterization of a *Pseudomonas* sp that mineralizes the s-triazine herbicide atrazine. *Appl. Environ. Microbiol.* 1995, 61, 1451-1457.

Mueller, T.C., et al. Enhanced atrazine degradation is widespread across the United States. *Pest. Manag.* 2017.

Newton, R.J.; McLellan, S.L. A unique assemblage of cosmopolitan freshwater bacteria and higher community diversity differentiate an urbanized estuary from oligotrophic Lake Michigan. *Frontiers in Microbiology*. 2015, 6, 1028.
Rousseaux, S., et al. Isolation and characterization of new Gram-negative and Gram-positive atrazine degrading bacteria from different French soils. *FEMS Microbiology Ecology.* 2001, 36, 211-222.
Rygwelski, K.R. (Ed.) Results of the Lake Michigan Mass Balance Project: atrazine modeling report. U.S. Environmental Protection Agency, ORD/NHEERL/MED, Grosse Ile, MI. EPA/600/R-08/111, 140 pp.
Rygwelski, K.R., et al. Model forecasts of atrazine in Lake Michigan in response to various sensitivity and potential management scenarios. *J. Great Lakes Res*. 2012, 38, 1-10.
Schottler, S.P.; Eisenreich, S.J. Herbicides in the Great Lakes. *Environ. Sci. Technol*. 1994. 28, 2228-2232.
Schottler, S.P.; Eisenreich, S.J. Mass balance model to quantify atrazine sources, transformation rates, and trends in the Great Lakes. *Environ. Sci. Technol*. 1997. 31, 2616-2625.
Smalling, K.L.; Aelion, C.M. Distribution of atrazine into three chemical fractions: impact of sediment depth and organic carbon content. *Environ. Toxicol. Chem.* 2004, 23 (5), 1164-1171.
Struger, J., et al. In-use pesticide concentrations in surface waters of the Laurentian Great Lakes, 1994-2000. *J. Great Lakes Res.* 2004, 30 (3), 435-450.
Tierney, D.P., et al. Predicted atrazine concentrations in the Great Lakes: Implications for biological effects. *J. Great Lakes Res.* 1999. 25 (3), 455-467.
Topp, E. A comparison of three atrazine-degrading bacteria for soil remediation. *Biol. Fertil. Soils.* 2001, 33, 529-534.

Report: Examining Legacy and Emerging Contaminants in Lake Michigan Tributaries

Authors:

Marta Venier, Indiana University

Jiehong Guo, Indiana University

Kevin Romanak, Indiana University

Stephen Westenbroek, USGS Wisconsin Water Science Center

An Li, University of Illinois at Chicago

Russell G. Kreis, Jr., USEPA ORD/NHEERL/MED (Retired)

Ronald Hites, Indiana University

Contact:

Marta Venier

Email: mvenier@indiana.edu

Phone: 812-855-1005

Address:

School of Public and Environmental Affairs

702 N. Walnut Grove ave.

Bloomington, IN 47405

Project Summary

High-volume water samples were collected every 3 weeks in 2015 from five tributaries to Lake Michigan, and were subsequently analyzed for PCB congeners, mercury, and emerging chemical flame retardants. The five tributaries were selected because they showed the highest loads of PCBs in the 1994-5 Lake Michigan Mass Balance Project (LMMBP); the tributaries sampled were the Grand, Kalamazoo, St. Joseph, and Lower Fox Rivers and from the Indiana Harbor and Ship Canal (IHSC). A total of 59 samples were collected from these five tributaries by two USGS field offices between April and December of 2015. The sampling procedure was similar to that in the LMMBP, where 80-160 L of water were pumped through a 0.7 µm filter and through XAD-2 packed resin columns.

The dissolved phase (XAD-2) and the particle phase (glass fiber filters) were analyzed separately to study how the chemicals partition between the two phases. The XAD-2 resin or filter was loaded in a Soxhlet extractor, spiked with the surrogate standards and extracted using a mixture of hexane and acetone. Following additional concentration and extraction steps, the samples were analyzed for PCBs and flame retardants, including organophosphate esters (OPEs), brominated flame retardants (BFRs), and dechlorane-related compounds.

In the five tributaries sampled in this study, the geometric mean concentrations of ΣPCB (sum of 85 congeners) ranged from 1.52 to 22.4 ng/L. The highest concentrations of PCBs were generally found in the Lower Fox River and in the Indiana Harbor and Ship Canal. The highest BFR concentrations were measured in either the IHSC or the St. Joseph River. OPEs were the most abundant among the targeted compounds with geometric mean concentrations ranging from 20 to 54 ng/L; OPE concentrations were comparable among the five tributaries. BFR concentrations were about 1 ng/L, and the most abundant compounds were bis(2-ethylhexyl) tetrabromophthalate, 2-ethylhexyl 2,3,4,5-tetrabromobenzoate, and decabromodiphenyl ether. The dechlorane-related compounds were detected at low concentrations (< 1 pg/L). The fraction of target compounds in the particulate phase relative to the dissolved phase varied by chemical and tended to increase with their octanol-water partition coefficient.

During the work on flame retardants, a relatively new compound named Marbon was identified. Marbon is isomeric with Dechlorane Plus (DP). Dechlorane Plus is commonly found in the environment throughout the world, but Marbon has, so far, only been detected at low levels in one sediment core collected near the mouth of the Niagara River in Lake Ontario. In addition to the 59 Lake Michigan Tributary water samples, 10 surface sediment samples from the IHSC, and 2 surface sediment samples from the Chicago Sanitary and Ship Canal were analyzed for Marbon. Three Marbon diastereomers were detected in the water and sediment samples from the IHSC, which is far from the location of its previous detection in Lake Ontario. The sum of the concentrations of the three Marbons was greater in the water from the IHSC (N = 11, median = 150 pg/L) compared to those in water from the other four tributaries (N = 11-13, medians = 0.9-2.0 pg/L). Marbon concentrations in sediment samples from the IHSC were up to 450 ng/g dry

weight. Anti-DP was also measured for comparison. Its concentrations were not significantly different among the water samples, but its sediment concentrations in the IHSC were significantly correlated with those of Marbon. The source of Marbon contamination in the IHSC is not clear.

Loads for PCB, mercury, and flame retardant compounds were calculated for the five tributaries. PCB data from this study were combined with PCB concentration data from other previous studies involving open lake water, air, and sediment to calculate an updated mass budget. The input flows of ΣPCBs from wet deposition, dry deposition, tributary loading, and air to water exchange, and the output flows due to sediment burial, volatilization from water to air, and transport to Lake Huron and through the Chicago Diversion were calculated as well as flows related to the internal processes of settling, resuspension, and sediment-water diffusion. The net transfer of PCBs was 1240 ± 531 kg/yr out of the lake. This net transfer is 46% lower than that estimated in 1994-5. PCB concentrations in most matrices in the lake are decreasing, which drove the decline of all the individual input and output flows. Tributary loads at the Lower Fox River and the Indiana Harbor and Ship Canal both decreased substantially relative to 1994-1995 loads. Atmospheric deposition to Lake Michigan has become negligible, while volatilization from the water surface is still a major route of loss, releasing PCB from the lake into the air. Large masses of PCB remain in the water column and surface sediments and are likely to contribute to future efflux of PCBs from the lake to the air.

Mercury loads from all five tributaries to Lake Michigan were on the order of 50% to 75% lower in 2015 relative to loads calculated for 1994-1995. The total mercury load in the Lower Fox River was about 160 kg/yr in 1994-1995; the total mercury load in the Lower Fox River was about 43 kg/yr in 2015. The total mercury load in the Grand River was about 36 kg/yr in 1994-1995; the total mercury load in the Grand River was about 8 kg/yr in 2015. Similar decreases were seen for the other three tributaries. Indiana Harbor and Ship Canal's total mercury load decreased from about 4.3 kg/yr (1994-1995) to about 1.7 kg/yr. St. Joseph River's total mercury load decreased from about 35 kg/yr (1994-1995) to about 12.6 kg/yr (2015). Kalamazoo River's total mercury loads decreased from about 21 kg/yr (1994-1995) to about 9 kg/yr (2015).

Publications Related to this Work

Guo, J.; Venier, M.; Romanak, K.; Westenbroek, S.; Hites, R. A., Identification of Marbon in the Indiana Harbor and Ship Canal. Environ. Sci. Technol. 2016, 50, (24), 13232-13238.

Guo, J.; Romanak, K.; Westenbroek, S.; Li., An, Kreis, R.G. Jr, Hites, R. A., Venier, M.; Updated Polychlorinated Biphenyl Mass Budget for Lake Michigan. Environ. Sci. Technol. 2017, 51, (21), 12455-12465.

Guo, J.; Romanak, K.; Westenbroek, S.; Hites, R. A.; Venier, M., Current-Use Flame Retardants in the Water of Lake Michigan Tributaries. Environ. Sci. Technol. 2017, 51, (17), 9960–9969.

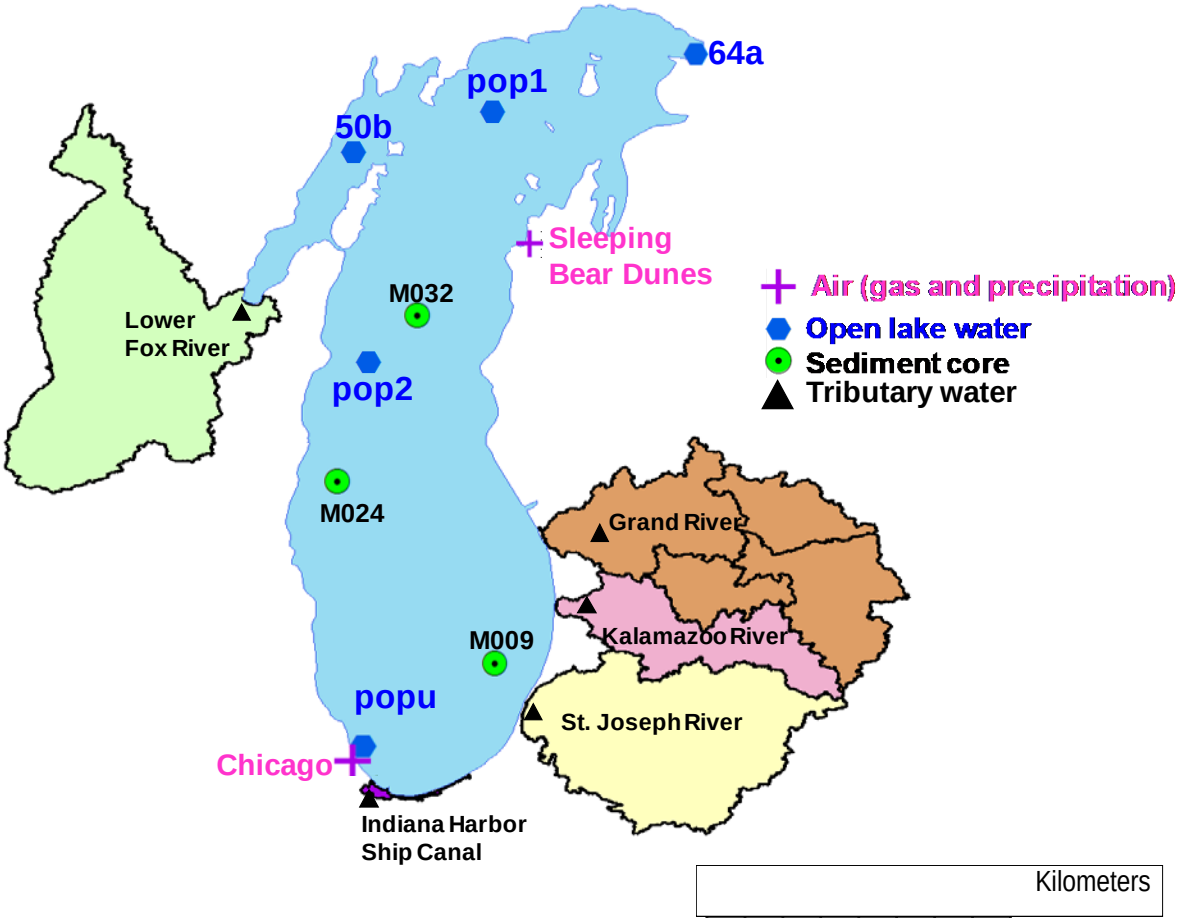

Figure 1. Sampling locations related to the 2015 CSMI Lake Michigan contaminant study referenced in subsequent plots and the text.

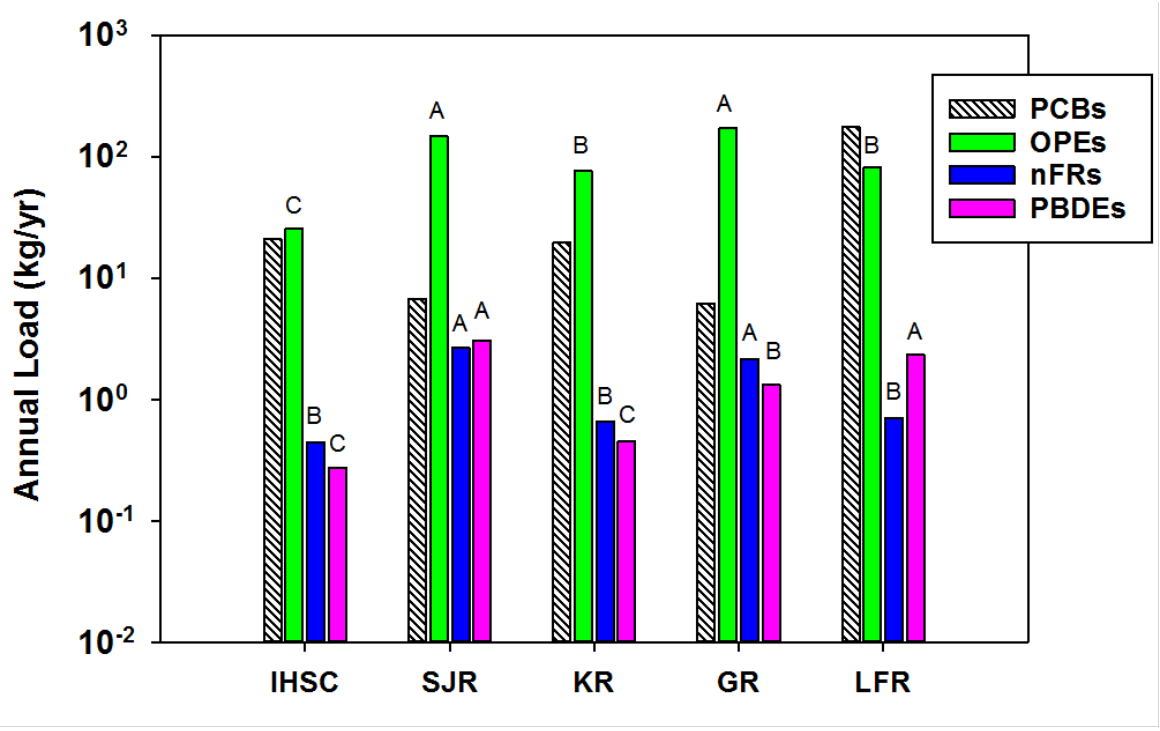

Figure 2. Tributary loading of organophosphate esters (OPEs), non-BDE novel flame retardants (nFRs), and polybrominated diphenyl ethers (PBDEs) to Lake Michigan. Loadings for polychlorinated biphenyls (PCBs) from 2005-06 are included for reference. Abbreviations: IHSC, Indiana Harbor and Ship Canal; SJR, St. Joseph River; KR, Kalamazoo River; GR, Grand River; and LFR, Lower Fox River. The rivers are arranged based on latitude from south to north. ANOVA results are to be read across the tributaries; water from tributaries sharing the same letter do not have statistically different ($p < 0.05$) concentrations.

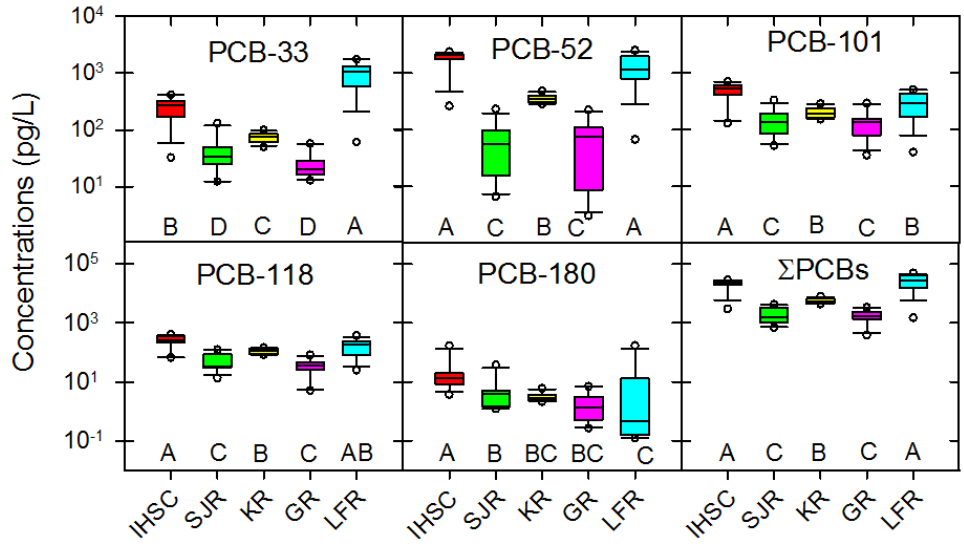

Figure 3. Box and whisker plots of concentrations of individual congeners and ΣPCBs in 2015 tributary water samples. Abbreviations: IHSC, Indiana Harbor and Ship Canal (N = 11); SJR, St. Joseph River (N = 12); KR, Kalamazoo River (N = 12); GR, Grand River (N = 11); and LFR, Lower Fox River (N = 13). Shown are the medians (black lines inside the box), the 25th to 75th percentiles (box), the 10th and 90th percentiles (whiskers), the minimum and maximum values (circles), and the one-way analysis of variance (ANOVA) results (letters at the bottom of each box). ANOVA results are to be read across the rivers; water from rivers sharing the same letter do not have statistically different ($p < 0.05$) concentrations. Rivers are arranged from south to north.

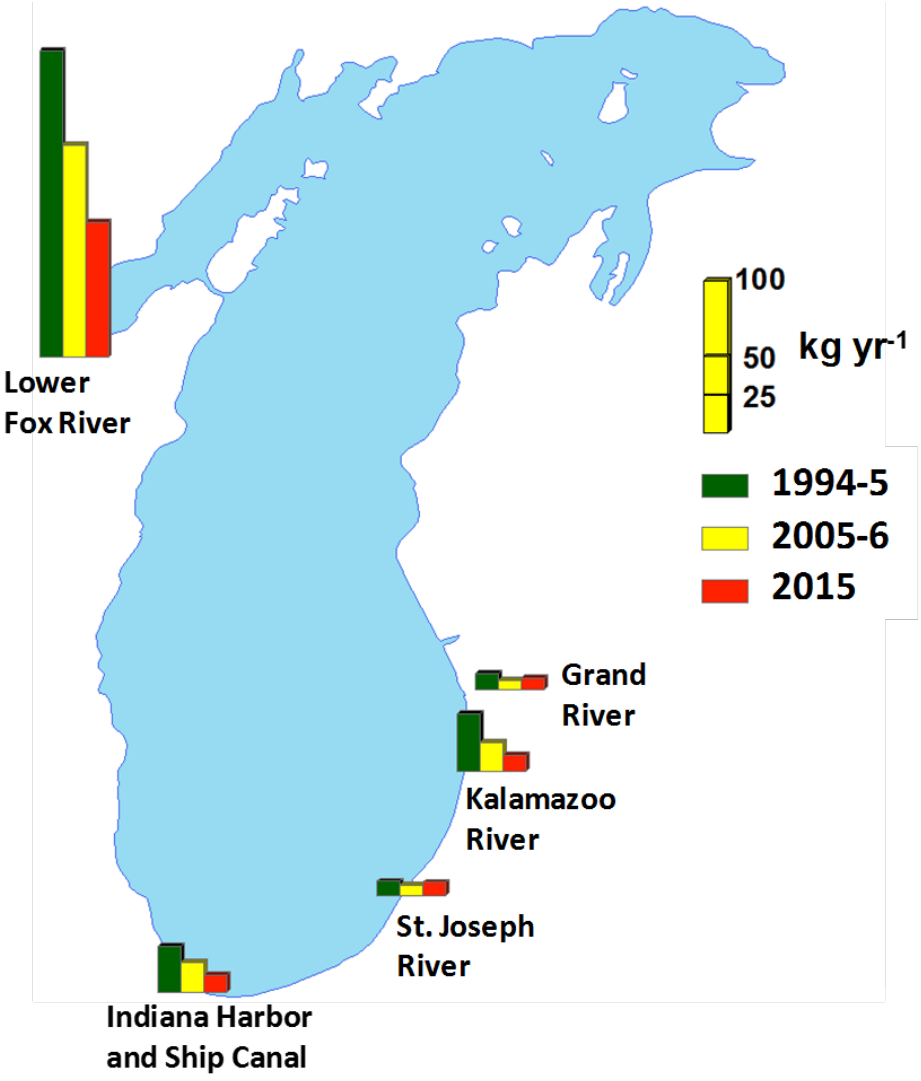

Figure 4. Tributary ΣPCB flows to Lake Michigan for 1994-5, 2005-6, and 2015. Estimates for 1994-5 and 2005-6 were obtained from a previous study.

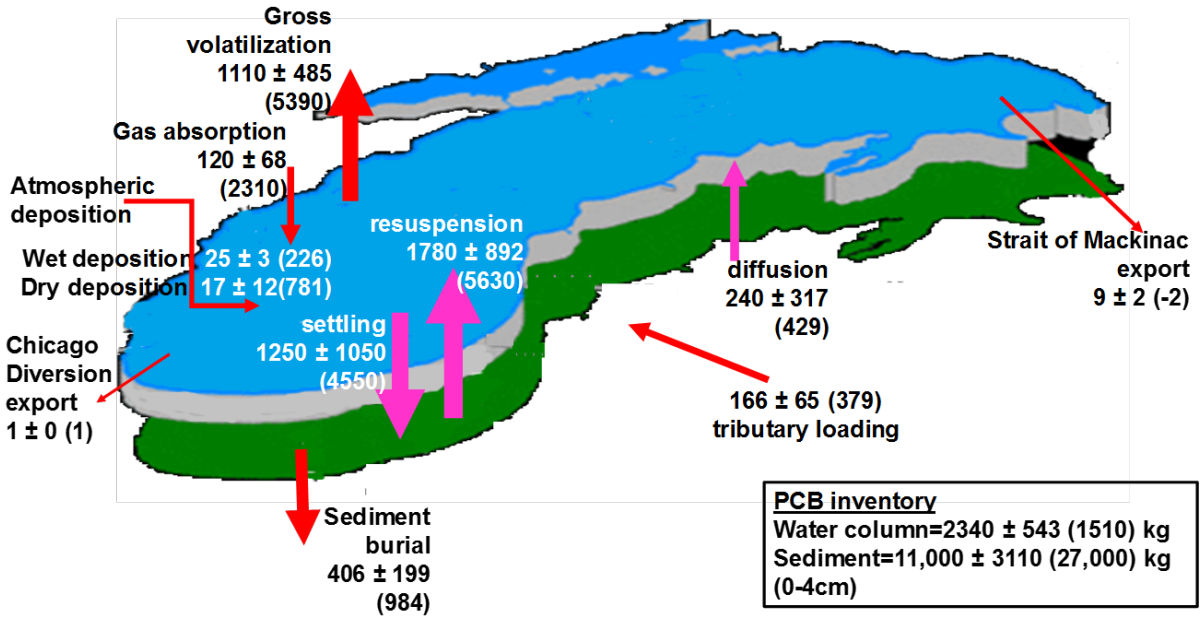

Figure 5. Estimated total PCB mass budget flows (kg yr^{-1}) and inventories (kg) for 2010-2015 and comparison to the 1994-5 mass balance results based on the MICHTOX model16 (in parentheses) in Lake Michigan. The blue and green layers represent water and sediment layers, respectively. The thickness of the arrows indicates the magnitude of flows in 2010-2015.

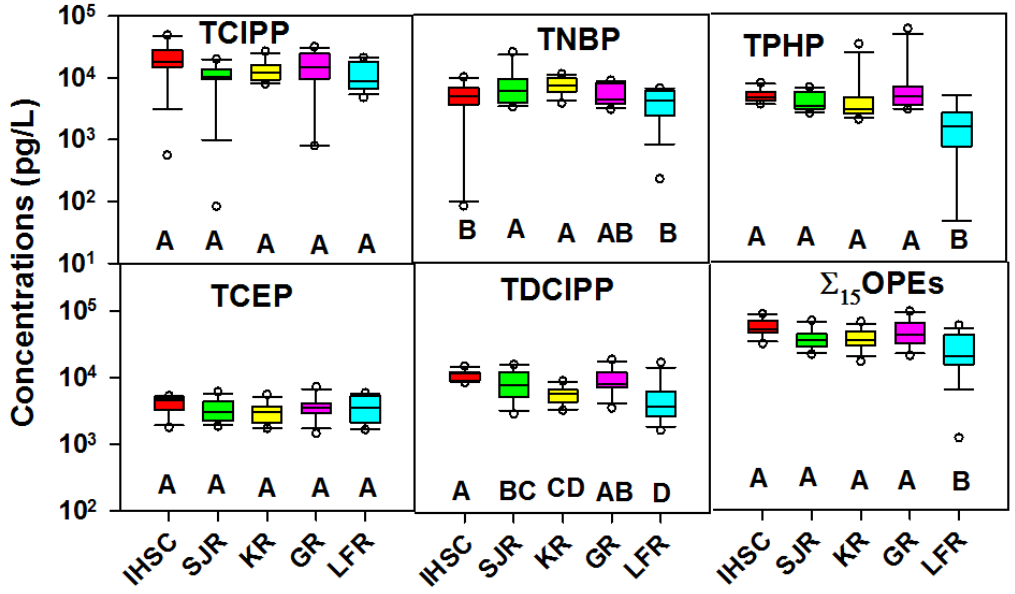

Figure 6. Box and whisker plots of concentrations of organophosphate esters (OPEs) in tributary water samples. Abbreviations: IHSC, Indiana Harbor and Ship Canal (N = 11); SJR, St. Joseph River (N = 12); KR, Kalamazoo River (N = 12); GR, Grand River (N = 11); and LFR, Lower Fox River (N = 13); TCIPP, tris[(2R)-1-chloro-2-propyl] phosphate; TNBP, tri-n-butyl phosphate; TPHP, triphenyl phosphate; TCEP, tris(2-chloroethyl) phosphate; TDCIPP, tris(1,3-dichloro-2-propyl) phosphate; $\sum_{15}$OPEs, sum of 15 OPEs. Shown are the medians (black lines inside the box), the 25th to 75th percentiles (box), the 10th and 90th percentiles (whiskers), the minimum and maximum values (circles), and the ANOVA results (letters at the bottom of each box). ANOVA results are to be read across the tributaries; water from tributaries sharing the same letter do not have statistically different ($p < 0.05$) concentrations. Tributaries are arranged based on latitude from south to north.

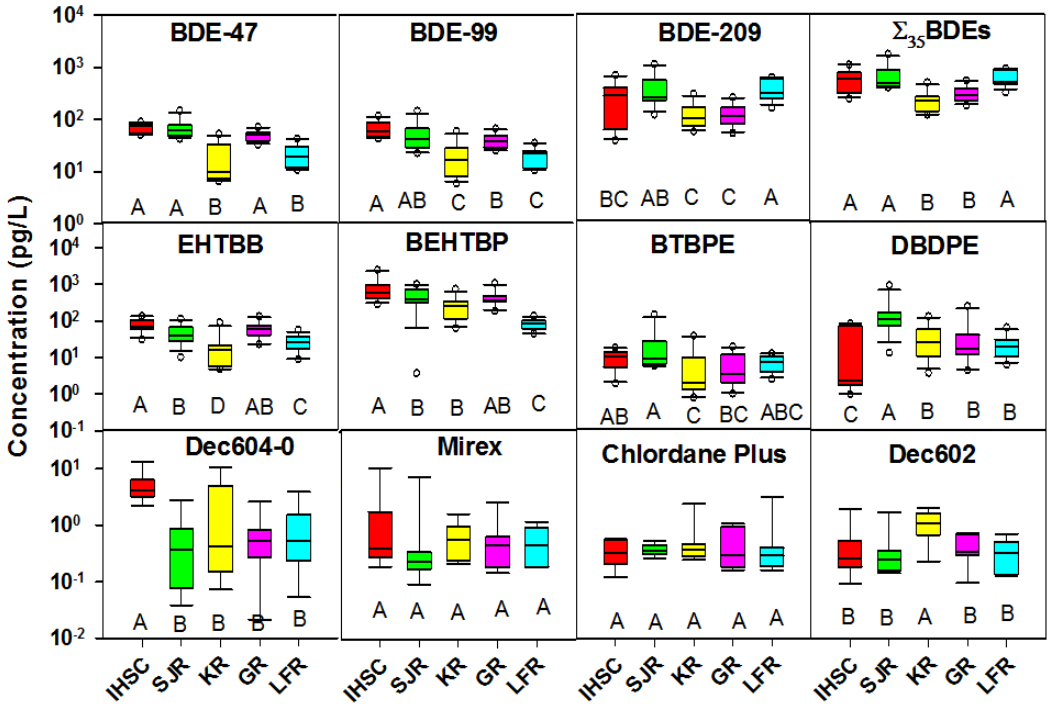

Figure 7. Box and whisker plots of concentrations of polybrominated diphenyl ethers (PBDEs), non-BDE novel flame retardants (nFRs), and dechlorane related compounds (Decs) in tributary water samples. Abbreviations: IHSC, Indiana Harbor and Ship Canal (N = 11 for PBDEs and nFRs, N=8 for Decs); SJR, St. Joseph River (N = 12 for PBDEs and nFRs, N=8 for Decs); KR, Kalamazoo River (N = 12 for PBDEs and nFRs, N=8 for Decs); GR, Grand River (N = 11 for PBDEs and nFRs, N=7 for Decs); and LFR, Lower Fox River (N = 13 for PBDEs and nFRs, N=7 for Decs); $\sum_{35}$BDEs, sum of 35 PBDEs; EHTBB, 2-ethylhexyl 2,3,4,5-tetrabromobenzoate; BEHTBP, di-(2-ethylhexyl)-tetrabromophthalate; BTBPE, 1,2-bis(2,4,6-tribromophenoxy)ethane; DBDPE, decabromodiphenylethane; Dec604-0, hexachlorophenyl-norbornene; Dec602, dechlorane 602. Shown are the medians (black lines inside the box), the 25th to 75th percentiles (box), the 10th and 90th percentiles (whiskers), the minimum and maximum values (circles), and the ANOVA results (letters at the bottom of each box). ANOVA results are to be read across the tributaries; water from tributaries sharing the same letter do not have statistically different ($p < 0.05$) concentrations. Rivers are arranged based on latitude from south to north.